IN THE UNITED STATES PATENT AND TRADEMARK OFFICE

In re application of: **YU et al.**

Application Serial No.: 09/333,966 Art Unit: 1646

Filed: June 16, 1999 Examiner: Ulm, J.

For: Death Domain Containing Receptors Attorney Docket No.: **PF267D1**

DECLARATION OF THI-SAU MIGONE UNDER 37 C.F.R. § 1.132

Assistant Commissioner for Patents
Washington, D.C. 20231

Sir:

I, Thi-Sau Migone Ph.D., hereby declare and state as follows:

1. I am currently employed as a Senior Scientist at Human Genome Sciences, Inc. (HGS), which I understand to be the assignee of the above-captioned patent application (the '966 Application). In 1991, I received my Ph.D. from the University of Pavia, Italy in Biochemistry. From 1991 to 1992, I served a professional apprenticeship at the Ospedale San Raffaele in Milan, Italy, where I carried out research in the Laboratory of AIDS-Immunopathogenesis. From 1992 to 1993, I was a guest researcher at the National Institute of Allergy and Infectious Disease in Bethesda, Maryland, where I carried out research in the Laboratory of Molecular Microbiology. From 1993 to 1996, I was a Special Volunteer-Fogarty Visiting Fellow at the National Heart, Lung, Blood Institute in Bethesda, Maryland, where I carried out research in the Laboratory of Molecular Immunology. From 1997 to 1999, I was a Postdoctoral Fellow at the DNAX Research Institute in Palo Alto, California, where I carried out research in the Department

of Cell Signaling. Since 1999 I have been employed by HGS, where my research has included both directly carrying out and supervising the discovery, recombinant expression, isolation, and biochemical and biological characterization of human therapeutic proteins. I have co-authored over twenty articles that have been published in peer-reviewed scientific journals. A copy of my curriculum vitae is attached hereto as Exhibit A.

2. I have been shown and have examined U.S. Patent Application No. 09/333,966 (the '966 Application), captioned above, which I understand was filed on June 16, 1999. I will refer to the '966 Application as "the Application."

3. I am the first named author of the publication entitled "TL1A Is a TNF-like Ligand for DR3 and TR6/DcR3 and Functions as a T Cell Costimulator" which was published in the peer-reviewed scientific journal Immunity in March 2002 (Immunity, Vol. 16, 479-492). I will refer to this publication as "the Migone paper." A copy of the Migone paper is attached hereto as Exhibit B.

4. I am familiar with the publication entitled "DR3 Regulates Negative Selection during Thymocyte Development" authored by Eddie Wang et al., which was published in the peer-reviewed scientific journal Molecular and Cellular Biology in May 2001 (Mol. Cell. Biol., Vol. 21, 3451-3461). I will refer to this publication as "the Wang paper." A copy of the Wang paper is attached hereto as Exhibit C.

5. I am familiar with the publication entitled "Signal Transduction by DR3, a Death Domain-Containing Receptor Related to TNFR-1 and CD95" authored by Arul Chinnaiyan et al., which was published in the peer-reviewed scientific journal Science in

November 1996 (Science, Vol. 274, 990-992). I will refer to this publication as "the Chinnaiyan paper." A copy of the Chinnaiyan paper is attached hereto as Exhibit D.

6. I am familiar with the publication entitled "A New Death Receptor 3 Isoform: Expression in Human Lymphoid Cell Lines and Non-Hodgkin's Lymphomas" authored by Krzysztof Warzocha et al., which was published in the peer-reviewed scientific journal Biochemical and Biophysical Research Communications in 1998 (Biochem. Biophys. Res. Comm., Vol. 242, 376-379). I will refer to this publication as "the Warzocha paper." A copy of the Warzocha paper is attached hereto as Exhibit E.

7. I have been asked by patent counsel for HGS to provide my understanding of the correlation between: (a) the characterization of the DR3 molecule as indicated in the Application and the Migone, Wang, Chinnaiyan and Warzocha papers; and (b) the usefulness of the DR3 molecule as disclosed in the Application.

CELLULAR RESPONSES TO DR3 ACTIVATION

8. The Application discloses that DR3 is a TNFR family member containing a death domain and describes the role DR3 plays in mediating intracellular signaling which can lead to various cellular responses including, for example, apoptosis and cell proliferation. *See e.g.*, the Application at Page 5, line 15 through Page 6, line 27; at Page 29, lines 9-16; at Page 39, lines 3-11; and at Page 41, lines 11-13 and lines 21-25.

9. Prior to March 12, 1996 it was known that signaling through TNFR-1 and Fas, the two characterized TNFR family members known to have death domains, can cause both apoptosis and NF-κB activation, with the cell's commitment to either pathway

being determined by the intracellular balance between divergent signaling pathways. *See e.g.*, Hsu, H. et al. (1996). "TRADD-TRAF2 and TRADD-FADD interactions define two distinct TNF receptor 1 signal transduction pathways." Cell 84(2), 299-308, published January 26, 1996. A copy of the Hsu paper is attached hereto as Exhibit F.

10. Prior to March 12, 1996 it was known that activation of NF-κB is responsible for a variety of immune cell responses, including cell proliferation. *See e.g.*, Snapper, C. M. et al. (1996). "B Cells from p50/NF-κB Knockout Mice Have Selective Defects in Proliferation, Differentiation, Germ-Line CH Transcription, and Ig Class Switching." J. Immunol. 156, 183-191, published January 1, 1996. A copy of the Snapper paper is attached hereto as Exhibit G.

11. Accordingly, the assertion in the Application that signaling through DR3 may induce apoptosis and proliferation would have been credible to a scientist in the field of molecular biology in light of the state of knowledge in the art at the time of filing of the Application.

12. In Example 6 of the Application, overexpression of DR3 is shown to specifically induce apoptosis in MCF7 breast carcinoma cells. Overexpression of TNF receptor family polypeptides is an art accepted means of mimicking receptor activation in mammalian cell culture. *See e.g.*, Boldin, M. et al., (1995). "Self-association of the "death domains" of the p55 tumor necrosis factor (TNF) receptor and Fas/APO1 prompts signaling for TNF and Fas/APO1 effects." J. Biol. Chem. 270(1), 387-391, published January 6, 1995. A copy of the Boldin paper is attached hereto as Exhibit H. Therefore,

this data confirms the assertion of the Application, that DR3 activation can cause apoptosis in certain cellular environments.

13. In Example 6 of the Application, overexpression of DR3 is shown to specifically induce apoptosis and proliferation in 293 cells. *See*, the Application at Page 72, lines 23-25. Therefore, this data confirms the assertion of the Application, that DR3 activation can lead to an apoptotic response or a proliferative response depending upon the cellular environment.

14. The Migone paper demonstrates that: (a) recombinant DR3 specifically binds the TNF ligand TL1A and specifically induces activation of NF-κB when expressed in 293T cells; (b) endogenous DR3 specifically binds the TNF ligand TL1A and specifically induces activation of NF-κB in the erythroleukemic cell line TF-1 and also in activated T cells; (c) activation of endogenous DR3 by addition of TL1A in the presence of cycloheximide specifically induces caspase activity and apoptosis in the erythroleukemic cell line TF-1, but not in activated T cells; and (d) TL1A was more effective than FasL in inducing apoptosis of TF-1 cells under similar conditions.

15. The data and conclusions presented in the Migone paper are consistent with, and do not contradict, the function of DR3 disclosed in the Application. In its totality, the Migone paper supports the disclosure of the Application and confirms that the effects of DR3 activation are context specific and that DR3 can act to promote apoptosis in certain cellular environments.

16. The Wang paper describes the generation and characterization of mice that lack expression of the DR3 gene. The Wang paper identifies a non-redundant role for DR3

in the removal of self-reactive T cells in the thymus and in so doing identifies a physiological context in which DR3 is responsible for T cell apoptosis. The Wang paper does not exclude the likelihood of other redundant roles for DR3 in the regulation of T cell death.

17. The data and conclusions presented in the Wang paper are consistent with the function of DR3 disclosed in the Application. In its totality, the Wang paper confirms that DR3 does indeed mediate T cell apoptosis in at least one physiological circumstance.

18. The Chinnaiyan paper demonstrates that: (a) recombinant DR3 specifically binds the TRADD signaling molecule *in vitro* and when expressed in 293T cells; (b) recombinant DR3 can specifically activate NF-κB when expressed in 293 cells; (c) recombinant DR3 can specifically induce apoptosis when expressed in 293 cells; and (d) overexpression of recombinant DR3 specifically induces apoptosis in MCF7 breast carcinoma cells.

19. The data and conclusions presented in the Chinnaiyan paper are consistent with the function of DR3 disclosed in the Application. In its totality, the Chinnaiyan paper confirms that the effects of DR3 activation are context specific and that DR3 can act to promote apoptosis in certain cellular environments.

20. The experimental results presented in the Application, as well as those in the Migone, Wang and Chinnaiyan papers, support the functional role of DR3 as disclosed in the Application. These data, individually and in combination, confirm that DR3 can induce apoptosis under certain conditions and stimulate cell proliferation under other conditions.

TISSUE AND CELLULAR DISTRIBUTION OF DR3 EXPRESSION

21. From analysis of numerous experiments performed by myself or performed by other employees at HGS, it is my belief that:

(a) DR3 is expressed at very low levels in normal resting T cells; and

(b) DR3 is expressed at very low levels in normal B cells where it is sometimes undetectable.

22. The Warzocha paper shows that DR3 is "abundantly expressed" in a panel of pre-B acute lymphoblastic leukemia cell lines as well as in each of eleven distinct clinical isolates of follicular lymphoma. *See*, Page 377, lines 26-28 of the right column; and Figure 2. Therefore, Warzocha confirms that DR3 overexpression is useful as a diagnostic marker for certain lymphoid cancers such as acute lymphoblastic leukemia and follicular lymphoma.

23. The Application discloses that DR3 is expressed in lymphoid tissue and that increased expression of DR3 may be used to detect the presence of certain cancers including, for example, cancers of lymphoid tissue, such as follicular lymphoma. *See e.g.*, the Application at Page 5, lines 10-14; at Page 36, line 25 through Page 37, line 8; and at Page 38, lines 5-8; and at Page 38, lines 18-25.

24. In light of the observed expression profile of DR3, together with the experimental results presented in the Warzocha paper, one of ordinary skill in the art would find it credible that DR3 is useful as a diagnostic marker for certain cancers, as disclosed in the Application.

PHYSIOLOGICAL ROLES OF DR3

25. As declared above (*see*, statements 14 and 15), the Migone paper shows that DR3 can act to promote apoptosis under certain conditions. Furthermore, the Migone paper shows that: (a) DR3 activation of activated T cells *in vitro* via TL1A lead to increased IL-2 responsiveness and increased secretion of pro-inflammatory cytokines; (b) activation of DR3 promoted splenocyte alloactivation in an animal model of GVHD and in so doing increased the severity of the graft versus host response; and (c) a solubleTL1A-binding DR3 fusion protein can reduce TL1A stimulated apoptosis of TF1 cells in a dose-dependent manner.

26. The data and conclusions presented in the Migone paper confirm that: (a) regulation of DR3 activation would modulate the physiological response believed to underlie inflammation and inflammatory diseases such as GVHD; (b) regulation of DR3 activation would regulate the unfettered cellular proliferation that is believed to underlie the development of certain cancers; and (c) regulation of DR3 activation would modulate development of immune responses which are necessary to control viral infections and which underlie autoimmune diseases such as rheumatoid arthritis.

27. As declared above (*see*, statements 16 and 17), the Wang paper shows that DR3 does act to promote T cell apoptosis under certain physiological conditions. Furthermore, the Wang paper does not exclude the likelihood of other redundant roles for DR3 in the regulation of T cell death.

28. The data and conclusions presented in the Wang paper provide further confirmation that regulation of DR3 activation would modulate immune responses which

underlie inflammation and inflammatory diseases such as GVHD, control of viral infections and certain autoimmune diseases such as rheumatoid arthritis.

29. The Application asserts that DR3 polypeptides and antibodies are useful in the treatment of diseases such as cancers, including follicular lymphomas; inflammatory diseases, including Graft Versus Host Disease (GVHD); viral infections; and certain autoimmune disease such as rheumatoid arthritis. *See e.g.*, the Application at Page 6, lines 1-11; at Page 29, lines 9-17; at Page 38, lines 5-25; and at Page 46, line 20 through Page 47, line 3. It is my considered opinion that the Migone and Wang papers, together and individually, provide credible and compelling support for such uses of DR3 polypeptides and antibodies.

CONCLUSIONS

30. On reviewing the documents described above in their entireties, it is my considered opinion that: (a) the Application discloses functional characteristics of DR3 which were credible in light of the state of biological knowledge at the time the Application was filed; (b) the Application discloses functional characteristics of DR3 which have been corroborated by the work described in the Migone, Wang and Chinnaiyan papers; (c) the Application discloses that DR3 overexpression may be diagnostic for certain cancers, the credibility of this assertion is corroborated by the expression pattern of DR3 and the data reported in the Warzocha paper; and (d) the Application asserts that DR3 is useful in the treatment of certain cancers and inflammatory disorders, the credibility of this assertion is corroborated by the functional characterization of DR3 provided in the Application and the Migone and Wang papers.

31. I hereby declare that all statements made herein of my own knowledge are true and that all statements made on information and belief are believed to be true; and further that these statements were made with the knowledge that willful false statements and the like so made are punishable by fine or imprisonment, or both, under § 1001 of Title 18 of the United States Code, and that such willful false statements may jeopardize the validity of the application captioned above or any patent issuing thereupon.

Date: 18 OCT 2002

Thi-Sau Migone Ph.D.

CURRICULUM VITAE

Thi-Sau Migone

Nationality: Italian

Marital status: married, two children

2001-date	Senior Scientist Department of Pre-clinical Development, Immunology Section, Human Genome Sciences, Inc. 9410 Key West Avenue, Rockville MD, 20850
1999-2001	Scientist Department of Cell Biology, Human Genome Sciences, Inc. 9410 Key West Avenue, Rockville MD, 20850

PROFESSIONAL TRAINING:

1997-1999	Post-doctoral fellow, Advisor: James A. Johnston, Ph.D Department of Cell Signaling, DNAX Research Institute, Palo Alto CA, 94304
1993-1996	Special Volunteer-Fogarty Visiting fellow, Laboratory of Molecular Immunology Chief: Warren J. Leonard, M.D. National Heart, Lung, Blood Institute, National Institutes of Health, Bethesda, MD, 20892
1992-1993	Guest Researcher, Laboratory of Molecular Microbiology Chief: Malcolm A. Martin, M.D. National Institute of Allergy and Infectious Diseases, National Institutes of Health, Bethesda, MD, 20892

EDUCATION:

1991-1992	Professional apprenticeship Laboratory of AIDS-Immunopathogenesis Chief: Professor Adriano Lazzarin Ospedale San Raffaele, Milan, Italy
1991	Doctoral Degree in Biological Sciences (cum laude) Laboratory of Macromolecular Biochemistry Department of Biochemistry, University of Pavia, Italy Thesis:" Role of the oxidation state of methionine residues in membrane proteins in erythrocytes".

FELLOWSHIPS:

1993-1995	Fellowship for AIDS-related research Istituto Superiore di Sanita', Rome, Italy
1995-1996	Fogarty Visiting Fellowship, National Institutes of Health, Bethesda, MD 20892

PUBLICATIONS

Roschke V, Sosnovtseva S, Ward CD, Hong JS, Smith R, Albert V, Stohl W, Baker KP, Ullrich S, Nardelli B, Hilbert DM, **Migone TS**
BLyS and APRIL form biologically active heterotrimers that are expressed in patients with systemic immune-based rheumatic diseases.
J. Immunol. (2002) 169: 4314-4321

Migone TS*, Zhang J*, Luo X, Zhuang Li, Chen C, Hu B, Hong JS , Perry JW, Chen SF, Zhou JXH, Cho YH, Ullrich S, Kanakaraj P, Carrell J, Boyd E, Olsen H, Hu G, Pukac L, Ding L, Ni J, Kim S, Gentz R, Feng P, Moore PA, Ruben SM and Wei P (* The authors contributed equally to this article)
TL1A is a Novel Ligand for DR3 and TR6/DcR3 and Functions as a T cell Costimulator
Immunity 2002, 16 (3), 479-492

Migone TS, Humbert M, Rascle A, Sanden D, D'Andrea A., Johnston JA
The Deubiquitinating enzyme UB-2 prolongs cytokine-induced STAT activation and suppresses apoptosis induced by cytokine withdrawal.
Blood 2001, 98(6), 1935-41.

Kankaraj P, **Migone TS**, Nardelli B, Ullrich S, Li Y, Olden HS, Salcedo TW, Kaufman T, Cochrane E, Gan Y, Hilbert DM, Giri JG
BlyS binds to B cells with high affinity and induces activation of the transcription factors NF-kB and ELF-1.
Cytokine 2001, 13 (1); 25-31

Nardelli B., Belvedere O, Roschke V, Moore PA, Olsen HS, **Migone TS**, Sosonovtseva S, Carrell JA, Feng P, Giri JG, Hilbert DM.
Synthesis and release of B-lymphocyte stimulator from myeloid cells.
Blood 2001 97 (1):198-204

Wu Y, Bressette D, Carrell JA, Kaufman T, Feng P, Taylor K, Gan Y, Cho YH, Garcia AD, Gollatz E, Dimke D, LaFleur D, **Migone TS**, Nardelli B, Wei P, Ruben SM, Ullrich SJ, Olsen HS, Kanakaraj P, Moore PA, Baker KP.
Tumor Necrosis Factor Receptor Superfamily Member TACI is a High Affinity Receptor for TNF Family Members APRIL and BLyS.
J Biol Chem. 2000 275 (45):35478-85

Aman MJ*, **Migone TS***, Sasaki A, Ascherman DP, Zhu M, Soldaini E, Imada K, Miyajima A, Yoshimura A, Leonard WJ. (* The authors contributed equally to this article)
CIS associates with the interleukin-2 receptor beta chain and inhibits interleukin-2-dependent signaling.
J Biol Chem. 1999 Oct 15;274(42):30266-72.

Cohney SJ, Sanden D, Cacalano NA, Yoshimura A, Mui A, **Migone TS,** Johnston JA.
SOCS-3 is tyrosine phosphorylated in response to interleukin-2 and suppresses STAT5 phosphorylation and lymphocyte proliferation.
Mol Cell Biol. 1999 Jul;19(7):4980-8.

Cacalano NA, **Migone TS**, Bazan F, Hanson EP, Chen M, Candotti F, O'Shea JJ, Johnston JA.
Autosomal SCID caused by a point mutation in the N-terminus of Jak3: mapping of the Jak3-receptor interaction domain.
EMBO J. 1999 Mar 15;18(6):1549-58.

Migone TS, Rodig S, Cacalano NA, Berg M, Schreiber RD, Leonard WJ.
Functional cooperation of the interleukin-2 receptor beta chain and Jak1 in phosphatidylinositol 3-kinase recruitment and phosphorylation.
Mol Cell Biol. 1998 Nov;18(11):6416-22.

Migone TS, Cacalano NA, Taylor N, Yi T, Waldmann TA, Johnston JA.
Recruitment of SH2-containing protein tyrosine phosphatase SHP-1 to the interleukin 2 receptor; loss of SHP-1 expression in human T-lymphotropic virus type I-transformed T cells.
Proc Natl Acad Sci U S A. 1998 Mar 31;95(7):3845-50.

Mulloy JC, **Migone TS**, Ross TM, Ton N, Green PL, Leonard WJ, Franchini G.
Human and simian T-cell leukemia viruses type 2 (HTLV-2 and STLV-2(pan-p)) transform T cells independently of Jak/STAT activation.
J Virol. 1998 May;72(5):4408-12.

Takemoto S, Mulloy JC, Cereseto A, **Migone TS**, Patel BK, Matsuoka M, Yamaguchi K, Takatsuki K, Kamihira S, White JD, Leonard WJ, Waldmann T, Franchini G.
Proliferation of adult T cell leukemia/lymphoma cells is associated with the constitutive activation of JAK/STAT proteins.
Proc Natl Acad Sci U S A. 1997 Dec 9;94(25):13897-902

Ascherman DP, **Migone TS,** Friedmann MC, Leonard WJ.
Interleukin-2 (IL-2)-mediated induction of the IL-2 receptor alpha chain gene. Critical role of two functionally redundant tyrosine residues in the IL-2 receptor beta chain cytoplasmic domain and suggestion that these residues mediate more than Stat5 activation.
J Biol Chem. 1997 Mar 28;272(13):8704-9.

Hilbert DM, **Migone TS**, Kopf M, Leonard WJ, Rudikoff S.
Distinct tumorigenic potential of abl and raf in B cell neoplasia: abl activates the IL-6 signaling pathway.
Immunity. 1996 Jul;5(1):81-9.

Friedmann MC, **Migone TS**, Russell SM, Leonard WJ.
Different interleukin 2 receptor beta-chain tyrosines couple to at least two signaling pathways and synergistically mediate interleukin 2-induced proliferation.
Proc Natl Acad Sci U S A. 1996 Mar 5;93(5):2077-82.

Russell SM, Tayebi N, Nakajima H, Riedy MC, Roberts JL, Aman MJ, **Migone TS**, Noguchi M, Markert ML, Buckley RH, et al.
Mutation of Jak3 in a patient with SCID: essential role of Jak3 in lymphoid development.
Science. 1995 Nov 3;270(5237):797-800.

Migone TS, Lin JX, Cereseto A, Mulloy JC, O'Shea JJ, Franchini G, Leonard WJ.
Constitutively activated Jak-STAT pathway in T cells transformed with HTLV-I.
Science. 1995 Jul 7;269(5220):79-81.

Lin JX, **Migone TS**, Tsang M, Friedmann M, Weatherbee JA, Zhou L, Yamauchi A, Bloom ET, Mietz J, John S, et al.
The role of shared receptor motifs and common Stat proteins in the generation of cytokine pleiotropy and redundancy by IL-2, IL-4, IL-7, IL-13, and IL-15.
Immunity. 1995 Apr;2(4):331-9.

Vicenzi E, Dimitrov DS, Engelman A, **Migone TS**, Purcell DF, Leonard J, Englund G, Martin MA.
An integration-defective U5 deletion mutant of human immunodeficiency virus type 1 reverts by eliminating additional long terminal repeat sequences.
J Virol. 1994 Dec;68(12):7879-90.

Morsica G, Panese S, Novati R, **Migone TS**, Barin P, Mustara D, Frigato A, Lazzarin A.
Hepatitis C virus infection in blood donors with indeterminate results in second-generation recombinant immunoblot assay.
Transfusion. 1994 Jun;34(6):555-6..

Gianotti N, Finazzi R, Uberti Foppa C, Danise A, **Migone TS**, Lazzarin A.
The thymic hormones in the treatment of immune deficiency related to HIV infection.
Pharmacol Res. 1992 Sep;26 Suppl 2:62-3.

Immunity, Vol. 16, 479–492, Mar.

TL1A Is a TNF-like Ligand for DR3 and TR6/DcR3 and Functions as a T Cell Costimulator

Thi-Sau Migone,[2] Jun Zhang,[2] Xia Luo, Li Zhuang, Cecil Chen, Bugen Hu, June S. Hong, James W. Perry, Su-Fang Chen, Joe X.H. Zhou, Yun Hee Cho, Stephen Ullrich, Palanisamy Kanakaraj, Jeffrey Carrell, Ernest Boyd, Henrik S. Olsen, Gang Hu, Laurie Pukac, Ding Liu, Jian Ni, Sunghee Kim, Reiner Gentz, Ping Feng, Paul A. Moore, Steve M. Ruben, and Ping Wei[1]
Human Genome Sciences, Inc.
Rockville, Maryland 20850

Summary

DR3 is a death domain-containing receptor that is upregulated during T cell activation and whose overexpression induces apoptosis and NF-κB activation in cell lines. Here we show that an endothelial cell-derived TNF-like factor, TL1A, is a ligand for DR3 and decoy receptor TR6/DcR3 and that its expression is inducible by TNF and IL-1α. TL1A induces NF-κB activation and apoptosis in DR3-expressing cell lines, while TR6-Fc protein antagonizes these signaling events. Interestingly, in T cells, TL1A acts as a costimulator that increases IL-2 responsiveness and secretion of proinflammatory cytokines both in vitro and in vivo. Our data suggest that interaction of TL1A with DR3 promotes T cell expansion during an immune response, whereas TR6 has an opposing effect.

Introduction

Members of the TNF and TNFR superfamilies of proteins are involved in the regulation of many important biological processes, including development, organogenesis, and innate and adaptive immunity (Locksley et al., 2001). Interaction of TNF ligands such as TNF, Fas, LIGHT, and BLyS with their cognate receptor (or receptors) has been shown to affect immune responses, as they are able to activate signaling pathways that link them to the regulation of inflammation, apoptosis, homeostasis, host defense, and autoimmunity. The TNFR superfamily can be divided into two groups based on the presence of different domains in the intracellular portion of the receptor. One group contains a TRAF binding domain that enables it to couple to TRAFs (TNFR-associated factors); these, in turn, activate a signaling cascade that results in the activation of NF-κB and initiation of transcription. The second group of receptors is characterized by a 60 aa globular structure named death domain (DD). Historically, death domain-containing receptors have been described as inducers of apoptosis via the activation of caspases. These receptors include TNFR1, DR3, DR4, DR5, DR6, and Fas. More recent evidence (Siegel et al., 2000 and references within) has shown that some members of this subgroup of receptors, such as Fas, also have the ability to positively affect T cell activation. A third group of receptors has also been described. The members of this group, which include DcR1, DcR2, OPG, and TR6 (also called DcR3), have been named decoy receptors, as they lack a cytoplasmic domain and may act as inhibitors by competing with the signal-transducing receptor for the ligand (Ashkenazi and Dixit, 1999). TR6, which exhibits closest homology to OPG, associates with high affinity to FasL and LIGHT and inhibits FasL-induced apoptosis both in vitro and in vivo (Pitti et al., 1998; Yu et al., 1999; Connolly et al., 2001). Its role in downregulating immune responses was strongly suggested by the observation that TR6 suppresses T cell responses against alloantigen (Zhang et al., 2001) and certain tumors overexpress TR6 (Pitti et al., 1998; Bai et al., 2000).

DR3 is a DD-containing receptor that shows highest homology to TNFR1 (Chinnaiyan et al., 1996; Kitson et al., 1996; Marsters et al., 1996; Bodmer et al., 1997; Screaton et al., 1997; Tan et al., 1997). In contrast to TNFR1, which is ubiquitously expressed, DR3 appears to be preferentially expressed by lymphocytes and is efficiently induced following T cell activation. TWEAK/Apo3L was previously shown to bind DR3 in vitro (Marsters et al., 1998). However, more recent work raised doubt about this interaction and showed that TWEAK functions through a TNFR, TweakR, and is able to induce NF-κB and caspase activation in cells lacking DR3 (Schneider et al., 1999; Kaptein et al., 2000; Wiley et al., 2001).

In this paper, we describe the identification and characterization of a ligand, which we have named TL1A, for both DR3 and TR6/DcR3. TL1A is a longer variant of TL1 (also called VEGI), which was previously identified as an endothelium-derived factor that inhibited endothelial cell growth in vitro and tumor progression in vivo (Tan et al., 1997; Zhai et al., 1999a, 1999b; Yue et al., 1999). We found that TL1A is the full-length gene product and is markedly upregulated by TNF and IL-1α. We show that interaction between TL1A and DR3 in a reconstituted system or in cells that naturally express DR3 results in activation of NF-κB and apoptosis. TR6 is able to inhibit these activities by competing with DR3 for TL1A. More importantly, we have found that in vitro, TL1A functions specifically on activated T cells to promote survival and secretion of proinflammatory cytokines, and in vivo, it potently enhances acute graft-versus-host reactions.

Results

TL1A Is a Longer Variant of TL1 (VEGI) and a Member of the TNF Ligand Superfamily

To identify TNF-like molecules, a database of over three million human expressed sequence tag (EST) sequences was analyzed using the BLAST algorithm. Several EST clones with high homology to TNF-like molecule 1, TL1 (or VEGI), were identified from endothelial cell cDNA

[1]Correspondence: ping_wei@hgsi.com
[2]These authors contributed equally to this work.

libraries. Sequence analysis of these cDNA clones revealed a 2.02 kb insert encoding an open reading frame of 251 aa. The predicted protein lacks an N-terminal signal peptide but contains a hydrophobic transmembrane region near the 5′ end and a carboxyl domain that shows highest sequence identity to TNF (24.6%), followed by FasL (22.9%) and LTα (22.2%). Interestingly, the C-terminal 151 aa of this protein (aa 101–251) and that of TL1 (aa 24–174) are identical, whereas the N-terminal regions share no sequence similarity (Figure 1A). To distinguish it from TL1, we have named it TL1A. The cloned mouse and rat TL1A cDNAs encode proteins of 252 aa and share 63.7% and 66.1% sequence homology to the human counterpart, respectively (Figure 1A). The presence of in-frame upstream stop codons in human, mouse, and rat cDNA clones indicated that these open reading frames are full length.

The 2.02 kb TL1A cDNA was blasted against the public human genome databases (www.ncbi.nlm.nih.gov/genome/guide/human; www.ensembl.org) and was mapped, as TL1 originally was, to chromosome 9q32 (Figure 1B). Detailed sequence alignment revealed that TL1A is encoded by four coding exons (shaded boxes) utilizing consensus splicing sites, while TL1 is encoded by a continuous DNA containing the exon 4 and its 5′ adjacent intron region (open box). As a result, TL1 lacks a transmembrane domain and the first conserved β strand seen in other TNF family of ligands. To our surprise, we found that the 3.3 kb TL1 cDNA matches completely a TL1A genomic DNA region of the same length that contains both the introns and exons (3 and 4) of TL1A (Figure 1B).

Like most TNF ligands, TL1A exists as a membrane bound protein (Figure 3A, fourth panel) and can also be processed into a soluble form when ectopically expressed (data not shown). The N-terminal sequence of soluble TL1A protein purified from full-length TL1A-transfected 293T cells was determined to be Leu72 (Figure 1A).

TL1A Is Predominantly Expressed by Endothelial Cells, Is More Abundant than TL1/VEGI, and Is Inducible by TNF and IL-1α

The expression pattern of TL1A mRNA was studied using quantitative real-time polymerase chain reaction (TaqMan) and reverse transcriptase polymerase chain reaction (RT-PCR) (see Experimental Procedures). We found that TL1A was expressed predominantly by human endothelial cells, including the umbilical vein endothelial cells (HUVEC), the adult dermal microvascular endothelial cells (HMVEC-Ad), and uterus myometrial endothelial cells (UtMEC-Myo), with highest expression seen in HUVEC (Figure 2A). An ~750 bp DNA fragment was readily amplified from these endothelial cells by RT-PCR, indicating the presence of full-length TL1A transcripts (Figure 2B). Very little expression was seen in human aortic endothelial cells (HAEC) or other human primary cells including adult fibroblasts (NHDF-Ad and HFL-1), aortic smooth muscle cells (AoSMC), skeletal muscle cells (SkMC), adult keratinocytes (NHEK-Ad), tonsillar B cells, T cells, NK cells, monocytes, or dendritic cells. In human tissues, TL1A mRNA was detected in kidney, prostate, placenta, and stomach, and low levels were seen in intestine, lung, spleen, and thymus. Very little if any was detected in heart, brain, liver, PBL, or adrenal gland (Figure 2A and data not shown). We did not detect significant levels of TL1A mRNA in any of the cancer cell lines tested, including 293T, HeLa, Jurkat, Molt4, Raji, IM9, U937, Caco-2, SK-N-MC, HepG2, KS4-1, and GH4C (data not shown).

Although the reported mRNA expression profile of TL1, detected by Northern hybridization (Tan et al., 1997; Zhai et al., 1999a), is very similar to that of TL1A, the Northern probes used for those analyses were derived from the shared region of TL1A and TL1 and therefore may have detected the total level of expression of the two RNA. To analyze the relative abundance of the two RNA species, we used TL1A and TL1-specific primers and fluorescent probes for conventional and quantitative RT-PCR. As shown in Figures 2B and 2C, both methods yielded a similar result: that TL1A mRNA is the more abundant form. The amount of TL1A-specific mRNA is at least 15-fold higher than that of TL1. Since TL1A is the predominant species of the two RNA and also appears to be the full-length form, we have focused our study on this form.

To determine if TL1A mRNA levels were inducible, HUVEC cells were stimulated with TNF, IL-1α, PMA, bFGF, or IFNγ. As shown in Figure 2D, PMA and IL-1α rapidly induced high levels of TL1A mRNA, with a peak in expression reached at 6 hr after treatment. TNF was also able to induce TL1A mRNA, and a weak stimulation by bFGF could be seen at the 6 hr time point. In contrast, IFNγ may have a negative effect on TL1A expression.

Identification of DR3 and TR6 as Receptors for TL1A

To identify the receptor for TL1A, we generated a 293F stable cell line expressing full-length TL1A on the cell surface (Figure 3A, fourth panel). These cells were used to screen the Fc-fusion form of the extracellular domain of TNFR family members, including TNFR1, Fas, HveA, DR3, DR4, DR5, DR6, DcR1, DcR2, TR6, OPG, RANK, AITR, TACI, CD40, and OX40. As shown in Figure 3A, DR3-Fc and TR6-Fc bound efficiently to cells expressing TL1A (second and third panels) but not to vector control transfected cells (first panel). In contrast, HveA-Fc (second panel) and all the other receptors tested (data not shown) did not bind to the TL1A-expressing cells. We then tested whether TR6 could compete with DR3 for TL1A binding. When a 2:1 molar ratio of a nontagged form of TR6 and DR3-Fc was used, no binding of DR3-Fc was detected on TL1A-expressing cells (third panel). These results demonstrated that both DR3 and TR6 can bind to the membrane bound form of the TL1A protein.

To determine whether TL1A protein could bind to the membrane bound form of DR3, a Flag-tagged soluble form of the TL1A (aa 72–251) protein was tested on cells transiently transfected with different members of the TNFR family, including TNFR2, LTβR, 4-1BB, CD27, CD30, BCMA, DR3, DR4, DR5, DR6, DcR1, DcR2, RANK, HveA, and AITR. We consistently detected binding of Flag-TL1A but not Flag-TRAIL to cells expressing full-length or DD-deleted DR3 (Figure 3B and data not shown). No association was seen with DD-deleted DR5 or any of the other receptors tested, demonstrating that TL1A interacts specifically with membrane-associated DR3.

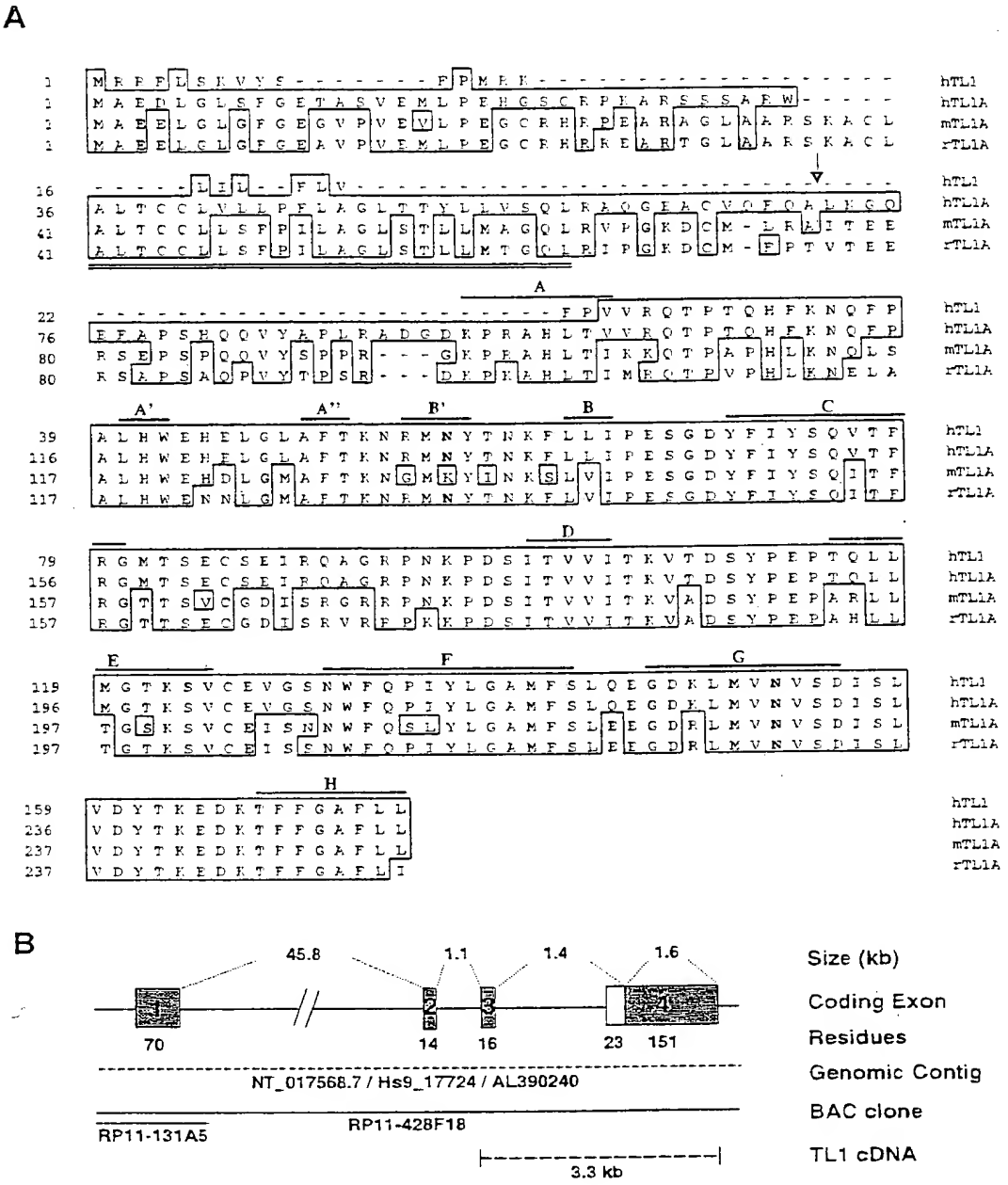

Figure 1. Sequence and Genomic Structure of TL1A

(A) Amino acid sequence alignment of TL1A from human (h), mouse (m), and rat (r), and human TL1. Identical aa are boxed. Dashes indicate gaps between regions of homology. The predicted transmembrane domain is underlined, and the potential N-linked glycosylation sites are in bold. Arrow represents the N-terminal cleavage site of soluble TL1A. Bars above sequences indicate the positions of β strand forming sequences (labeled A–H) according to the crystal structure of LTα (Eck et al., 1992). Alignments were generated using Megalign (Clustal Method, DNASTAR) software.

(B) Diagram of the TL1A genomic structure. Intron/exon sizes are shown above the DNA. The shaded boxes represent TL1A coding exons 1–4, and the open box depicts the intron region encoding the first 23 aa of TL1. The number of residues encoded by each exon, the genomic contigs, and BAC clones that contain the genomic DNA are shown. The 3.3 kb TL1 cDNA matches to the 3′ region of the genomic DNA is also shown.

Coimmunoprecipitation studies were also performed to confirm the specific interaction between the soluble forms of TL1A and the receptors. We found that DR3-Fc and TR6-Fc specifically interacted with Flag-TL1A (Figure 3C). In contrast, TACI-Fc or Fas-Fc could not immunoprecipitate Flag-TL1A but efficiently bound their

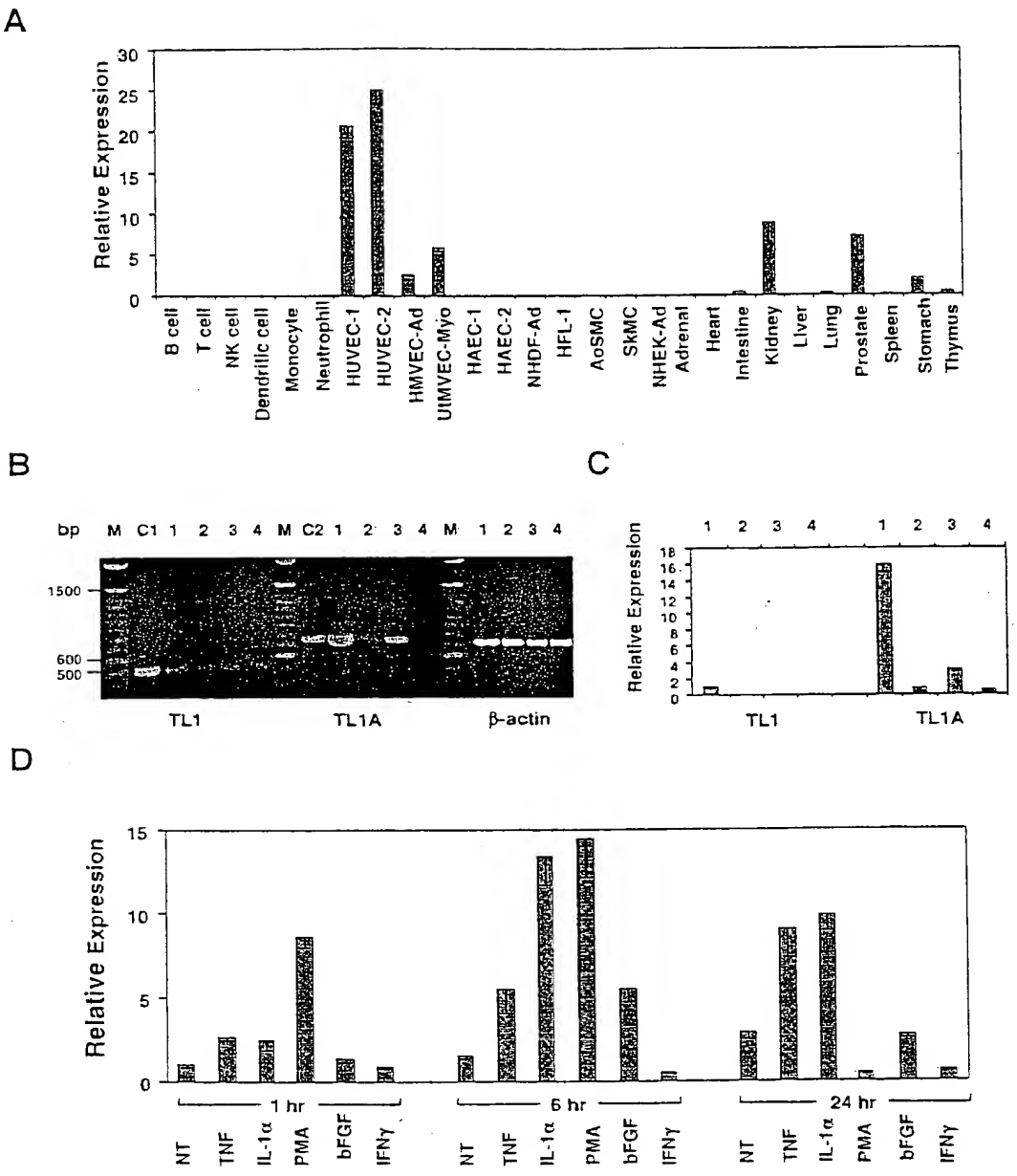

Figure 2. Expression Analysis of TL1A mRNA

(A) Taqman (quantitative real-time PCR) analysis of TL1A mRNA expression. TL1A-specific primer and fluorescence probe were used. All values were normalized to 18S ribosomal RNA internal control. Standard deviations were calculated from triplicate reactions. The relative level of expression was displayed in arbitrary units in which one is equivalent to 1×10^{-5} fraction of the 18S RNA amount.

(B) RT-PCR analysis of expression of TL1 and TL1A mRNA in endothelial cells. 0.5 micrograms of total RNA was amplified using gene-specific sense and antisense primers for TL1 (522 bp product) or TL1A (750 bp product). β-actin (600 bp product) was used as internal control. Lane 1, HUVEC; lane 2, HMVEC-Ad; lane 3, UtMVEC-Myo; lane 4, HAEC. TL1 cDNA (C1, 2 pg) and TL1A cDNA (C2, 2 pg) were used as positive controls. M, 100 bp DNA ladder.

(C) Taqman analysis of TL1 and TL1A mRNA expression in endothelial cells. TL1 or TL1A-specific primer and fluorescence probe were used and the data were derived from triplicate reactions and analyzed as in (A). Lane 1, HUVEC; lane 2, HMVEC-Ad; lane 3, UtMVEC-Myo; lane 4, HAEC. The amount of TL1 expression in HUVEC was set as 1.

(D) Inducible expression of TL1A mRNA in HUVEC cells. HUVEC were either untreated (NT) or treated with IL-1α (2 ng/ml), TNF (50 ng/ml), PMA (100 ng/ml), bFGF (50 ng/ml), or IFNγ (10 ng/ml) for 1, 6, or 24 hr. TL1A mRNA expression at each time point was analyzed as described in (A). TL1A level in untreated sample at 1 hr time point was set as 1.

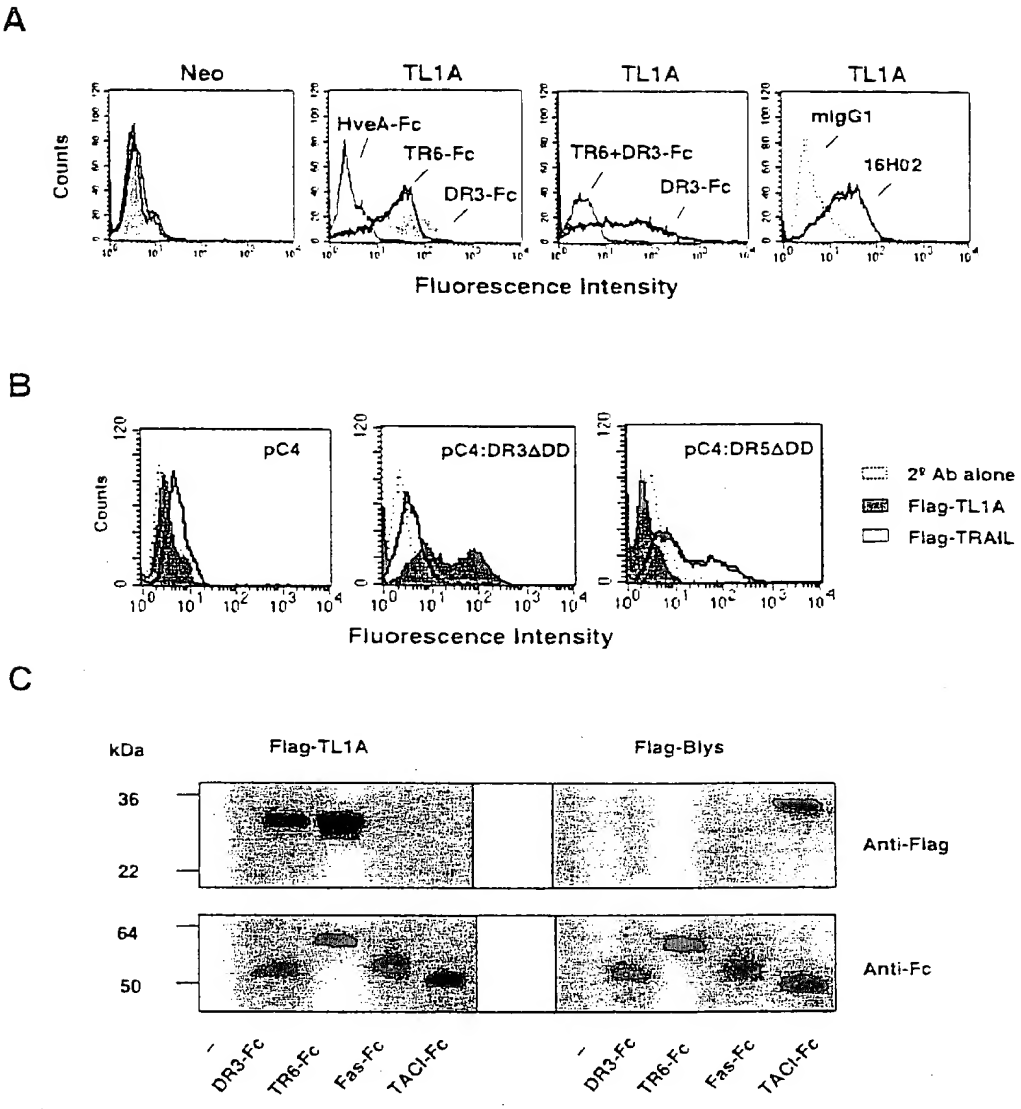

Figure 3. TL1A Interacts with DR3 and TR6/DcR3

(A) Flow cytometric analyses of TNFR-Fc binding to TL1A-expressing cells. 293F cells stably transfected with vector (Neo, first panel) or full-length TL1A (second and third panels) were incubated with DR3-Fc, TR6-Fc, or HveA-Fc (negative control) and stained with PE-conjugated goat anti-human IgG antibody. In the third panel, nontagged TR6, at a 2:1 molar ratio, was used together with DR3-Fc. In the fourth panel, TL1A cells were stained with TL1A monoclonal Ab 16H02 or a mouse isotype control Ab.

(B) Flow cytometric analyses of binding of Flag-TL1A (aa 72–251) protein to membrane-bound DR3 receptor. 293T cells were transiently transfected with either vector control (pC4), or DD-deleted mutant DR3 (pC4:DR3ΔDD) or DR5 (pC4:DR5ΔDD). Cells were stained 40 hr later with either secondary Ab alone (dashed line) or Flag-tagged protein (Flag-TL1A, filled histogram; Flag-TRAIL, dark line) followed by anti-Flag Ab.

(C) Coimmunoprecipitation of DR3-Fc and TR6-Fc with TL1A. Flag-tagged TL1A (aa 72–251) or BlyS (aa 134–285) protein was incubated with or without recombinant DR3-Fc, TR6-Fc, Fas-Fc, or TACI-Fc protein and precipitated with Protein A-agarose beads. The bound proteins were analyzed by Western blotting with anti-Flag M2 antibody (upper panel) or with anti-human Fc antibody (lower panel).

known ligands, Flag-BlyS (Figure 3B) and Flag-FasL (not shown), respectively.

To determine the binding affinity of solubleTL1A to DR3-Fc and TR6-Fc, we performed a BIAcore analysis using a nontagged TL1A (aa 72–251) protein purified from *E. coli*. The kinetics of TL1A binding to DR3-Fc was determined using three different batches of the TL1A protein. The K_A and K_D values were found to be 6.39E + 05 Ms^{-1} and 4.13E − 03M^{-1}, respectively. The average Kd value was 6.45 ± 0.2 nM. TL1A was also examined for its ability to bind to several other TNF-related receptors (HveA, BCMA, TACI, and TR6). Besides DR3, only TR6 was found to exhibit significant and specific binding to TL1A. The K_A and K_D values were 1.04E + 06 Ms^{-1} and 1.9E − 03 M^{-1}, respectively, which gives a Kd of 1.8 nM. The specificity of binding of TL1A

to DR3-Fc and TR6-Fc was confirmed by the competition of TL1A binding in the presence of excess soluble receptor-Fc (data not shown). These Kd values for binding of TL1A to DR3-Fc and TR6-Fc are comparable to those determined for other TNFR-ligand interactions.

Interaction of TL1A with DR3 Induces Activation of NF-κB

It was reported previously that ectopic expression of DR3 results in the activation of the transcription factor NF-κB (Chinnaiyan et al., 1996; Kitson et al., 1996; Marsters et al., 1996; Bodmer et al., 1997). We therefore decided to study TL1A-induced signaling in a reconstitution system in 293T cells in which DR3 and an NF-κB-SEAP reporter were introduced by transient transfection. To avoid spontaneous apoptosis or NF-κB activation caused by DR3 overexpression, we used a limited amount of DR3-expression DNA that by itself minimally activated these pathways (Figure 4A). Under these conditions, cotransfection of cDNA encoding full-length or the soluble form of TL1A resulted in significant NF-κB activation. This signaling event was dependent on the ectopic expression of DR3 and the presence of the DR3 death domain, as TL1A alone or in combination with a DD-deleted DR3 did not induce NF-κB activation in these cells. Interestingly, cotransfection of DR3 with cDNAs encoding TL1 (full-length or N-terminal 24 aa truncated) failed to induce NF-κB activation, suggesting that TL1A and TL1 may utilize distinct receptors and/or transduction pathways and the shared region between TL1A and TL1 is not sufficient to mediate NF-κB activation. A similar induction of NF-κB activity was observed when recombinant TL1A protein (aa 72–251, from *E. coli* or Flag-tagged from 293T cells) was added to DR3-expressing cells (Figure 4B and data not shown). This induction of NF-κB was completely inhibited by the addition of an excess amount of TR6-Fc and partially by the amount of DR3-Fc used but not by the addition of twice as much of TNFR1-Fc or Fas-Fc. These results demonstrated that TL1A is a signaling ligand for DR3 that induces NF-κB activation and that TR6 can specifically inhibit this event.

To study the signaling events mediated by TL1A on cells that naturally express DR3, we analyzed various cell lines for the expression of DR3 and found that the erythroleukemic cell line TF-1 expressed high levels of DR3 (data not shown). In addition, DR3 has been shown to be upregulated in activated T cells (Screaton et al., 1997; Tan et al., 1997). Therefore, we studied whether TL1A could induce NF-κB activation in TF-1 cells and in activated T cells. We analyzed the degradation of IκBα, the cytoplasmic inhibitor of NF-κB, and found that in both cell types TL1A rapidly induced the degradation of IκBα (Figure 4C) and that the TL1A-induced degradation of IκBα could be inhibited by increasing amounts of TR6-Fc. These results indicate that TL1A can activate NF-κB in cells expressing endogenous DR3.

TL1A Induces IL-2 Responsiveness and Cytokine Secretion from Activated T Cells

As DR3 expression is mostly restricted to lymphocytes and is upregulated upon T cell activation, we decided to study the biological activity of TL1A on T cells. Recombinant TL1A (aa 72–251) protein was tested for its ability to induce proliferation of resting or costimulated T cells (treated with amounts of anti-CD3 and anti-CD28 that are not sufficient to induce optimal proliferation). In resting (data not shown) or costimulated T cells, we did not observe a significant increase in proliferation over background (Figure 5A, compare the light bars of untreated versus TL1A-treated samples). Interestingly, cells that were previously treated with TL1A for 72 hr were able to proliferate better in response to IL-2 compared to T cells that had not been pretreated with TL1A (Figure 5A, compare the dark bars of untreated versus TL1A-treated samples), indicating that TL1A increases the IL-2 responsiveness of costimulated T cells.

As enhanced IL-2 responsiveness has been associated with increased IL-2 receptor expression and altered cytokine secretion, it was of interest to assess these responses on costimulated T cells treated with TL1A. As shown in Figure 5B, TL1A treatment increased the number of cells expressing IL-2Rα (CD25) and the level of IL-2Rβ (CD122) expression in these cells. We next measured cytokine secretion from these cells and found that both IFNγ and GMCSF (Figure 5C) were significantly induced, whereas IL-2, IL-4, IL-10, or TNF were not (data not shown). This effect was mostly dependent on anti-CD28, as treatment with anti-CD3 and TL1A, in the absence of the signal induced by crosslinking CD28, did not result in significant secretion of cytokines (Figure 5C). The effect that we observed on T cells was specifically mediated by TL1A, as addition of monoclonal neutralizing antibody to TL1A or addition of DR3-Fc or TR6-Fc proteins was able to inhibit TL1A-mediated IFNγ secretion (data not shown). TL1A was also tested on a variety of primary cells, including tonsil B cells, NK cells, monocytes, and endothelial cells, but no significant activity was detected (data not shown), suggesting a specific activity of TL1A on T cells.

TL1A Induces Caspase Activation in TF-1 Cells but Not in T Cells

It has been shown previously that overexpression of DR3 in cell lines induces apoptosis (Chinnaiyan et al., 1996; Kitson et al., 1996; Marsters et al., 1996; Bodmer et al., 1997). We then studied the effect of recombinant TL1A on caspase activation and apoptosis in DR3-containing cells: primary activated T cells and TF-1 cells. Activated T cells were incubated with recombinant TL1A or FasL in the presence of cycloheximide (CHX). No induction of caspase activity was detected in TL1A-treated T cells, but it was readily measured when cells were triggered with FasL (Figure 6A, left panel), suggesting that under these experimental conditions, TL1A does not activate caspases in T cells (the assay we used detects activation of caspases 2, 3, 6, 7, 8, 9, and 10). In TF-1 cells, in contrast to T cells, TL1A was able to induce caspase activation efficiently in the presence of CHX (Figure 6A, right panel). FasL was also able to induce caspase activation in this cell line, although less efficiently than TL1A. Both DR3-Fc and TR6-Fc but not a control Fc protein efficiently inhibited the TL1A-induced caspase activation in TF-1 cells (Figure 6B, left panel). A TL1A monoclonal antibody 16H02 was also shown to completely inhibit this activity (Figure 6B, right panel),

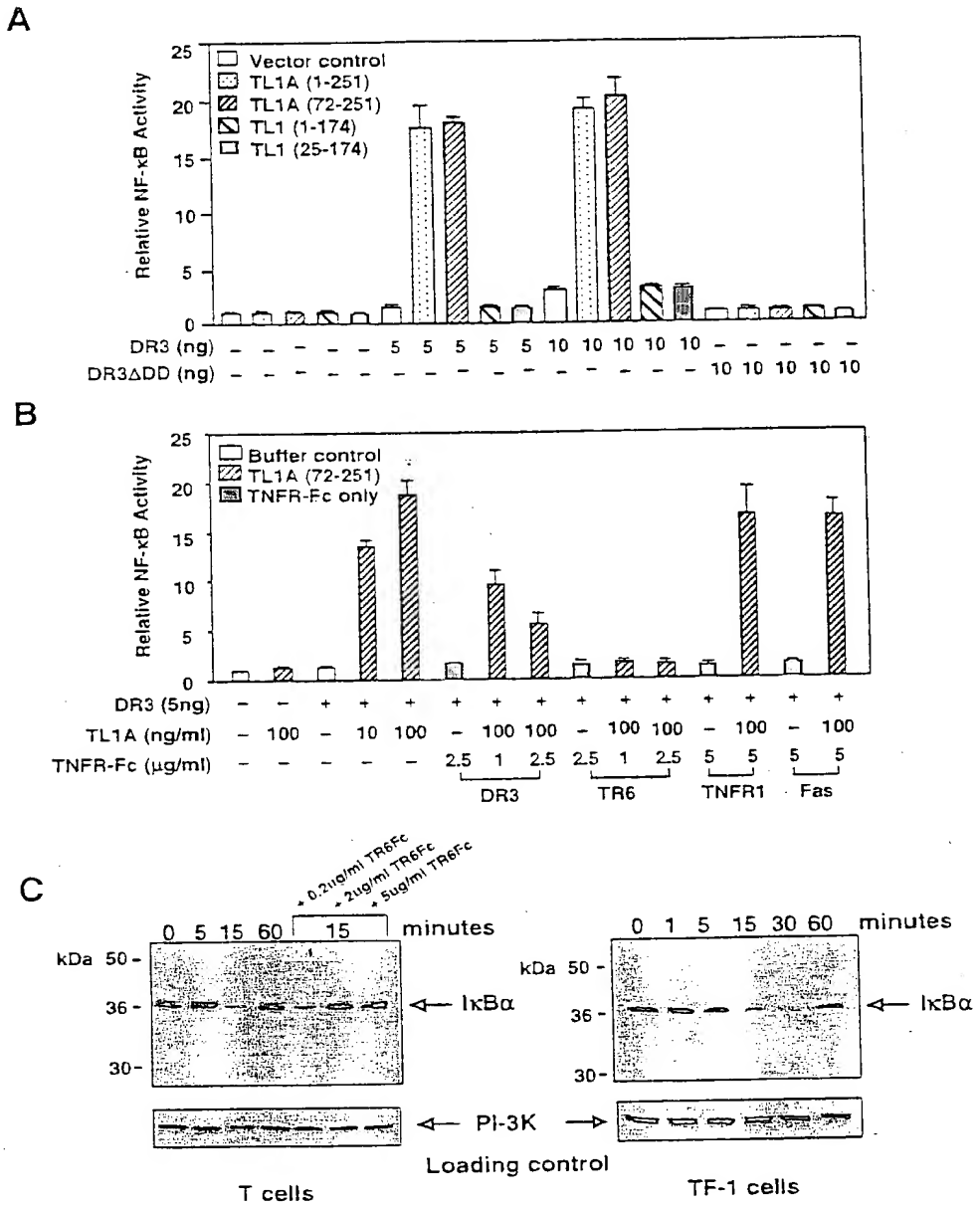

Figure 4. Interaction of DR3 and TL1A Induces NF-κB Activation

(A) 293T cells in 6-well plates were cotransfected with 4× NF-κB-SEAP reporter (0.1 μg), pCMV-lacZ reporter (internal control, 10 ng), pC4:DR3 (5 or 10 ng), or pC4:DR3ΔDD (10 ng). In addition to these constructs, the cells were cotransfected with the indicated forms of either TL1A or TL1 in pC4. SEAP activity was measured 20 hr later from the supernatant and normalized to β-galactosidase activity. Standard deviation was calculated from triplicate experiments.

(B) 293T cells were cotransfected with 4× NF-κB-SEAP reporter (0.1 μg), pCMV-lacZ reporter (10 ng), pC4, or pC4:DR3 (5 ng) for 5 hr. Cells were then treated with the indicated amounts of recombinant TL1A protein from *E. coli* in combination with the indicated amounts of DR3-Fc, TR6-Fc, TNFR1-Fc, or Fas-Fc. SEAP activity was measured and displayed as in (A).

(C) PHA-activated primary T cells (left panel) or TF-1 cells (right panel) were treated for the indicated time points with 100 ng/ml of TL1A in the presence or absence of the indicated amounts of TR6-Fc (left panel). Cell lysates were prepared and analyzed by Western blotting using a polyclonal antibody to IκBα. Equal loading was confirmed by reprobing with an anti-PI-3K polyclonal antibody.

confirming that the caspase activation was mediated by TL1A. No significant caspase activation was observed in the absence of CHX in either cell type (data not shown).

To confirm that the observed caspase activation following TL1A treatment correlated with induction of cell death, we analyzed both TF-1 cells and primary activated T cells by annexin V and propidium iodide staining. As shown in Figure 6C, significant apoptosis (annexin

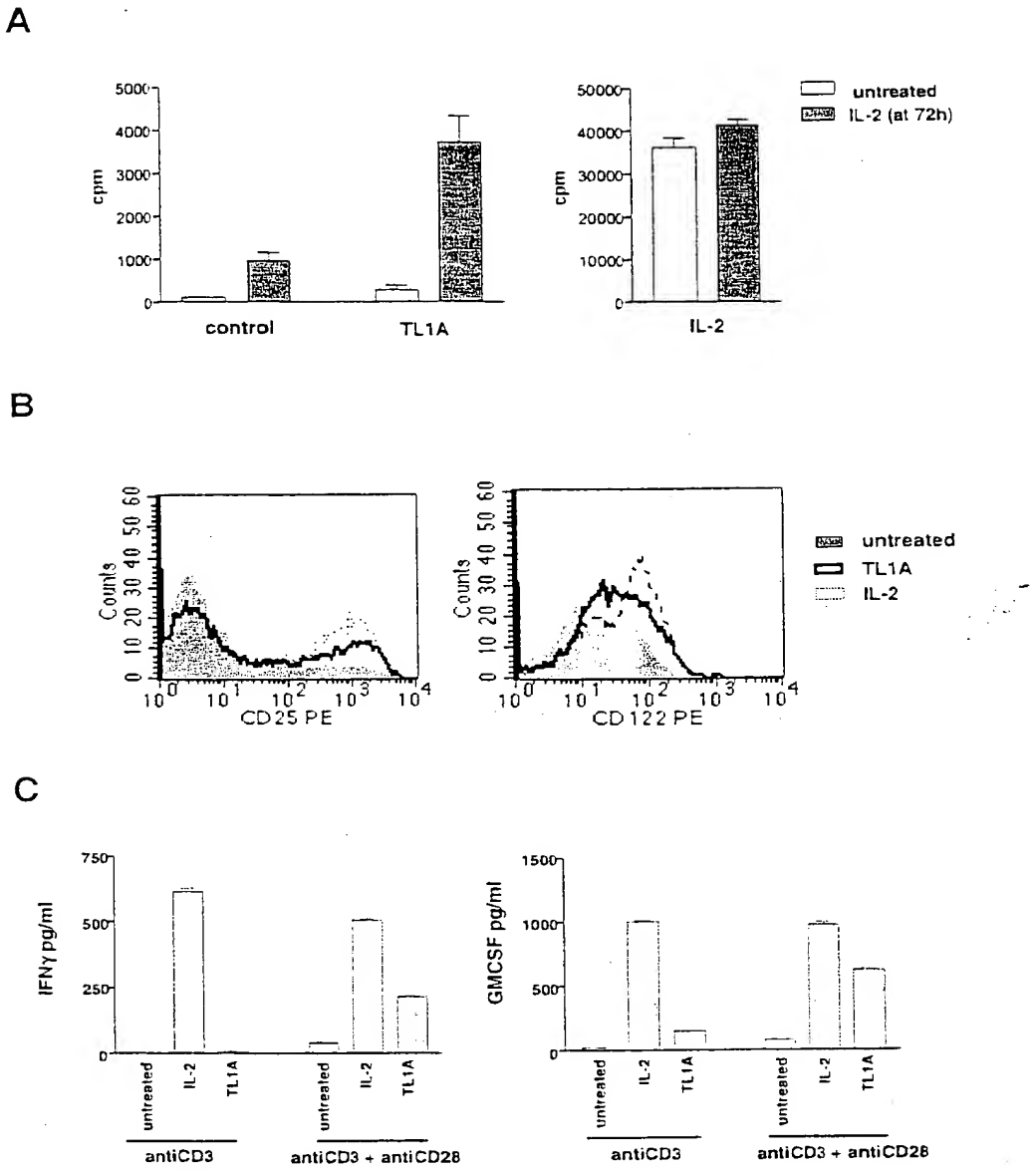

Figure 5. TL1A Increases IL-2 Responsiveness and Induces Cytokine Release in Anti-CD3- and Anti-CD28-Treated T Cells

Human T cells (1×10^5/ml) in plates coated with suboptimal levels of anti-CD3 (0.3 μg/ml) and anti-CD28 (5 μg/ml) were either untreated or treated with rhIL-2 (1 ng/ml) or TL1A (aa 72–251, 100 ng/ml) for 72 hr.

(A) Cells were then incubated with medium alone (RPMI) or with rhIL-2 (1 ng/ml) and pulsed with 0.5 μCi ^{3}H-thymidine for 24 hr to measure proliferation. Results are expressed as an average of triplicate reactions plus standard error.

(B) Cells were stained with PE-conjugated antibodies against IL-2Rα (CD25) and IL-2Rβ (CD122).

(C) Human T cells (1×10^5/ml) were seeded in 24-well plates that had been precoated with either anti-CD3 alone, or anti-CD3 and anti-CD28 as shown above. The cells were then treated with either rhIL-2 (5 ng/ml) or TL1A (100 ng/ml). Supernatants were collected after 3 days and analyzed for the presence of IFNγ and GMCSF by ELISA. Results are expressed as an average of triplicate reactions plus standard error.

V/PI positive cells, upper right quadrant of each panel) was seen only in TF-1 cells treated with TL1A and CHX (32.25%). No dramatic apoptosis occurred in T cells 24 hr post TL1A treatment in the presence or absence of CHX. These results are consistent with our measurement of caspase activation.

TL1A Promotes Splenocyte Alloactivation in Mice

To determine if the in vitro activities of TL1A could be reproduced in vivo, a mouse model of acute graft-versus-host-response (GVHR) was developed in which parental C57BL/6 splenocytes were injected intravenously into (BALB/c × C57 BL/6) F1 mice (CB6F1), and the

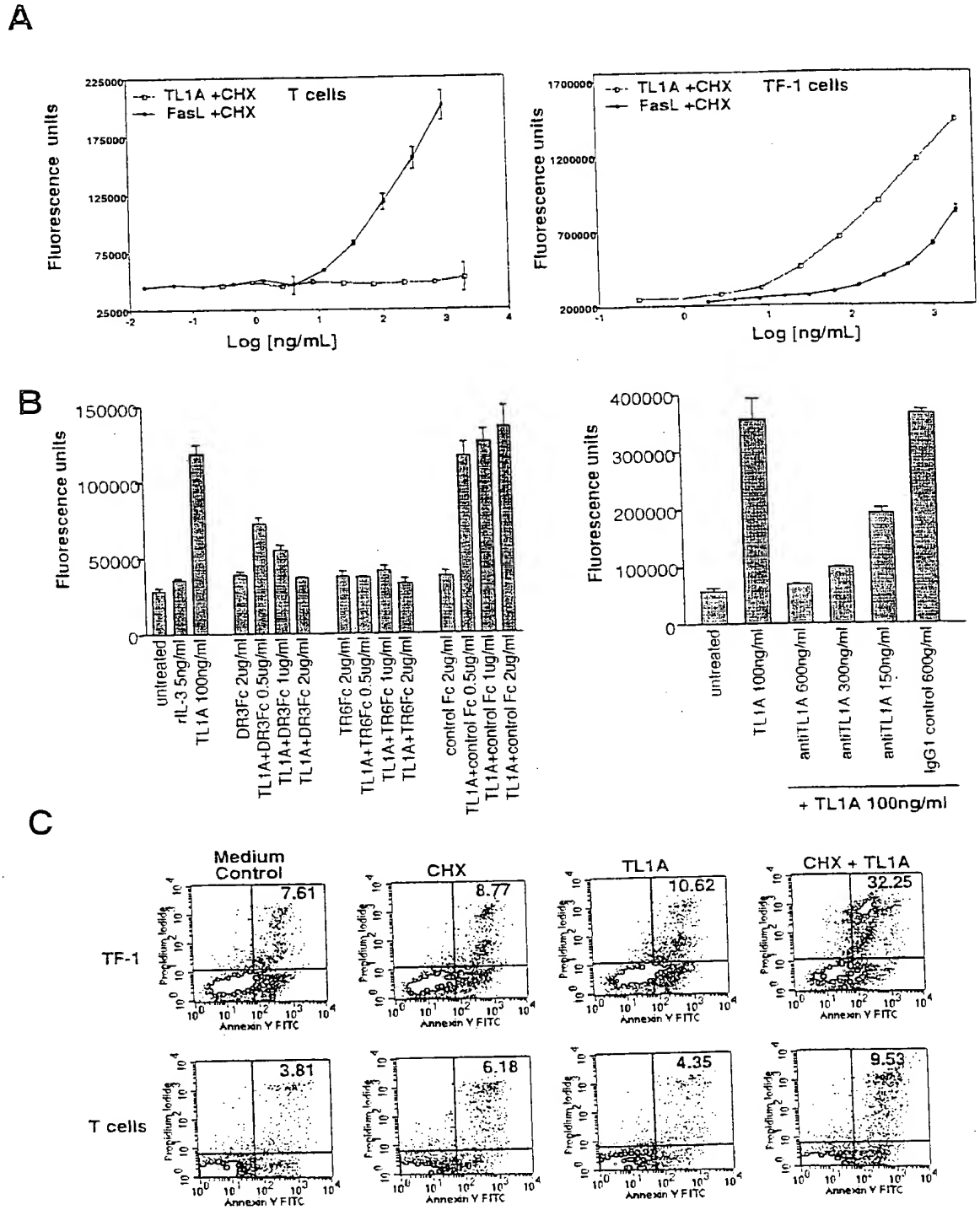

Figure 6. TL1A Induces Caspase Activation in the Erythroleukemic Line TF-1, but Not in Activated T Cells

(A) Activated T cells (left panel) or TF-1 cells were treated with increasing concentrations of recombinant FasL (aa 130–281) or TL1A (aa 72–251), 0.1 ng/ml–3 μg/ml, in the presence of cycloheximide (CHX, 10 μg/ml) for 6 hr. Caspase activity was measured as described in the Experimental Procedures.

(B) TF-1 cells (7.5×10^4/well) were treated with recombinant TL1A (100 ng/ml) in the presence of CHX for 6 hr. In the left panel, DR3-Fc, TR6-Fc, and a control Fc protein were added at the indicated concentrations either alone or in combination with TL1A. In the right panel, an anti-TL1A antibody or an IgG1 control were added at the indicated concentrations in combination with TL1A. Caspase activity was measured as described in the Experimental Procedures. Results are expressed as an average of triplicate samples plus standard error.

(C) TF-1 cells and activated T cells were treated with CHX (10 μg/ml), TL1A (200 ng/ml), or CHX in combination with TL1A for 24 hr. Cells were then stained for annexin V/propidium iodide and analyzed by FACS. The relative percent of annexin V/PI positive cells is shown.

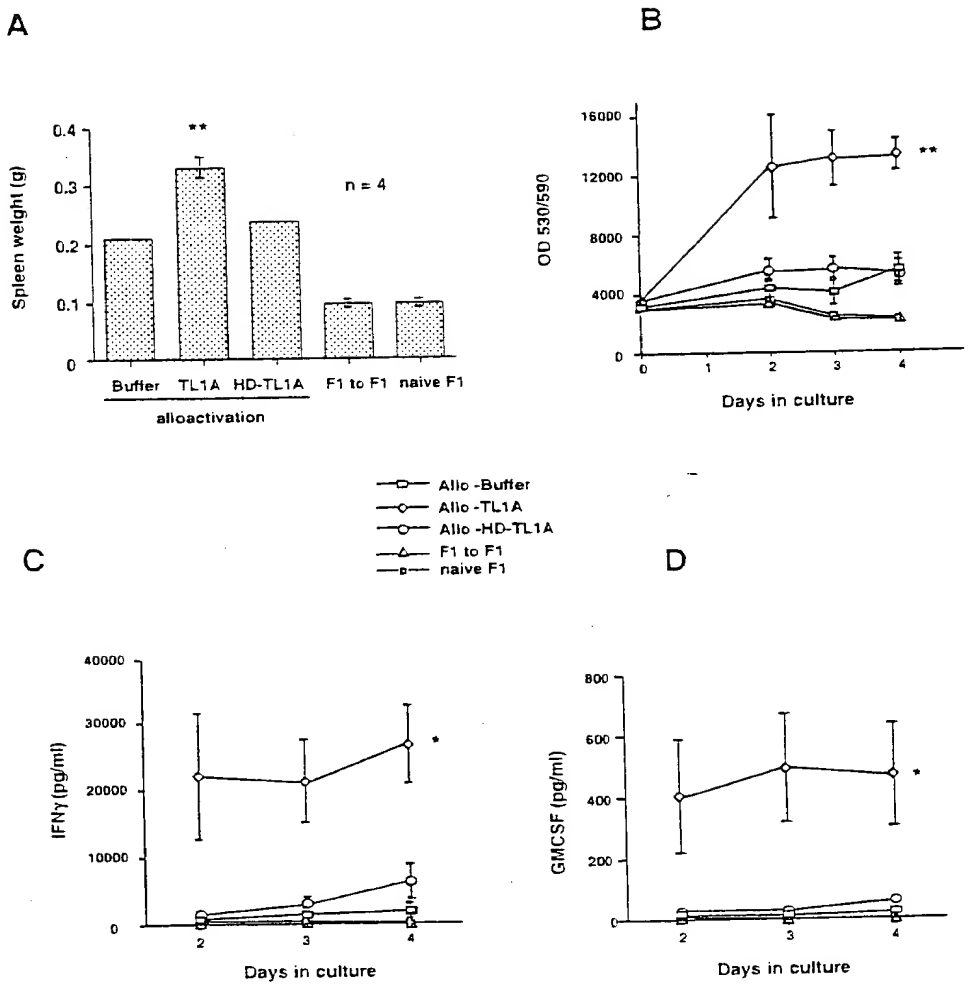

Figure 7. TL1A Enhances In Vivo and Ex Vivo Splenic Alloactivation

CB6F1 (H-2^{bxd}) mice were injected intravenously with 1.5×10^6 of splenocytes from either C57BL/6 (H-2^b, alloactivation) or CB6F1 (H-2^{bxd}, F1 to F1) on day 0, followed by a daily intravenous treatment with recombinant TL1A (aa 72–251, 3 mg/kg), heat-denatured TL1A (HD-TL1A), or buffer for 5 days from day 0 to day 4. Spleen weight (A), spontaneous splenocyte ex vivo proliferation (B), and IFNγ (C) and GMCSF (D) production from ex vivo culture were measured. Representative results from one experiment (n = 4 mice) were shown as the mean ± SEM, and similar results were obtained in two other experiments. The data were analyzed by ANOVA t tests for spleen weight. Kinetic splenocyte proliferation and cytokine production were analyzed by using a two-way ANOVA model for repeated measurements. Symbols * and ** represent significant ($p < 0.05$) and highly significant difference ($p < 0.005$), respectively.

recipient's immune responses were measured. Typical alloactivation results in splenomegaly of the recipient mice and enhanced proliferation and cytokine production of the splenocytes cultured ex vivo (Via, 1991; Zhang et al., 2001). The large number of T cells in the spleen and their expected upregulation of DR3 in response to alloactivation makes this an ideal model to assess the effect of TL1A on a defined in vivo immune response. As shown in Figure 7, 5 day administration of 3 mg/kg/day of the recombinant TL1A protein markedly enhanced the graft-versus-host responses. The same mean spleen weight (0.095 g) was seen for both naive mice and mice transferred with CB6F1 syngeneic splenocytes (Figure 7A). Alloactivation alone (transfer only C57BL/6 splenocytes into CBF1 mice and treat the mice with buffer only) resulted in a 2.2-fold increase in splenic weight (~0.22 g). Treatment of allografted CB6F1 mice with recombinant TL1A protein (aa 72–251) further increased splenic weight about 50% to a mean value of 0.34 g (Figure 7A). TL1A treatment also significantly enhanced ex vivo splenocyte expansion (Figure 7B) and secretion of IFNγ (Figure 7C) and GMCSF (Figure 7D). This effect is dependent on the TL1A protein as heat-denatured TL1A (HD-TL1A) lost most of these in vivo and ex vivo activities. Thus, TL1A strongly enhances GVHR in vivo, and this effect is consistent with the observed in vitro activities.

Discussion

Death domain-containing receptors have historically been defined as proteins that can induce apoptotic cell

death through activation of caspases. Recent work performed with TNF, FasL, and Fas (Siegel et al., 2000 and references within) has shown that while these proteins are potent inducers of cell death they also have the more subtle ability to act as costimulatory signals during T cell activation. FasL was shown to promote proliferation and IL-2 secretion from T cells treated with suboptimal doses of anti-CD3, whereas Fas-Fc inhibited T cell costimulation. This positive effect on T cells has been further confirmed by the studies of the FADD$^{-/-}$ mice (Varfolomeev et al., 1998; Zhang et al., 1998; Newton et al., 2001). Cells lacking FADD, which associates with DD and is required for the recruitment of caspase-8, not only are impaired in their ability to induce apoptosis but also exhibit a defect in T cell proliferation in response to mitogens. This suggests that DD-induced signals may result in different effects depending on the activation state of the responding T cell or on the specific stage of an immune response or of development. Therefore, during the initial stage of an immune response or in the presence of suboptimal antigen presentation, factors that signal through DD-containing receptors may act as costimulatory signals. In contrast, at the end of an immune response, they may contribute to the specific elimination of the excess activated T cells, or they may contribute to the regulation of negative selection in the thymus during development.

DR3 was initially described as a TNFR capable of inducing NF-κB activation and apoptosis when ectopically overexpressed in cell lines. TWEAK/Apo3L was shown to be a ligand for DR3 (Marsters et al., 1998). Neither others nor ourselves were able to demonstrate this interaction using similar methods (Schneider et al., 1999; Kaptein et al., 2000; our unpublished data). Recently, a novel TWEAK receptor, TweakR, was identified (Wiley et al., 2001). Therefore, the nature of DR3 and TWEAK interaction remains unclear.

In this paper, we describe the identification of a longer variant of TL1/VEGI, called TL1A, and provide evidence that it is a ligand for both DR3 and TR6. TL1A is expressed primarily in endothelial cells, and its expression is highly inducible by TNF and IL-1α. As for the relationship between TL1A and TL1, several lines of evidence strongly suggest that TL1A is the predominant, full-length gene product for this TNF family member and that TL1 is very likely a cloning artifact. First, TL1A mRNA is readily detected from endothelial cells, and several EST clones encoding the full-length TL1A exist. In contrast, a single TL1 clone with 3.3 kb insert was obtained through cDNA library screening (Zhai et al., 1999a), and no EST sequence corresponding to the full-length TL1 has been found from either the public or other databases. Furthermore, we were unable to clone the mouse or rat TL1 counterparts (L.Z. and P.W., unpublished data). Second, the human genomic information (Figure 1B) clearly shows that the TL1A cDNA was derived from normally spliced, multiexon mRNA, like that of other TNF family members. Consistent with this, TL1A has the characteristics of a full-length type II membrane protein. The complete matching of TL1 cDNA to a continuous TL1A genomic DNA region that contains both the introns and exons with intact consensus splicing sites strongly suggests that TL1 cDNA was derived from nonspliced/incompletely spliced nuclear RNA, a common source of cloning artifact. The low level of TL1-specific RNA detected by RT-PCR and Taqman (Figures 2B and 2C) may reflect the small proportion of nuclear RNA in total RNA preparations. Third, TL1A but not TL1 cDNA has an optimal eukaryotic Kozak sequence (−6 AGGAG CATGG+4 versus −6 AATGATATGA+4), suggesting that TL1 may not be properly translated. In line with this, no activity of the full-length TL1 has been reported, and the full-length TL1 did not show antiangiogeneic activity in vivo (Zhai et al., 1999a).

We have found that TL1A functions specifically as a T cell costimulator, which is consistent with DR3 being mainly expressed on activated T cells. The signal induced by TL1A on T cells results in increased responsiveness to IL-2 and in the secretion of proinflammatory cytokines. As TL1A production is significantly elevated in activated endothelial cells, the interaction with DR3 would occur when T cells are recruited to the site of inflammation and increase their ability to expand and to secrete proinflammatory cytokines. This, in turn, will result in recruitment and activation of macrophages and neutrophils. The ability of TL1A to enhance and amplify an immune response is evident from our in vivo work using the acute GVHR model. In this setting, in which a high proportion of T cells are activated and are therefore expected to express DR3, treatment with TL1A resulted in the exacerbation of the response. We, in fact, found an increase in T cell expansion (increase in splenic weight and ex vivo proliferation) and in the secretion of IFNγ and GMCSF.

Interestingly, we have observed that while TL1A was able to induce NF-κB activation and a costimulatory signal in primary T cells, it did not induce significant caspase activation or apoptosis. In contrast, TL1A was able to induce caspase activity and apoptosis in the tumor cell line TF-1, which is consistent with the possibility that binding of TL1A to DR3 may couple to distinct signaling pathways in different contexts. The fact that caspase activation and apoptosis were observed mainly in the presence of CHX indicates that, as seen for other TNF family members, signaling by TL1A results in a balance between positive and negative effects on cell viability. Therefore, apoptosis in this cell line can be detected only when protein synthesis is blocked and proliferative signals are inhibited.

Although TL1A (aa 72–251) protein exerts potent activity on activated T cells, we did not observe significant antiangiogenic activity of it in both in vitro and in vivo experiments (our unpublished data). It is known that many antiangiogenic factors are processed protein products whose full-length proteins have different biological activities. The fact that truncated TL1 proteins, which correspond to aa 101–251 and 106–251 of TL1A (Zhai et al., 1999a, 1999b; Yue et al., 1999), have an antiangiogenic effect is consistent with this notion.

Recently, mice with a disrupted DR3 gene have been described (DR3$^{-/-}$ mice; Wang et al., 2001) as having a partial defect in negative selection during thymocyte development. It will be interesting to see whether TL1A contributes to the complex regulation of the removal of autoreactive thymocytes that occurs during development or whether this effect is mediated by another member of the TNF family that is able to interact with DR3.

In addition to TL1A's binding to DR3, we show that, as seen in the case of Fas and LIGHT, the decoy receptor TR6 can compete with DR3 for TL1A binding. Our data

obtained from the BIAcore analysis and from the inhibition studies with DR3-Fc and TR6-Fc suggest that TL1A can bind both receptors with high affinity of the order of what has been previously reported for other members of the TNFR family and their ligands. TR6 has been shown previously to negatively regulate cytotoxic T lymphocyte activity in vitro and T cell responses to alloantigens in acute GVHR in vivo (Zhang et al., 2001). TR6 has also been shown to be overexpressed in certain tumors (Pitti et al., 1998; Bai et al., 2000), suggesting that some tumors may escape FasL-dependent cell death by expressing a decoy receptor that blocks FasL. Its ability to bind FasL, Light, and TL1A with high affinity suggests that it may modulate the duration and the magnitude of an immune response or it might protect tumor cells from apoptosis. A careful analysis of TL1A, DR3, and TR6 expression in human diseases may reveal a role for these molecules in autoimmune, inflammation, or tumor genesis.

Experimental Procedures

Cells, Constructs, and Other Reagents

All human cancer cell lines and normal lung fibroblasts (HFL-1) were purchased from the American Tissue Culture Collection. Human primary cells were purchased from Clonetics Corp. Cells were cultured as recommended. Human cDNA encoding the full-length TL1, TL1A, and DR3; the extracellular domain of TL1 (aa 25–174), TL1A (aa 72–251), BlyS (aa 134–285), and FasL (aa 130–281); and death domain-truncated DR3 (DR3ΔDD, aa 1–345) and DR5 (DR5ΔDD, aa 1–321) were amplified by PCR and cloned into the mammalian expression vectors pC4 and/or pFLAGCMV1 (Sigma). The extracellular domains of human DR3 (aa 1–199), TACI (aa 1–159), HveA (aa 1–192), Fas (aa 1–169), and full-length TR6 (aa 1–300) were each fused in-frame, at their C terminus, to the hinge and Fc domain of human IgG1 and cloned into pC4. Monoclonal antibody against TL1A, 16H02 (IgG1), was raised and purified as described (Kohler and Milstein, 1975). Stable cell lines expressing pcDNA3.1 vector control (Neo) or full-length TL1A were selected in 293F cells in 0.5 mg/ml Geneticin (Invitrogen).

Cloning of Human, Mouse, and Rat TL1A cDNA

TL1A was identified from human EST databases. The mouse and rat TL1A cDNA was isolated by low-stringency PCR amplification from mouse or rat kidney Marathon-Ready cDNAs (Clontech). Each sequence was derived and confirmed from more than two independent PCR products.

Quantitative Real-Time PCR (Taqman) and RT-PCR Analysis

Total RNA was isolated from human cell lines and primary cells using TriZOL (Invitrogen). Taqman was carried out in a 25 μl reaction containing 25 ng of total RNA, 0.6 μM each of gene-specific forward and reverse primers, and 0.2 μM of gene-specific fluorescence probe. TL1A-specific primers (forward: CACCTCTTAGAGCAGACG GAGATAA; reverse: TTAAAGTGCTGTGTGGGAGTTTGT; probe: CCA AGGGCACACCTGACAGTTGTGA) amplify an amplicon spanning nt 257 to 340 of the TL1A cDNA. TL1-specific primers (forward: CAAAGTCTACAGTTTCCCAATGAGAA; reverse: GGGAACTGATTT TTAAAGTGCTGTGT; probe: TCCTCTTTCTTGTCTTTCCAGTTGTGA GACAAAC) amplify nt 17 to 113 of the TL1 cDNA. Gene-specific PCR products were measured using an ABI PRISM 7700 Sequence Detection System following the manufacturer's instructions (PE Corp.). The relative TL1A mRNA level was normalized to the 18S ribosomal RNA internal control in the same sample.

For RT-PCR analysis, 0.5 μg of total RNA was amplified with TL1- (GCAAAGTCTACAGTTTCCCAATGAGAAAATTAATCC) or TL1A-specific sense primer (ATGGCCGAGGATCTGGGACTGAGC) and an antisense primer (CTATAGTAAGAAGGCTCCAAAGAAGGTTTTATC TTC) using SuperScript One-Step RT-PCR System (Invitrogen). β-actin was used as an internal control.

Recombinant Protein Purification

Flag fusion proteins were produced from 293T cells by transient transfection and purified on anti-Flag M2 affinity columns (Sigma) according to the manufacturer's instructions. Receptor proteins with or without Fc fusion were produced from Baculovirus or CHO stable cell lines as described (Zhang et al., 2001). Recombinant, untagged TL1A protein (aa 72–251) was generated and purified from *E. coli*. In brief, *E. coli* cell extract was separated on an HQ-50 anion exchange column (Applied Biosystems) and eluted with a salt gradient. The 0.2 M NaCl elution was diluted and loaded on an HQ-50 column, and the flow-through was collected, adjusted to 0.8 M ammonium sulfate, and loaded on a Butyl-650s column (Toso Haus). The column was eluted with a 0.8–0 M ammonium sulfate gradient, and the fractions containing TL1A protein were pooled and further purified by size exclusion on a Superdex-200 column (Pharmacia) in PBS. All recombinant proteins were in trimer form and confirmed by NH_2-terminal sequencing on an ABI-494 sequencer (Applied Biosystem). The endotoxin level of the purified protein was less than 10 EU/mg as measured on a LAL-5000E (Cape Cod Associates).

Flow Cytometry, Immunoprecipitation, and Western Blotting

One million cells, in 0.1 ml of FACS buffer (PBS, 0.1% BSA, and 0.1% NaN_3), were incubated with 0.1–1 μg of protein or antibody at room temperature for 15 min. The cells were washed with 3 ml of FACS buffer, reacted with biotinylated primary antibody, and stained with PE-conjugated secondary antibody at room temperature for 15 min. Cells were then washed again and resuspended in 0.5 μg/ml of propidium iodide, and live cells were gated and analyzed on a FACScan using the CellQuest software (BD Biosciences). For annexin V/PI staining, one million cells in 250 μl PBS containing calcium (BDPharmingen) were incubated with annexin V FITC and propidium iodide for 15 min at room temperature in the dark and analyzed.

For coimmunoprecipitation studies, 2 μg each of purified TNFR-Fc proteins was incubated with 1 μg of Flag-tagged TL1A, FasL, or BlyS protein and 20 μl of protein A-Sepharose beads in 0.5 ml of IP buffer (DMEM, 10% FCS, and 0.1% Triton X-100) at 4°C for 4 hr. The beads were then precipitated and washed extensively with PBST buffer (PBS and 0.5% Triton X-100) before being boiled in SDS-sample buffer.

For IκBα degradation studies, activated T cells or TF-1 cells were treated with 100 ng/ml of TL1A for the indicated time points in the presence or absence of the indicated amounts of TR6-Fc. Cells were then washed and lysed in RIPA buffer. Proteins were separated on SDS-PAGE (NOVEX), transferred onto PVDF membranes (Millipore), and immunoblotted with a polyclonal antibody to IκBα (Santa Cruz).

BIAcore Analysis

Recombinant TL1A (from *E. coli*) binding to various human TNF receptors was analyzed on a BIAcore 3000 instrument. TNFR-Fc were covalently immobilized to the BIAcore sensor chip (CM5 chip) via amine groups using N-ethyl-N'-(dimethylaminopropyl) carbodiimide/N-hydroxysuccinimide chemistry. A control receptor surface of identical density was prepared with BCMA-Fc that was negative for TL1A binding and used for background subtraction. Eight different concentrations of TL1A (range: 3–70 nM) were flowed over the receptor-derivatized flow cells at 15 μl/min for a total volume of 50 μl. The amount of bound protein was determined during washing of the flow cell with HBS buffer (10 mM HEPES [pH 7.4], 150 mM NaCl, 3.4 mM EDTA, and 0.005% Surfactant P20). The flow cell surface was regenerated by displacing bound protein by washing with 20 μl of 10 mM glycine-HCl (pH 2.3). For kinetic analysis, the on and off rates were determined using the kinetic evaluation program in BIAevaluation 3 software using a 1:1 binding model and the global analysis method.

T Cell Proliferation Assays

Whole blood from human donors was separated by Ficoll (ICN Biotechnologies) gradient centrifugation, and cells were cultured overnight in RPMI containing 10% FCS (Biofluids). T cells were separated using the MACS PanT separation kit (Milteny Biotech). The T cell purity achieved was usually higher that 90%. The cells were seeded

on anti-CD3 (0.3 μg/ml, Pharmingen) and anti-CD28 (5.0 μg/ml) coated 96-well plates at 2 × 10^4/well and were incubated with medium alone, 1 ng/ml of IL-2 (R&D Systems), or 100 ng/ml of TL1A (aa 72–251) at 37°C. After 72 hr in culture, the cells were either untreated or treated with 1 ng/ml of IL-2 and pulsed with 0.5 μCi of ^{3}H-thymidine for another 24 hr, and incorporation of ^{3}H was measured on a scintillation counter.

Cytokine ELISA Assays for Primary Cells

1 × 10^5 cells/ml of purified T cells were seeded in a 24-well tissue culture plate that had been coated with anti-CD3 (0.3 μg/ml) and anti-CD28 (5.0 μg/ml) overnight at 4°C. Recombinant TL1A (aa 72–251) protein (100 ng/ml) was added to cells, and supernatants were collected 72 hr later. ELISA assays for IFNγ, GM-CSF, IL-2, IL-4, IL-10, and TNFα were performed using kits purchased from R&D Systems. Recombinant human IL-2 (5 ng/ml) was used as a positive control. All samples were tested in duplicate and results were expressed as an average of duplicate samples plus or minus error.

Caspase Assay

TF-1 cells or PHA-activated primary T cells were seeded at 75,000 cells/well in a black 96-well plate with clear bottom (Becton Dickinson) in RPMI medium containing 1% fetal bovine serum (Biowhittaker). Cells were treated with TL1A or FasL in the presence or absence of cycloheximide (10 μg/ml) for 6 hr. Caspase activity was measured directly in the wells by adding an equal volume of a lysis buffer containing 25 μM DEVD-rodamine 110 (Roche Molecular Biochemicals) and allowing the reaction to proceed at 37°C for 1 to 2 hr. Release of rodamine 110 was monitored with a Wallac Victor2 fluorescence plate reader with excitation filter 485 nm and emission filter 535 nm.

Murine Graft-Versus-Host Reaction

CB6F1 (H-2^{bxd}) mice (C57BL/6 × BALB/c) were transfused intravenously with 1.5 × 10^6 spleen cells either from C57BL/6 mice (H-2^b) or from CB6F1 mice on day 0. Recombinant TL1A (aa 72–251) protein, heat-denatured TL1A (56°C for 45 min), or buffer alone was administered intravenously for 5 days at 3 mg/kg/day starting on the same day as the transfusion. The spleens of the recipient F1 mice were harvested on day 5 and weighed. Single cell suspensions were prepared for ex vivo assays.

Ex Vivo Mouse Splenocyte Proliferation and Cytokine Assays

Splenocytes from normal and the transfused F1 mice were cultured in triplicate in 96-well flat-bottomed plates (4 × 10^5 cells/200 μl/well) for 2–4 days. After removing 100 μl of supernatant per well on the day of harvest, 10 μl Alamar Blue (Biosource) was added to each well, and the cells were cultured for an additional 4 hr. The cell number in each well was assessed according to OD_{590nm} minus OD_{530nm} background, using a CytoFluor apparatus (PerSeptive Biosystems). Cytokines in the culture supernatant were measured with commercial ELISA kits from Endogen or R&D Systems following the manufacturer's instructions.

Acknowledgments

The authors wish to thank Victor Kao, Thomas Kaufmann, Susie Kirchhof, Soo Kim, and Kara Taylor for technical assistance, and Drs. Ricardo Cibotti, David Hilbert, and Theodora Salcedo for reviewing the manuscript.

Received July 30, 2001; revised January 25, 2002.

References

Ashkenazi, A., and Dixit, V.M. (1999). Apoptosis control by death and decoy receptors. Curr. Opin. Cell Biol. *11*, 255–260.

Bai, C., Connolly, B., Metzker, M.L., Hilliard, C.A., Liu, X., Sandig, V., Soderman, A., Galloway, S.M., Liu, Q., Austin, C.P., and Caskey, C.T. (2000). Overexpression of M68/DcR3 in human gastrointestinal tract tumors independent of gene amplification and its location in a four-gene cluster. Proc. Natl. Acad. Sci. USA *97*, 1230–1235.

Bodmer, J., Burns, K., Schneider, P., Hofmann, K., Steiner, V., Thome, M., Bornand, T., Hahne, M., Schroter, M., Becker, K., et al. (1997). TRAMP, a novel apoptosis-mediating receptor with sequence homology to tumor necrosis factor receptor 1 and Fas(Apo-1/CD95). Immunity *6*, 79–88.

Chinnaiyan, A.M., O'Rourke, K., Yu, G.L., Lyons, R.H., Garg, M., Duan, D.R., Xing, L., Gentz, R., Ni, J., Dixit, V.M. (1996). Signal transduction by DR3, a death domain-containing receptor related to TNFR-1 and CD95. Science *274*, 990–992.

Connolly, K., Cho, Y.H., Duan, R., Fikes, J., Gregorio, T., LaFleur, D.W., Okoye, Z., Salcedo, T.W., Santiago, G., Ullrich, S., et al. (2001). In vivo inhibition of fas ligand-mediated killing by TR6, a fas ligand decoy receptor. J Pharmacol Exp. Ther. *298*, 25–33.

Eck, M.J., Ultsch, M., Rinderknecht, E., de Vos, A.M., and Sprang, S.R. (1992). The structure of human lymphotoxin (tumor necrosis factor beta) at 1.9 Å resolution. J. Biol. Chem. *267*, 2119–2122.

Kaptein, A., Jansen, M., Dilaver, G., Kitson, J., Dash, L., Wang, E., Owen, M.J., Bodmer, J., Tschopp, J., and Farrow, S.N. (2000). Studies on the interaction between TWEAK and the death receptor WSL-1/TRAMP (DR3). FEBS Lett. *485*, 135–141.

Kitson, J., Raven, T., Jiang, Y.P., Goeddel, D.V., Giles, K.M., Pun, K.T., Grinham, C.J., Brown, R., and Farrow, S.N. (1996). A death-domain-containing receptor that mediates apoptosis. Nature *384*, 372–375.

Kohler, G., and Milstein, C. (1975). Continuous cultures of fused cells secreting antibody of predefined specificity. Nature *256*, 503–519.

Locksley, R.M., Killeen, N., and Lenardo, M.J. (2001). The TNF and TNF receptor superfamilies: integrating mammalian biology. Cell *104*, 487–501.

Marsters, S.A., Sheridan, J.P., Donahue, C.J., Pitti, R.M., Gray, C.L., Goddard, A.D., Bauer, K.D., and Ashkenazi, A. (1996). Apo-3, a new member of the tumor necrosis factor receptor family, contains a death domain and activates apoptosis and NF-κB. Curr. Biol. *6*, 1669–1676.

Marsters, S.A., Sheridan, J.P., Pitti, R.M., Brush, J., Goddard, A., and Ashkenazi, A. (1998). Identification of a ligand for the death-domain-containing receptor Apo3. Curr. Biol. *8*, 525–528.

Newton, K., Kurts, C., Harris, A.W., and Strasser, A. (2001). Effects of a dominant interfering mutant of FADD on signal transduction in activated T cells. Curr. Biol. *11*, 273–276.

Pitti, R.M., Marsters, S.A., Lawrence, D.A., Roy, M., Kischkel, F.C., Dowd, P., Huang, A., Donahue, C.J., Sherwood, S.W., Baldwin, D.T., et al. (1998). Genomic amplification of a decoy receptor for Fas ligand in lung and colon cancer. Nature *396*, 699–703.

Schneider, P., Schwenzer, R., Haas, E., Muhlenbeck, F., Schubert, G., Scheurich, P., Tschopp, J., and Wajant, H. (1999). TWEAK can induce cell death via endogenous TNF and TNF receptor 1. Eur. J. Immunol. *29*, 1785–1792.

Screaton, G.R., Xu, X., Olsen, A.L., Cowper, A.E., Tan, R., McMichael, A.J., and Bell, J.I. (1997). LARD: a new lymphoid-specific death domain containing receptor regulated by alternative pre-mRNA splicing. Proc. Natl. Acad. Sci. USA *94*, 4615–4619.

Siegel, R.M., Chan, F.K., Chun, H.J., and Lenardo, M.J. (2000). The multifaceted role of Fas signaling in immune cell homeostasis and autoimmunity. Nature *1*, 469–474.

Tan, K.B., Harrop, J., Reddy, M., Young, P., Terrett, J., Emery, J., Moore, G., and Truneh, A. (1997). Characterization of a novel TNF-like ligand and recently described TNF ligand and TNF receptor superfamily genes and their constitutive and inducible expression in hematopoietic and non-hematopoietic cells. Gene *204*, 35–46.

Varfolomeev, E.E., Schuchmann, M., Luria, V., Chiannikulchai, N., Bechmann, J.S., Mett, I.L., Rebrikov, D., Brodianski, V.M., Kemper, O.C., Kollet, O., et al. (1998). Target disruption of the mouse caspase 8 gene ablates cell death induction by the TNF receptors, Fas/Apo1, and DR3 and is lethal prenatally. Immunity *9*, 267–276.

Via, C.S. (1991). Kinetics of T cell activation in acute and chronic forms of murine graft-versus-host disease. J. Immunol. *146*, 2603–2609.

Wang, E.C.Y., Thern, A., Denzel, A., Kitson, J., Farrow, S.N., and

Owen, M.J. (2001). DR3 regulates negative selection during thymocyte development. Mol. Cell. Biol. *12*, 3451–3461.

Wiley, S.R., Cassiano, L., Lofton, T., Davis-Smith, T., Winkles, J.A., Lindner, V., Liu, H., Daniel, T.O., Smith, C.A., and Fanslow, W.C. (2001). A novel TNF receptor family member binds TWEAK and is implicated in angiogenesis. Immunity *15*, 837–846.

Yu, K.Y., Kwon, B., Ni, J., Zhai, Y., Ebner, R., and Kwon, B.S. (1999). A newly identified member of tumor necrosis factor receptor superfamily (TR6) suppresses LIGHT-mediated apoptosis. J. Biol. Chem. *274*, 13733–13736.

Yue, T., Ni, J., Romanic, A.M., Gu, J., Keller, P., Wang, C., Kumar, S., Yu, G., Hart, T.K., Wang, X., et al. (1999). TL1, a novel tumor necrosis factor-like cytokine, induces apoptosis in endothelial cells. J. Biol. Chem. *274*, 1479–1486.

Zhai, Y., Ni, J., Jiang, G.W., Lu, J., Xing, L., Lincoln, C., Carter, K.C., Janat, F., Kozak, D., Xu, S., et al. (1999a). VEGI, a novel cytokine of the tumor necrosis factor family, is an angiogenesis inhibitor that suppresses the growth of colon carcinomas in vivo. FASEB J. *13*, 181–189.

Zhai, Y., Yu, J., Iruela-Arispe, L., Huang, W.Q., Wang, Z., Hayes, A.J., Lu, J., Jiang, G., Rojas, L., Lippman, M.E., et al. (1999b). Inhibition of angiogenesis and breast cancer xenograft tumor growth by VEGI, a novel cytokine of the TNF superfamily. Int. J. Cancer *82*, 131–136.

Zhang, J., Cado, D., Chen, A., Kabra, N.H., and Winoto, A. (1998). Fas-mediated apoptosis and activation-induced T-cell proliferation are defective in mice lacking FADD.Mort/1. Nature *392*, 296–300.

Zhang, J., Salcedo, T.W., Wan, X., Ullrich, S., Hu, B., Gregorio, T., Feng, P., Qi, S., Chen, H., Cho, Y.H., et al. (2001). Modulation of T-cell responses to alloantigens by TR6/DcR3. J. Clin. Invest. *107*, 1459–1468.

Immunity

Volume 16, Number 3

March 2002

Salmonella-Specific CD4 T Cells

MOLECULAR AND CELLULAR BIOLOGY, May 2001, p. 3451–3461 Vol. 21, No. 10
0270-7306/01/$04.00+0. DOI: 10.1128/MCB.21.10.3451–3461.2001

DR3 Regulates Negative Selection during Thymocyte Development

EDDIE C. Y. WANG,[1]† ANETTE THERN,[1] ANGELA DENZEL,[1] JEREMY KITSON,[2] STUART N. FARROW,[2] AND MICHAEL J. OWEN[1]*

Imperial Cancer Research Fund, Lincoln's Inn Fields, London WC2A 3PX,[1] and Glaxo Wellcome, Stevenage, Herts SG1 2NY,[2] United Kingdom

Received 16 October 2000/Returned for modification 6 December 2000/Accepted 22 February 2001

DR3 (Ws1, Apo3, LARD, TRAMP, TNFSFR12) is a member of the death domain-containing tumor necrosis factor receptor (TNFR) superfamily, members of which mediate a variety of developmental events including the regulation of cell proliferation, differentiation, and apoptosis. We have investigated the in vivo role(s) of DR3 by generating mice congenitally deficient in the expression of the DR3 gene. We show that negative selection and anti-CD3-induced apoptosis are significantly impaired in DR3-null mice. In contrast, both superantigen-induced negative selection and positive selection are normal. The pre-T-cell receptor-mediated checkpoint, which is dependent on TNFR signaling, is also unaffected in DR3-deficient mice. These data reveal a nonredundant in vivo role for this TNF receptor family member in the removal of self-reactive T cells in the thymus.

The tumor necrosis factor receptor (TNFR) superfamily comprise a growing family of type I membrane bound glycoproteins which interact with the TNF family of soluble mediators and type II transmembrane proteins. At least 23 TNFR superfamily members and 17 known ligands have been identified in mammals (reviewed in references 3, 35, and 44). These receptors trigger pleiotropic responses, ranging from apoptosis and differentiation to proliferation, and have been implicated in immune regulation, host defense and lymphoid organ development.

Members of the TNFR family are characterized by the presence of varying numbers (three to six) of cysteine-rich repeats in their cytoplasmic domains (52). TNFRs are subdivided based on the presence or absence of a 70- to 80-amino-acid region of homology in the cytoplasmic region called the death domain, through which these receptors trigger apoptosis (20, 48). DR3 (also called Ws1, Apo3, TRAMP, LARD, TR3, and TNFRSF12) is one of six death domain-containing TNFR family members (the others are TNFR1, CD95/FAS, DR4, DR5, and DR6) and is the one most closely related to TNFR1. Studies on the TNFR1 crystal structure suggest that ligand binding or receptor overexpression results in receptor trimerization and recruitment of trimeric intracellular signaling molecules (4, 36). DR3, like TNFR1, recruits TNFR1-associated death domain protein (TRADD) and Fas-associated death domain-containing protein (FADD) (5, 6, 11, 12, 24) as downstream effectors of apoptosis. These, in turn, interact with caspase 8 (FLICE/MACH) (7, 31), and a cascade of interleukin-1β-converting enzyme-like cysteine proteases which trigger cell death (13, 17, 27). DR3 also recruits TRAF2 via TRADD (18, 24, 29, 39) and thus activates the transcription factor, NF-κB, that induces the transcription of a number of immune genes (19). In this respect, DR3 (like TNFR1) is capable of inducing both apoptosis and expression of survival/activation genes and is likely to have multiple functions depending on the context of its expression.

DR3 was first reported as the only death domain-containing TNFR family member with lymphoid organ-restricted expression (11, 24). More recent studies have, however, shown DR3 expression to be less restricted, though not as ubiquitous expression of as its other death domain-containing TNFR relatives (47, 51). DR3 expression patterns may be further complicated by the presence of at least 13 human (24, 42, 53) and 3 mouse (51) splice variants. DR3 splicing may be developmentally regulated since human peripheral blood leukocytes have been shown to express full-length DR3 mRNA only following activation (42). While the ligand for DR3 has been reported as TWEAK (30, 10), it has also been shown that TWEAK can bind and signal in a DR3-negative cell line via a TNF/TNFR1-related mechanism (40). Thus, the problems with identifying a single ligand together with the complex expression of DR3 have contributed to the lack of functional data for this gene. To date, the only ex vivo indication, albeit indirect, that DR3 has an apoptotic role stems from the detection of translocations affecting the DR3 gene in several neuroblastoma cell lines (16).

To determine the in vivo function(s) of DR3, we generated mice that are deficient in the expression of its murine homologue. DR3-deficient mice show no defects in organ development (lymphoid or otherwise), lymphoid proliferation, or apoptosis triggered by glucocorticoids or DNA-damaging agents. There is also no defect in the progression of double-negative (DN) thymocytes through the pre-T-cell receptor (TCR)-mediated checkpoint, a developmental transition at which TNFR signaling has been shown to be important (33). However, an impairment of negative selection, as well as anti-CD3-mediated cell death of thymocytes, is observed in DR3-deficient mice, suggesting a nonredundant role in TCR-induced apoptosis that establishes central tolerance in vivo.

* Corresponding author. Mailing address: Imperial Cancer Research Fund, P.O. Box 123, Lincoln's Inn Fields, London, WC2A 3PX, United Kingdom. Phone: 44 020 7269 3069. Fax: 44 020 7269 3479 E-mail: m.owen@icrf.icnet.uk.

† Present address: Department of Medicine, University of Wales College of Medicine, Heath Park, Cardiff CF14 4XX, United Kingdom.

MATERIALS AND METHODS

Generation of DR3$^{-/-}$ mice. A human cDNA corresponding to the full-length DR3 gene was used as a probe to isolate clones from an EMBL3A phage library of 129/Sv mouse strain genomic DNA (51). A 6-kb *SmaI-MfeI* fragment covering the whole of the coding region of the DR3 gene was replaced with a cassette containing an internal ribosome entry site (IRES), *lacZ* poly(A), and neomycin resistance (*neo*) gene flanked by *loxP* sequences (a gift from Andrew Smith, University of Edinburgh, Edinburgh, United Kingdom). The DR3 gene targeting construct was linearized and transfected into GK129 embryonic stem (ES) cells by electroporation. ES cell clones were selected in G418-containing medium on a monolayer of mitotically inactivated STO feeder cells. Clones were picked and screened for homologous recombinants using the probes shown in Fig. 1A. ES clones with correct 5′ and 3′ recombinations were microinjected into C57BL/6 blastocysts and introduced into pseudopregnant C57BL/6 mice. Male chimeric offspring were bred to obtain germ line mutant mice which were screened either by Southern blotting or by PCR.

Maintenance and breeding of mouse strains. All mice were kept under barrier conditions at the Imperial Cancer Research Fund animal unit. H-Y TCR transgenic mice were kindly provided by H. von Boehmer (22). Rag 1$^{-/-}$ mice were acquired from the Jackson Laboratory. For H-Y TCR transgenic studies, DR3$^{-/-}$ × H-Y TCR mice were obtained by crossing DR3$^{-/-}$ mice with DR3$^{+/-}$ H-Y TCR heterozygote transgenics, thus deriving DR3$^{+/-}$ and DR3$^{-/-}$ mice with and without the H-Y TCR transgene. All mice analyzed were between 6 and 14 weeks of age. For analysis of each age group (6, 10, and 14 weeks), mice were sacrificed within one day of their weekly age.

Flow cytometric analysis. Fluorescence-activated cell sorting (FACS) analysis was performed on a FACScan (Becton Dickinson) using CellQuest software. Single-cell suspensions were prepared from freshly isolated bone marrow, lymph nodes (inguinal), spleen, and thymus. All samples were gated on standard forward scatter versus-side scatter gates. Thymocytes were stained using combinations of the antibodies from Becton Dickinson (anti-CD4-fluorescein isothiocyanate [FITC], anti-CD4-phycoerythrin [PE], anti-CD8-FITC, anti-CD8-biotin, anti-CD30, anti-CD44-PE, anti-CD25-biotin, anti-Vβ8-FITC [F23.1], anti-CD3-FITC [2C11], anti-αβTCR-FITC, anti-γδTCR-FITC, anti-B220-FITC, and anti-5-bromo-2′-deoxyuridine [BrdU]) or Caltag Laboratories (anti-CD8-Tricolor, streptavidin-Tricolor, anti-neutrophil-FITC, and anti-monocyte-FITC) or kindly donated by P. Kieselow and H. von Boehmer for H-Y transgenic analysis (T3.70 and T3.70-FITC specific for Vα3 [49]). BrdU and unconjugated T3.70 or CD30 were visualized using anti-mouse immunoglobulin G (IgG)-FITC (Dako).

Lymphocyte proliferation assays. In vivo BrdU incorporation assays were carried out as described elsewhere (56). In brief, 1 mg of BrdU (Sigma) was injected twice intraperitoneally, 30 min apart. Mice were then sacrificed after 6 h, thymuses were extracted, and single-cell-suspension thymocytes were isolated. BrdU incorporation was visualized using a standard BrdU-labeling protocol (28) with an anti-BrdU antibody (Becton Dickinson) and anti-mouse Ig-FITC secondary (Dako) and analyzed on a FACScan (Becton Dickinson).

For in vitro [^{3}H]thymidine uptake assays, 2 × 10^5 lymphocytes, isolated as described above, were aliquoted into 96-well flat-bottomed plates and stimulated with anti-CD3 (2C11), anti-CD3, and anti-CD28 (37.51; Pharmingen), 1 ng of phorbol myristate acetate (PMA) and ionomycin (Sigma) per ml, or 5 μg of concanavalin A (Sigma) per ml. For antibody stimulations, plates were previously coated with the monoclonal antibodies (MAbs) overnight at 4°C at 10 μg/ml in phosphate-buffered saline (PBS) and washed five times with PBS before use. Cultures were performed in RPMI medium supplemented with 10% heat-inactivated fetal calf serum and 50 μM β-mercaptoethanol. Stimulations were carried out in triplicate and incubated for 72 h before pulsing for 18 to 24 h with [^{3}H]thymidine (1 mCi/well; Dupont NEN, Boston, Mass.). Cells were then harvested onto fiberglass filter mats (Pharmacia, Uppsala, Sweden) and washed with a cell harvester (Skatron). Beta emission was counted on a Betaplate counter (Pharmacia). Results are presented as a stimulation index, calculated as the geometric mean of stimulated cultures/geometric mean of control cultures with medium only ± 1 standard deviation. No significant differences were observed between the medium-only controls of DR3$^{+/-}$ and DR3$^{-/-}$ lymphocytes.

Apoptosis assays. For anti-CD3-induced apoptosis assays, experiments were carried out as described elsewhere (46). In brief, 96-well flat-bottomed plates were coated with anti-CD3 MAb 2C11 (2, 10, or 50 μg/ml) or anti-CD3 and anti-CD28 MAb (each at 10 μg/ml) in PBS, overnight at 4°C, or with rat Ig as a control. Plates were washed three times with PBS before use. Thymocytes were extracted, resuspended in single-cell suspension in Dulbecco's modified Eagle's medium (Gibco BRL) supplemented with 10% heat-inactivated fetal calf serum, and aliquoted into plates at 5 × 10^5 cells/well. For PMA (Sigma) stimulation, a final concentration of 1 ng/nl was used. Samples were then incubated at 37°C for the indicated times before analysis for apoptosing cells using annexin V-FITC (Pharmingen) and propidium iodide staining to gate out dead cells. All samples were performed in triplicate. Values for percent anti-CD3-induced apoptosis were calculated using the following formula: (% annexin V$^+$ cells after anti-CD3 − % annexin V$^+$ cells in rat Ig controls)/(100 − % annexin V$^+$ cells in rat Ig controls) × 100. For other apoptosis assays, thymocytes were cultured in vitro in standard RPMI medium supplemented with 10% heat-inactivated fetal calf serum and 50 μM β-mercaptoethanol, and apoptosis was induced by stimulation with the following reagents: cycloheximide (30 μg/ml) and anti-Fas antibody (1 μg/ml); dexamethasone (2 μM); and etoposide (50 μM). Samples were taken at 4, 8, 12, 24, and 48 h poststimulation. Apoptosis was visualized using both annexin V-FITC staining, or pre-G$_1$ peak DNA staining with propidium iodide.

RESULTS

Generation of DR3$^{-/-}$ mice. The strategy used to inactivate the DR3 gene in ES cells is shown in Fig. 1A. We chose to disrupt exon 1 and replace all of the coding exons of the gene to exclude the possibility of any expression of DR3 splice variants. The entire coding region of the DR3 gene, from exon 1 (56 bp upstream of the ATG initiation codon) to 297 bp downstream of the polyadenylation site, was replaced with a construct containing an IRES, β-galactosidase (*lacZ*) gene, and *neo* gene flanked by *laxP* sites. ES cell clones with correct 5′ and 3′ recombinations were detected by screening using probes outside the recombination arms of the targeting vector. 5′ recombination was detected by the reduction of a 6.5-kb wild-type *Bam*HI fragment to 3.9 kb and 3′ recombination by the reduction of an 11.5-kb wild-type *Xba*I band to 10 kb (Fig. 1A and B). The homologous recombination frequency was 4.2%. Four clones were chosen for injection into blastocysts. Mice heterozygous for the targeted allele, as detected by screening for 5′ recombination in genomic Southern blots of tail DNA (Fig. 1C), were generated from two ES cell clones with correct 5′ and 3′ integrations of the targeting construct.

Breeding of heterozygous (DR3$^{+/-}$) mice generated homozygote DR3-null (DR3$^{-/-}$) mice (Fig. 1C) in normal Mendelian and male/female ratios (data not shown). Due to the targeting strategy (deletion of the entire coding region of the DR3 gene), the mutation must clearly be null. In agreement with this, no transcripts were detected by PCR analysis using any combination of primers specific for the DR3 coding sequence. A representative reverse transcription-PCR demonstrating this using primers encoding sequences within the DR3 death domain is shown in Fig. 1D.

Normal development of major organs, peripheral lymphoid organs, and lymphocyte subsets in DR3$^{-/-}$ mice. The pattern of expression of mouse DR3 in the brain, heart, and kidney as well as lymphoid organs (51) prompted us to investigate whether there were any general developmental defects in DR3$^{-/-}$ mice. Histological analysis of all major organs (including brain, heart, and kidney) revealed no abnormalities (data not shown). In particular, the peripheral lymphoid organs such as thymus, spleen, lymph nodes, and Peyer's patches all showed normal development. Primary B-cell follicles and follicular dendritic cell networks were present in the peripheral lymphoid organs from DR3$^{-/-}$ mice (data not shown), unlike their TNFR1$^{-/-}$ counterparts (25, 32, 37).

A more detailed analysis of the B- and T-lymphocyte populations in peripheral lymphoid organs from DR3-deficient mice was carried out by FACS analysis using a battery of antibodies that define the various lymphoid populations. No

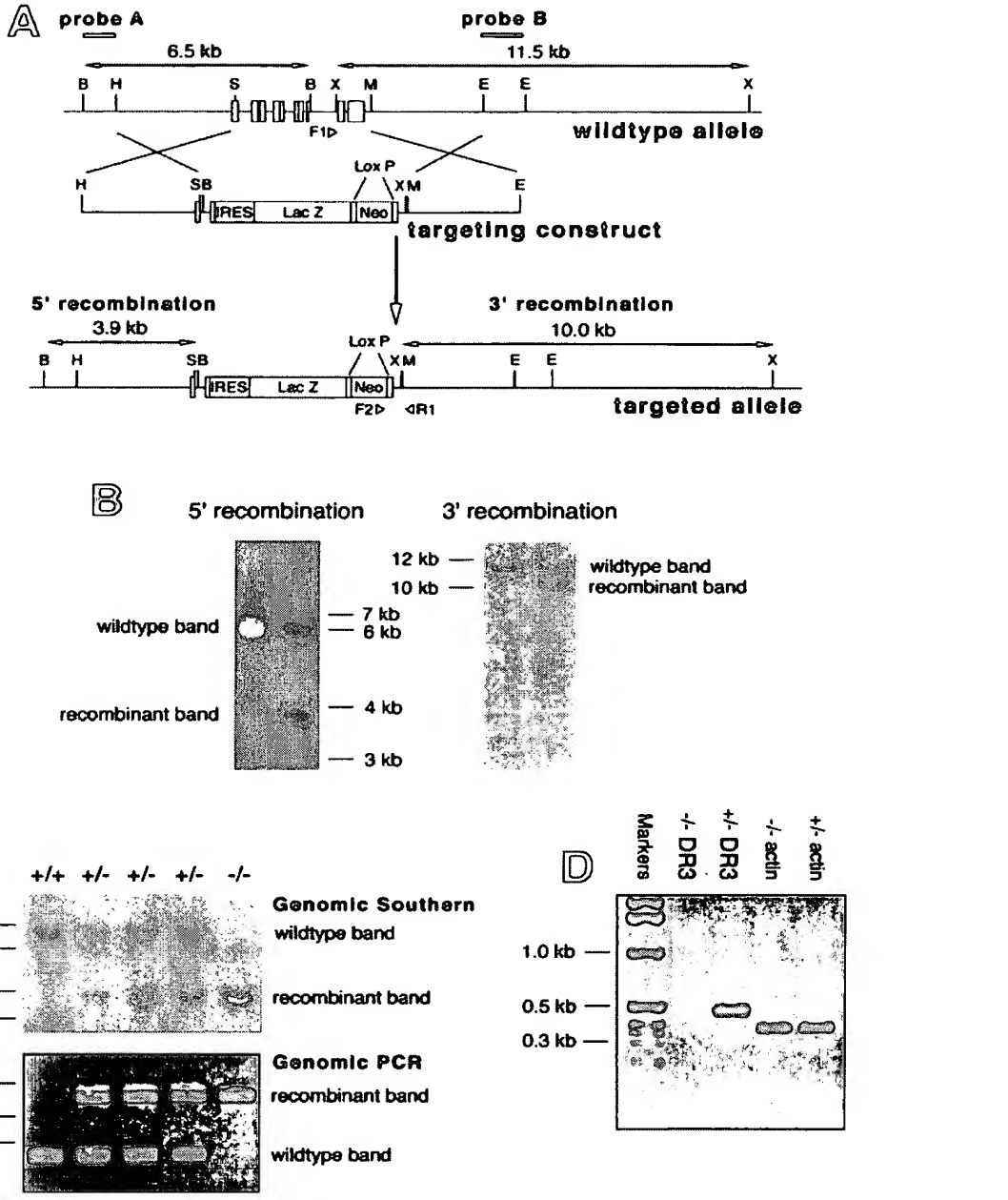

FIG. 1. Generation and screening of DR3$^{-/-}$ mice. (A) Map of the coding region of the DR3 gene (top), the targeting construct (middle), and the targeted locus (bottom). Restriction enzyme sites are indicated by single letters; B, *Bam*HI; E, *Eco*RI; H, *Hin*dIII; M, *Mfe*I; S, *Sma*I; X, *Xba*I. The positions of the DR3 exons are shown. An IRES/*lacZ*/*loxP*/*neo* vector was used to replace the whole coding region of the DR3 gene. The 5′ arm was generated using a 3-kb *Hin*dIII-*Sma*I fragment, while the 3′ arm consisted of a 3-kb *Mfe*I-*Eco*RI fragment. (B) Southern blot screening for homologous recombination in ES cell clones. Genomic DNA was isolated from transfected ES cell clones, digested with either *Bam*HI or *Xba*I, and screened with probe A (left) for 5′ recombination or probe B (right) for 3′ recombination, respectively. Only ES cell clones with correct recombination at both ends were used for injections. Sizes of fragments are indicated. (C) Southern blot analysis and genomic PCR of representative mouse tail DNA. Genomic DNA was isolated from mouse tails, screened for correct 5′ recombination by Southern blotting using a *Bam*HI digest and probe A, and screened for correct 3′ recombination by genomic PCR using the three primers (filled triangles) F1, F2 (in the *neo* gene), and R1. Sizes of fragments, recombinant and wild-type bands are indicated. (D) Reverse transcription-PCR analysis of thymus cDNA. cDNA prepared from total thymus RNA was subjected to PCR analysis using specific primers corresponding to sequences within the DR3 death domain exon. Actin primers were used a positive control. Sizes of fragments are indicated.

significant differences were observed between DR3$^{-/-}$ mice and their heterozygous or wild-type littermates (data not shown). There were also no significant differences in the weight and size of spleens or lymph nodes at any age examined (data not shown).

Increased thymus size but normal turnover in DR3$^{-/-}$ mice. TNFR family members have been shown to be important regulators of developmental processes. The expression of DR3 in developing thymocytes suggested that DR3 may be a regulator of thymocyte development. To determine whether DR3 is required for normal thymocyte development, thymocyte subpopulations were analyzed by flow cytometry. There were no significant differences in the four major thymocyte populations defined by the expression of the CD4 and CD8 markers. However, a small but significant increase in the average total number of thymocytes derived from DR3-deficient mice, compared to heterozygous littermates, was observed (Fig. 2A). At 2 to 5 weeks of age, DR3$^{-/-}$ thymuses were generally about 10% larger than their heterozygote counterparts, and by 29 to 32 weeks this difference had increased to about 30%. A larger study (data not shown), covering mice aged from 26 to 233 days, showed these differences to be significant using a different statistical analysis (Mann-Whitney U test; $U = 5{,}965$, $P < 0.05$). No difference in thymocyte number was observed between wild-type and heterozygous mice (data not shown). This increase in thymus size appeared not to be a consequence of an increase in thymocyte proliferation and/or turnover, since neither the proportion nor the numbers of thymocytes which incorporated BrdU differed significantly between DR3$^{-/-}$ and DR3$^{+/-}$ mice (Fig. 2B).

Early thymocyte development is unaffected by the absence of DR3. The small but significant increase in total thymocyte numbers in DR3-deficient mice was consistent with a regulatory role of DR3 at one or more stages of thymocyte development. There are two major checkpoints at which thymocyte development is controlled. The DN-to-double-positive (DP) thymocyte transition selects immature thymocytes with in-frame TCRβ rearrangements and is regulated by the pre-TCR. The DP-to-single-positive (SP) thymocyte transition selects major histocompatibility complex (MHC)-restricted, nonautoreactive thymocytes and is regulated by the mature αβTCR. To investigate whether DR3 plays an essential role in early thymocyte development, we initially analyzed DN thymocyte subsets, as defined by the absence of CD4, CD8, αβTCR, γδTCR, and B220 surface markers and the differential expression of CD44 and CD25, by flow cytometry. As shown in Fig. 2C (upper panels), this analysis revealed no consistent differences in the relative proportions of DN populations in DR3$^{-/-}$ compared to DR3$^{+/-}$ mice.

Analysis of transgenic mice expressing dominant negative FADD (DN-FADD)/MORT1 (which binds to TNFR death domains) has implicated a role for death receptor signaling in early thymocyte development at the pre-TCR checkpoint (33). This study showed that the DN-FADD transgene bypassed the requirement for pre-TCR signaling, promoting the survival and differentiation, but not the proliferation, of CD25$^+$ CD44$^-$ thymocytes in Rag-deficient mice. These results have suggested a model in which dual signaling, via the pre-TCR and death receptors, triggers the development of early pre-T cells, whereas death receptor signaling in thymocytes that lack a pre-TCR induces apoptosis. To test whether FADD recruitment to DR3 is essential for the regulation of the pre-TCR-mediated checkpoint, Rag1 × DR3 doubly deficient mice were analyzed. As shown in Fig. 2C (lower panels), thymocyte development was completely arrested at the CD25$^+$ CD44$^-$ DN stage in Rag$^{-/-}$ × DR3$^{-/-}$ mice, demonstrating that DR3 is not essential for FADD-mediated deletion of DN thymocytes that fail to make in-frame rearrangements at the TCRβ locus.

Negative selection is impaired in DR3$^{-/-}$, H-Y transgenic mice. The DP-to-SP thymocyte transition is a checkpoint at which a developmental decision is made between cell death and survival. Thymocytes expressing αβTCRs that have no detectable affinity for ligand, or which are autoreactive, undergo apoptosis, whereas cells expressing αβTCRs with intermediate affinities receive survival signals and generate the pool of mature SP thymocytes and αβT cells. To investigate whether DR3 is essential for efficient negative selection of thymocytes, the H-Y TCR transgenic mouse model was used (22). The H-Y TCR recognizes a male-specific antigen in the context of *H-2^b* In male mice, thymocytes expressing the transgenic TCR are deleted, whereas in female mice, transgene-expressing cells undergo positive selection, resulting in an increased proportion of CD8 SP cells.

In male H-Y TCR *H-2^b* transgenic mice, CD8$^+$ TCR-expressing cells are efficiently deleted by negative selection. To determine whether this deletion was dependent on the expression of DR3, the proportion of CD8$^+$ TCR-expressing thymocytes from DR3-deficient, H-Y TCR male mice was analyzed by flow cytometry using MAb T3.70, which recognizes the Vα3 chain of the H-Y TCR. This analysis was carried out using male mice 6, 10, and 14 weeks of age. As shown in Fig. 3A and B, and as reported previously (22), an age-dependent deletion of transgenic TCR-positive, CD8$^+$ thymocytes was observed in male mice. At 14 weeks of age, the total numbers and proportion of H-Y TCR CD8 SP thymocytes were barely detectable. A striking increase in the numbers and proportions of CD8$^+$ T3.70$^+$ thymocytes, was observed in DR3-deficient H-Y TCR transgenic male mice compared to DR3$^{+/-}$ littermates. A significant difference was apparent in 10-week-old male mice and, by 14 weeks of age there was at least a fourfold difference in the numbers of transgenic TCR-positive CD8$^+$ SP cells in DR3-deficient male mice.

The observed increase in the numbers of CD8$^+$ T3.70$^+$ thymocytes could be a consequence of either an increase in proliferation and/or a decrease in apoptosis of this subset. To distinguish between these possibilities, the turnover of thymocytes in male DR3$^{-/-}$ H-Y and DR3$^{+/-}$ H-Y TCR transgenic littermates was investigated by examining their BrdU incorporation. Mice 10 weeks age were chosen, as no significant differences in CD8$^+$ T3.70$^+$ thymocyte numbers or thymus size were observed at 6 weeks (Fig. 3B and data not shown), while at 14 weeks around half the DR3$^{+/-}$ H-Y mice had virtually undetectable thymuses. The proportion of thymocytes incorporating BrdU into DNA did not differ in the DR3$^{+/-}$ or DR3$^{-/-}$ background, but as expected from the increase in thymus size, there was a significant increase in the numbers of BrdU$^+$ thymocytes in DR3$^{-/-}$ H-Y male mice (Fig. 3C). Significantly, the numbers of transgenic Vβ8$^+$ thymocytes were increased and accounted for the rise in observed BrdU uptake (Fig. 3C).

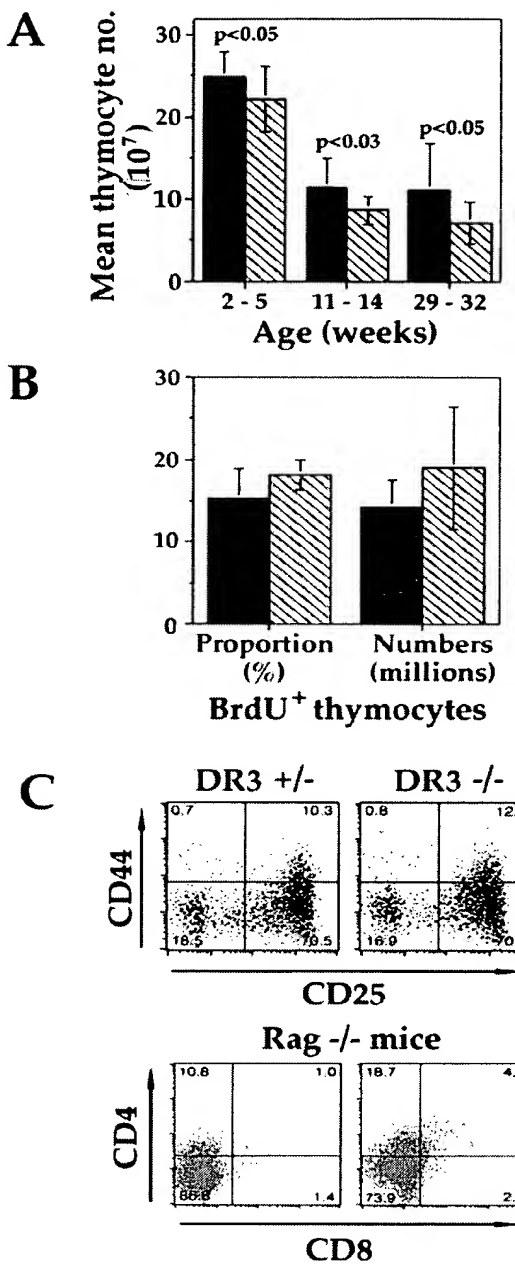

FIG. 2. Analysis of thymocyte development in $DR3^{+/-}$ and $DR3^{-/-}$ mice. (A) Thymus size in $DR3^{-/-}$ mice. Total thymocyte numbers were collected for mice at the ages indicated ($DR3^{+/-}$ and $DR3^{-/-}$, $n \geq 11$ and $n \geq 10$, respectively, for each age group), and means were generated. $DR3^{-/-}$ thymuses were generally larger than their $DR3^{-/-}$ counterparts, irrespective of age. Significance using t tests is indicated. (B) Turnover and proliferation in $DR3^{-/-}$ thymus. The proportion (left) and number (right) of $BrdU^+$ thymocytes were estimated as described in Materials and Methods. Filled bars, $DR3^{-/-}$; hatched bars, $DR3^{+/-}$. (C) Early thymocyte development in $DR3^{-/-}$ mice. Upper panels depict representative FACS plots showing expression of CD44 and CD25 in early thymocyte subsets from $DR3^{+/-}$ (left) and $DR3^{-/-}$ (right) mice. Thymocytes were extracted and depleted of cells expressing CD4 and CD8 using specific antibodies and complement. The remaining thymocytes were stained with anti-CD44-PE, anti-CD25-biotin with streptavidin-Tricolor and anti-CD4-FITC, anti-CD8-FITC, anti-B220-FITC, γδTCR-FITC, and αβTCR-FITC. DN thymocytes were analyzed by gating on the $CD4^-$, $CD8^-$, $B220^-$, $\alpha\beta TCR^-$, and $\gamma\delta TCR^-$ populations. Lower panels depict representative FACS plots showing CD4 and CD8 thymocyte subsets in Rag-1-deficient $DR3^{+/-}$ (left) and $DR3^{-/-}$ (right) mice.

One means by which thymocytes escape negative selection in male H-Y transgenic mice is by down-regulation of the CD8 coreceptor, allowing a small proportion of $T3.70^+$ transgenic thymocytes to migrate to the periphery (22). Thus, $CD8^{lo}$ $T3.70^+$ T cells can be detected in the peripheral lymphoid organs, though these cells remain unresponsive to H-Y antigen due to undefined peripheral tolerance mechanisms. Increased down-regulation of the CD8 coreceptor may therefore be one possible mechanism for the defect in negative selection that is observed in $DR3^{-/-}$ H-Y TCR transgenic mice. However, as shown in Fig. 3A and D, there was an increased proportion of $CD8^+$ $T3.70^+$ thymocytes in male $DR3^{-/-}$ mice compared to their heterozygous littermates, demonstrating that coreceptor down-regulation is not the major mechanism of escape from negative selection in these mice. A reduction in the surface level of the H-Y TCR may also enable thymocytes to escape negative selection. However, as shown in Fig. 3D, surface H-Y TCR levels were equivalent in $DR3^{-/-}$ and $DR3^{+/-}$ mice.

Defective negative selection in male H-Y TCR transgenic $DR3^{-/-}$ mice might be expected to result in an equivalent increase in the $CD8^+$ $T3.70^+$ T-cell load in the peripheral lymphoid organs. To test this possibility, the number of transgenic peripheral T cells was determined. As no differences in the development of different lymph nodes were observed in $DR3^{-/-}$ mice (data not shown), inguinal lymph nodes from H-Y TCR transgenic mice were used as a representative lymph node. While no differences were detected in inguinal lymph nodes, a significant increase (~40%) in the numbers of $CD8^+$ $T3.70^+$ T cells was observed in the spleens of $DR3^{-/-}$ mice.

A previous analysis has revealed that mice deficient in the expression of CD30, a TNFR family member that lacks a death domain, exhibit defective negative selection (2). Since CD30 maps to the same chromosomal location as DR3 (8), it is possible that the observed negative selection defect in DR3-null mice is a consequence of an indirect effect of the gene targeting strategy on CD30 gene expression. To rule out this possibility, CD30 expression on thymocytes from $DR3^{-/-}$ mice was assayed by flow cytometry. There were no differences in the overall proportions of CD30-expressing thymocytes between $DR3^{-/-}$ thymocytes and their heterozygous or wild-type littermates. However, a more detailed analysis identified a $CD4^{lo}$ $CD8^{lo}$ $CD30^+$ population that was significantly reduced in $DR3^{-/-}$ mice compared to their $DR3^{+/-}$ counterparts (data not shown). The reduction in this thymocyte subset is age dependent, but $CD4^{lo}$ $CD8^{lo}$ $CD30^+$ cells were generally lower in both proportion and number in $DR3^{-/-}$ mice. There were no significant differences in this subset between $DR3^{+/-}$ and $DR3^{+/+}$ mice (data not shown).

Endogenous superantigen-mediated deletion of T cells is unaffected in DR3-deficient mice. T cells expressing TCRs that recognize minor lymphocyte-stimulating determinants en-

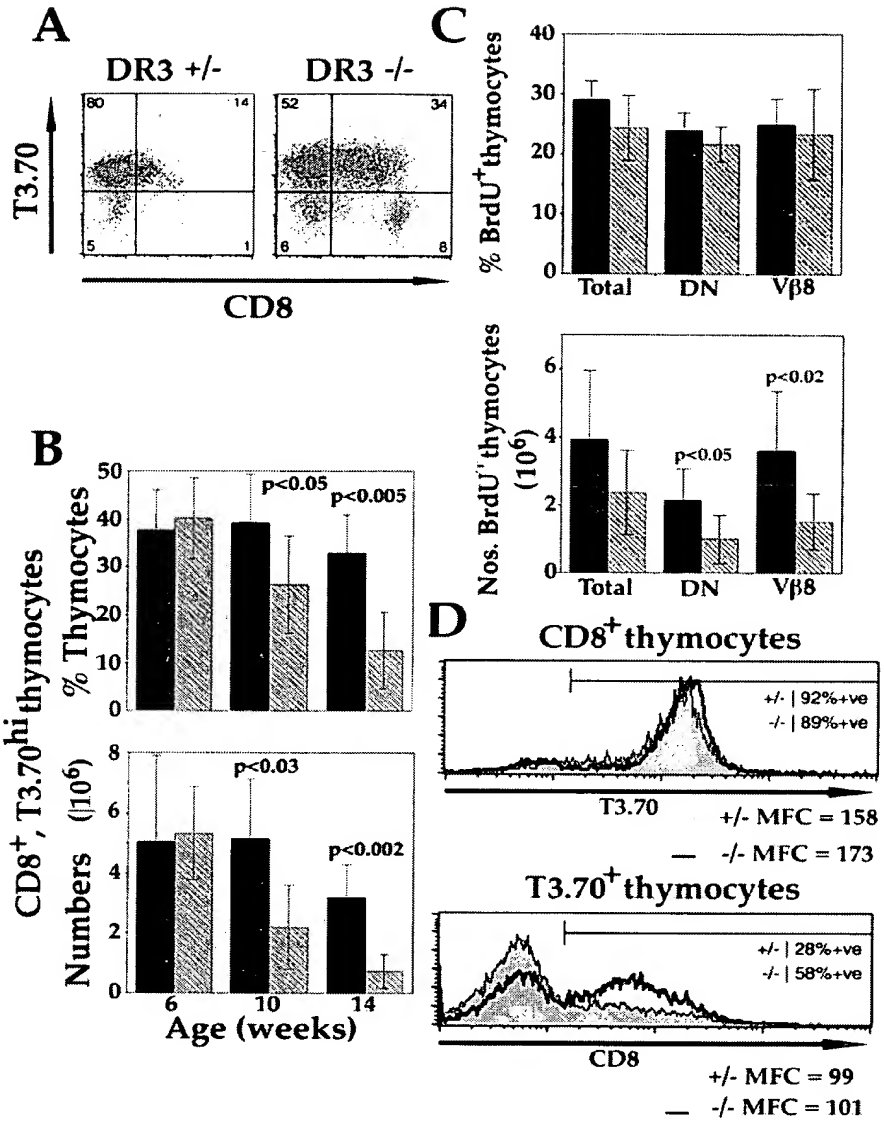

FIG. 3. Negative selection in male DR3$^{-/-}$ × H-Y transgenic mice. (A) Representative FACS plots showing expression of CD8 and T3.70 in 14-week-old male H-Y transgenic mice. Thymocytes were extracted and stained with anti-CD4-PE, anti-CD8-Tricolor, and anti-T3.70-FITC. DR3$^{-/-}$ × H-Y mice (right) showed an increase in the proportions of CD8$^+$ T3.70$^+$ thymocytes compared to their DR3$^{+/-}$ × H-Y littermates. (B) Proportions and numbers of CD8$^+$ T3.70$^+$ thymocytes in H-Y TCR transgenic DR3$^{-/-}$ and DR3$^{+/-}$ mice with age. Male DR3$^{-/-}$ × H-Y mice showed higher proportions (top) and numbers (bottom) of CD8$^+$ T3.70$^+$ thymocytes with age compared to their DR3$^{+/-}$ × H-Y littermates. Differences were statistically significant using parametric (for numbers) or nonparametric (for percentages) t tests from 10 weeks of age and are indicated on the graphs. Means were calculated from $n \geq 7$ mice. Standard deviations of the means are indicated by bars. Filled bars, DR3$^{-/-}$; hatched bars, DR3$^{+/-}$. (C) BrdU uptake of male DR3$^{-/-}$ × H-Y transgenic mice, determined as described in Materials and Methods. The mean from $n \geq 5$ mice for each thymocyte population is shown. All mice were 10 weeks of age (±1 day). Proportions (top) of BrdU$^+$ thymocytes did not differ between H-Y transgenic, DR3$^{-/-}$ and DR3$^{+/-}$ mice, but numbers (bottom) of BrdU$^+$ thymocytes were increased in DR3$^{-/-}$ × H-Y mice compared to their DR3$^{+/-}$ littermates at 10 weeks of age. Increased numbers of total BrdU$^+$ cells were due to increases in the BrdU$^+$ DN and transgenic Vβ8$^+$ thymocyte populations. Filled bars, DR3$^{-/-}$; hatched bars, DR3$^{+/-}$. (D) CD8 and T3.70 expression on DR3$^{-/-}$ × H-Y transgenic thymocytes. Thymocytes were extracted from 10-week-old mice and stained with anti-CD4-PE, anti-CD8-Tricolor, and anti-T3.70-FITC. Thymocytes were either gated for CD8 expression and their T3.70 expression (top) or gated for high T3.70 expression and their CD8 expression shown (bottom). Representative overlay histograms are displayed and labeled with the proportion of positive cells and the level of each surface marker, as measured by their mean fluorescence channel (MFC). Male DR3$^{-/-}$ × H-Y mice (thick line) showed an increase in the proportion of T3.70^{hi} thymocytes expressing CD8 compared to their DR3$^{+/-}$ × H-Y (shaded) littermates but no difference in the level of CD8 expression (lower panel). There was no significant difference in the proportion of CD8$^+$ thymocytes expressing T3.70 or the level of T370 expression on CD8$^+$ thymocytes compared with male DR3$^{-/-}$ and DR3$^{+/-}$ H-Y transgenic mice.

TABLE 1. MMTV superantigen deletion of CD4 and CD8 SP cells

SP cell type	Thymus		Spleen		Lymph node	
	Vβ5	Vβ8	Vβ5	Vβ8	Vβ5	Vβ8
CD4						
$DR3^{+/+}$	3.0 ± 0.4	15.0 ± 1.3	2.7 ± 0.6	17.5 ± 1.8	2.2 ± 0.3	19.0 ± 0.8
$DR3^{-/-}$	3.2 ± 0.9	13.7 ± 1.3	2.5 ± 0.3	17.3 ± 1.5	2.2 ± 0.1	18.5 ± 0.2
CD8						
$DR3^{+/+}$	10.7 ± 0.9	9.9 ± 1.3	12.4 ± 0.6	17.9 ± 1.2	13.3 ± 0.8	16.0 ± 1.5
$DR3^{-/-}$	11.0 ± 4.1	7.4 ± 1.1	14.8 ± 2.0	19.7 ± 3.7	13.0 ± 0.3	16.6 ± 1.7

coded by endogenous superantigens in the mouse genome together with MHC class II molecules are deleted. Minor lymphocyte-stimulating determinants expressed on the 129 × C57BL/6 background of DR3-deficient mice result in the deletion of several Vβ-expressing $CD4^+$ T cells including Vβ5 (1). To determine whether endogenous superantigen-driven deletion is defective in DR3-null mice, lymph node T cells, splenic T cells, and SP thymocytes were analyzed using antibodies to specific Vβ families. As shown in Table 1, Vβ5-bearing $CD4^+$ T cells were efficiently deleted in DR3-null mice, whereas the proportion of nondeleting Vβ8 cells was unaffected. These data show that DR3 is not essential for superantigen-mediated deletion.

Anti-CD3-induced, but not non-antigen receptor-mediated, apoptosis is impaired in DR3-deficient mice. Immature DP thymocytes and T cells are susceptible to an array of cell death-inducing stimuli, including anti-CD3 cross-linking, glucocorticoid treatment, Fas ligation, and DNA-damaging agents. To assess whether these forms of apoptosis are also dependent on DR3 expression, thymocytes and peripheral T cells were subjected to treatment with anti-CD3 cross-linking, the steroid dexamethasone, the DNA-damaging agent etoposide, and the protein synthesis inhibitor cycloheximide in conjunction with an anti-Fas signal.

Using propidium iodide to exclude all dead cells and annexin V surface labeling, the proportion of live thymocytes undergoing early stages of apoptosis was measured at different time points up to 48 h after stimulation. Cross-linking of surface CD3 on $DR3^{-/-}$ thymocytes resulted in significantly reduced levels of apoptosis compared to $DR3^{+/-}$ thymocytes at lower concentrations of anti-CD3 MAb (2 μg/ml [Fig. 4A and B] and 10 μg/ml [data not shown]) but not higher concentrations (50 μg/ml) of coating anti-CD3 MAb (data not shown). The reduction in the proportion of apoptosing cells induced by anti-CD3 treatment was observed at 12 h (data not shown) 24 and 48 h (Fig. 4B) and ranged from 15 to 45%. In contrast, the levels of apoptosis of thymocytes induced by PMA or anti-CD3 and anti-CD28 (Fig. 4B) were indistinguishable between $DR3^{+/-}$ and $DR3^{-/-}$ thymocytes.

In contrast, neither $DR3^{-/-}$ thymocytes nor lymphocytes extracted from inguinal lymph nodes were resistant to any of the other apoptosis-inducing agents used. There were no differences in the rate of apoptosis over 48 h following treatment with these agents compared to lymphocytes from $DR3^{+/+}$ and $DR3^{+/-}$ mice (Fig. 5).

We extended these investigations by performing proliferation assays using a variety of polyclonal stimulators. Previous studies have shown that lymphocytes from transgenic mice expressing a dominant negative form of FADD, a downstream signaling molecule of DR3, have impaired proliferative ability (34, 56). Therefore, the ability of DR3-deficient thymocytes and T cells to respond to a variety of proliferative stimuli was assessed. $DR3^{-/-}$ lymph node cells, splenocytes, and thymocytes exhibited no impairments in proliferation to anti-CD3, anti-CD3, and anti-CD28, concanavalin A, or PMA plus iono-

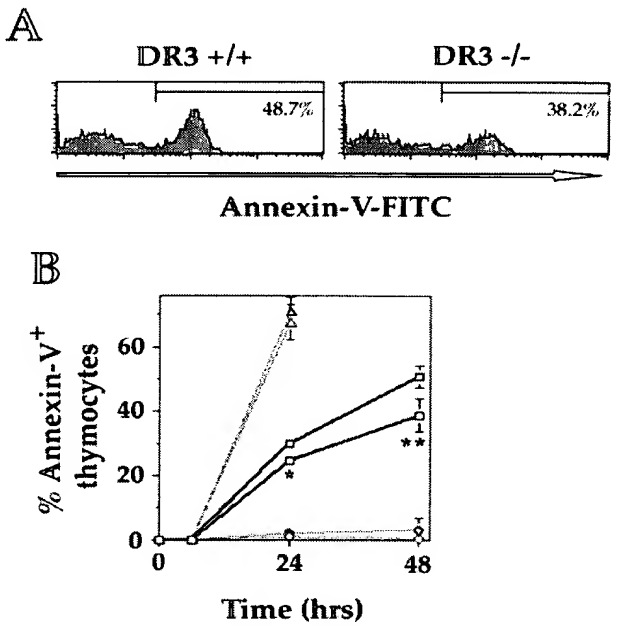

FIG. 4. Apoptosis of thymocytes following CD3 ligation. (A) Representative FACS histograms showing reduced proportions of annexin V-positive thymocytes from $DR3^{-/-}$ mice compared to $DR3^{+/+}$ age- and sex-matched controls after CD3 cross-linking. A stimulation of 2 μg/ml was used, and thymocytes were stained after 48 h. Dead cells were gated out using propidium iodide. (B) Thymocyte suspensions were stimulated for up to 48 h with plate bound anti-CD3 or rat Ig as a negative control. Percent apoptosis was measured as the proportion of propidium iodide-negative thymocytes, which were positive for annexin V. Anti-CD3 treatment at 2 μg/ml resulted in an increase of 50.7% in apoptosing thymocytes above rat Ig controls by 48 h in $DR3^{+/-}$ thymocytes (filled squares) compared to 38.7% in $DR3^{-/-}$ thymocytes (open squares). There were no differences in apoptosis of $DR3^{-/-}$ (open) and $DR3^{+/+}$ (filled) thymocytes following stimulation with PMA (triangles) or anti-CD3 and anti-CD28 (circles). Results are the means of 3 $DR3^{-/-}$ and $DR3^{+/-}$ littermates, with duplicate cultures performed on each mouse. Standard deviations are shown as bars. * and ** represent $P < 0.0003$ and $P < 0.004$, respectively, using *t* tests assuming unequal variance.

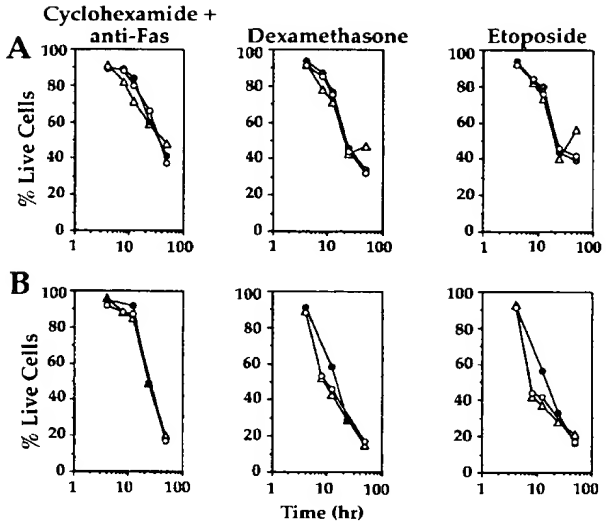

FIG. 5. Apoptosis of thymocytes and lymphocytes after exposure to various apoptosis inducing agents. Assays were carried out over 48 h with apoptosis measured using annexin V-FITC staining or sub-G_1 peak following staining with propidium iodide as described in Materials and Methods. There were no differences in the induction of apoptosis using cycloheximide and anti-Fas, dexamethasone, or etoposide on thymocytes (A) or lymphocytes (B) derived from inguinal lymph nodes from $DR3^{+/+}$ (open triangles), $DR3^{+/-}$ (closed circles), or $DR3^{-/-}$ (open circles) mice.

mycin compared to heterozygote or wild-type littermates (Fig. 6).

Positive selection is unimpaired in $DR3^{-/-}$ mice. The αβTCR is first expressed at the DP stage, resulting in a population of $\alpha\beta TCR^{lo}$ and $CD3^{lo}$ thymocytes which then undergo positive selection to generate the $\alpha\beta TCR^{hi}$ and $CD3^{hi}$ SP subsets. Positively selected thymocytes also transiently up-regulate the expression of CD69. Analysis of CD3 and CD69 expression on thymocytes from DR3-deficient mice showed no significant difference in the proportions of $CD3^{hi}$ or CD69-positive cells between DR3-null mice and their heterozygous littermates, suggesting that DR3 is not absolutely required for positive selection (data not shown). This conclusion was consistent with a flow cytometric analysis of DR3-deficient female mice expressing the H-Y TCR. No difference was observed in the numbers or proportions of H-Y TCR-expressing CD8 SP cells between DR3-expressing or -deficient thymocytes (Table 2). The H-Y TCR is $H\text{-}2K^b$ restricted and therefore selects on both C57BL/6 and 129 mouse strain backgrounds. Thus, the mixed strain nature of the knockouts should not affect the efficiency of positive or negative selection. Taken together, these results demonstrate that DR3 is not required for positive selection during thymocyte development.

DISCUSSION

DR3 belongs to a family of receptors that plays an important role in regulating cell survival and proliferation. These processes are tightly regulated during T-cell development. Thus, signals originating from the pre-TCR mediate the survival and

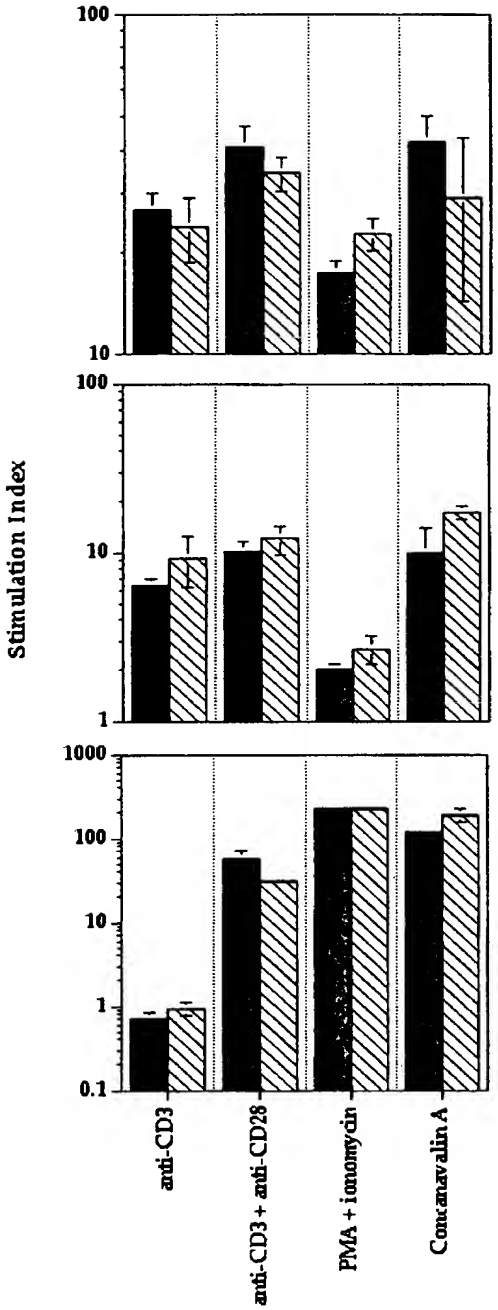

FIG. 6. Proliferation of lymphocytes, thymocytes, and splenocytes to various stimuli Assays were carried out over 96 h with proliferation measured by [^{3}H]thymidine uptake over the final 18 to 24 h as described in Materials and Methods. There were no significant differences in thymidine uptake of lymphocytes (top), splenocytes (middle), or thymocytes (bottom) between $DR3^{+/-}$ and $DR3^{-/-}$ cells using anti-CD3, anti-CD3, and anti-CD28, PMA and ionomycin, or concanavalin A as stimuli. Data are presented as a stimulation index over medium-only controls, which were not significantly different between $DR3^{+/-}$ and $DR3^{-/-}$ cells. Filled bars, $DR3^{-/-}$; hatched bars, $DR3^{+/+}$.

TABLE 2. Positive selection in female H-Y transgenic DR3$^{-/-}$ and DR3$^{+/-}$ mice

Organ (cell type)	Age (wk)	No. of cells (10^6 ± SD)[a]	
		KO (*n*)	HET (*n*)
Thymus (all thymocytes)	6	129 ± 29 (7)	134 ± 42 (10)
	10	95 ± 29 (7)	98 ± 31 (12)
	14	74 ± 49 (7)	75 ± 24 (6)
Thymus (CD8$^+$ T370$^+$)	6	33.2 ± 12.1 (7)	51.8 ± 30.3 (10)
	10	25.4 ± 7.3 (7)	31.1 ± 13.3 (12)
	14	24.4 ± 10.0 (7)	22.2 ± 6.5 (6)
Spleen (CD8$^+$ T370$^+$)	6	2.9 ± 0.4 (7)	3.3 ± 2.1 (10)
	10	4.7 ± 4.0 (7)	4.8 ± 2.1 (12)
	14	2.7 ± 1.6 (7)	3.2 ± 1.7 (6)
Inguinal LN (CD8$^+$ T370$^+$)	6	0.38 ± 0.21 (7)	0.68 ± 0.56 (10)
	10	0.39 ± 0.16 (7)	0.66 ± 0.35 (12)
	14	0.73 ± 0.52 (7)	0.63 ± 0.34 (6)

[a] In all cases, the difference between KO and HET values was nonsignificant.

proliferation of pre-T cells that have undergone in-frame TCRβ gene rearrangements. The αβTCR controls the survival of DP thymocytes, selecting those cells expressing TCR with intermediate affinity for MHC ligand and inducing programmed cell death of high-affinity, autoreactive T cells. DP thymocytes that fail to express an αβTCR also undergo apoptosis. The expression of DR3 in developing thymocytes prompted the hypothesis that it is a key regulator of life/death decisions during thymocyte development. This notion was tested by generating and analyzing mice deficient in DR3 expression.

TNFR family members containing death domains (TNFR1, Fas, DR3, DR4, DR5, and DR6) transduce death signals by interaction of their death domains with FADD, a death domain-containing cytoplasmic protein. FADD then recruits other cytoplasmic effectors such as caspase 8, TRADD, TRAF2, and RIP that activate the apoptotic machinery (41). Studies of transgenic mice expressing DN-FADD in developing thymocytes have given rise to the hypothesis that stimulation of death domain-containing TNFRs on early pre-T cells induces cell death via FADD only in the absence of pre-TCR-derived signals (33). In the presence of pre-TCR-derived signals, the TNFR signals proliferation. The present study demonstrates that DR3, which is expressed on early and late pre-T cells, is not essential for the transduction of apoptosis or proliferation signals at the pre-TCR-mediated developmental checkpoint. It may, however, participate in the regulation of β-selected thymocytes in concert with other death receptors, such as DR5, Fas, and TNFR1. An analysis of mice deficient in the expression of multiple death receptors would resolve this question.

The DP-to-SP thymocyte transition is associated with extensive cell death. The pathway(s) that, in concert with signals derived from high-affinity TCRs, induce apoptosis in DP thymocytes have not been defined. TNFRs have, however, been implicated in negative selection in the thymus. Thus, a role for Fas in negative selection at high doses of antigen has been proposed (23). Also, negative selection has been shown to be either enhanced following CD30 overexpression (9) or partially impaired in mice deficient in the expression of CD30, a non-death domain-containing member of the TNFR superfamily (2). We show here that DR3 is also important for negative selection, which is impaired in the absence of this receptor. Thus, the induction of apoptosis in DP thymocytes by anti-CD3, an agonist that is presumed to mimic a high-affinity TCR interaction, is impaired at least at low concentrations of anti-CD3 (2 and 10 μg/ml) in DR3-null mice. Interestingly, this effect is abrogated by high anti-CD3 concentrations, suggesting a greater contribution of DR3 to apoptosis when the signaling strength is not maximal. Also, the deletion of H-Y TCR transgenic thymocytes in male mice is partially inhibited, an effect which is manifested most clearly in older mice. Although the numbers and proportions of H-Y TCR transgenic thymocytes were indistinguishable between DR3$^{-/-}$ and DR3$^{+/-}$ backgrounds in 6-week-old male mice, a significant inhibition of negative selection occurred in DR3-null mice at 10 weeks, at 14 weeks, when H-Y TCR-expressing thymocytes were virtually undetectable in most male mice expressing DR3, transgene-positive cells were easily detectable in all DR3-null mice analyzed. However, substantial negative selection had clearly occurred in male DR3-null mice, since at 14 weeks, male thymuses contained only about 1/100 the numbers of cells found in the thymuses of female transgenic mice.

The notion that death domain-containing TNFRs play a role in negative selection is in apparent contradiction to studies of mice expressing DN-FADD in thymocytes. In one such study, negative selection was unaffected by DN-FADD, although in this study negative selection was assayed in 6-week-old H-Y TCR male mice (50). At this age, we observed no difference in negative selection in the presence or absence of DR3. In an independent study, the deletion of autoreactive thymocytes was enhanced in H-Y TCR$^+$ DN-FADD$^+$ male thymocytes (34). These studies suggest that FADD signaling does not lead exclusively to cell death in thymocytes. This, in turn, suggests that FADD-independent pathways from death domain-containing TNFRs activate caspases in negative selection. Adapter molecules such as RIP, RAIDD, and Daxx have been shown to interact with the CD95 death domain, thereby activating a caspase cascade leading to apoptosis (15, 55). It is possible that these cytoplasmic signaling molecules also transduce DR3-mediated signals in thymocytes. A recent study has, however, failed to support a role for caspase activity in negative selection. In this study, mice expressing an inhibitor (p35) of caspase activity in thymocytes showed unimpaired negative selection (14). However, an independent study, using an identical strategy, revealed a reduction of negative selection upon inhibition of caspase activity (21). Therefore, the role of caspases in thymocyte negative selection remains unresolved.

The observation that DR3-null mice exhibit a partial impairment of negative selection can be interpreted within a model in which several different surface molecules act in concert to control the removal of autoreactive thymocytes (23). According to this model, disruption of a single surface receptor or signal transduction pathway would not be expected to result in a complete block in negative selection, a prediction that is observed in practice. The age dependency of the negative selection defect in DR3-null mice in H-Y TCR-transgenic mice may be due to developmental regulation of the ligand(s) for DR3 or, alternatively, to the developmental stage at which deletion occurs in the H-Y TCR model which is likely to be at the DN stage or in the transition from DN to DP thymocytes.

Thus, the relative importance of a particular deletional mechanism may vary with age or with the stage of thymocyte development at which deletion of a particular TCR occurs.

Despite the impairment of negative selection in DR3-null mice, there were no signs of autoimmunity in these mice as indicated by the presence of DNA autoantibodies, nor was development of autoimmunity significantly accelerated on an *lpr* (Fas mutant) background (unpublished data). Furthermore, several other forms of apoptosis were unaffected. There was no difference in the rate of spontaneous cell death of thymocytes in culture or of the rate of apoptosis of thymocytes or T cells after treatment with glucocorticoids, DNA-damaging agents, or anti-Fas in the presence of protein synthesis inhibitors. Moreover, no difference in endogenous superantigen-mediated deletion of T cells was detected. This observation is consistent with the analysis of other transgenic models with defects in negative selection. For example, CD30-null mice (2) and mice lacking expression of the helix-loop-helix inhibitor protein Id3 (38) have impaired negative selection, but T cells specific for endogenous superantigens are efficiently deleted. Conversely, the antiapoptotic protein Bcl-2 inhibits multiple forms of apoptosis but not endogenous superantigen-induced negative selection in thymocytes (43), although *bcl-2* transgenic mice have impaired negative selection when tested on a TCR transgenic background (45, 54). Taken together with the present study, these data suggest that there are qualitatively or quantitatively distinct cell death programs that operate at different stages of T-cell development to ensure effective central tolerance.

ACKNOWLEDGMENTS

We thank J. Williamson for chromosome counting of ES cell clones, I. Rosewell and his group for microinjections and chimeric mouse breeding, P. Hagger and colleagues for breeding and maintenance of the $DR3^{-/-}$ mouse colony, and P. Kieselow and H. von Boehmer for the kind gift of MAb T3.70.

This work was supported by the Imperial Cancer Research Fund. Eddie Wang was the recipient of a fellowship from the Beit Memorial Foundation for Medical Research, Anette Thern is a fellow of the Swedish Cancer Society, and Angela Denzel was the recipient of a Glaxo-Wellcome-BBSRC CASE Studentship.

REFERENCES

1. **Acha-Orbea, H.** 1995. Superantigens and tolerance, p. 224–265. *In* J. I. Bell M. I. Owen, and E. Simpson (ed.), T cell receptors. Oxford University Press, Oxford, United Kingdom.
2. **Amakawa, R., A. Hakem, T. M. Kundig, T. Matsuyama, J. J. L. Simard, E. Timms, A. Wakeham, H.-W. Mittruecker, H. Griesser, H. Takimoto, R. Schmits, A. Shahinian, P. S. Ohashi, J. M. Penninger, and T. W. Mak.** 1996. Impaired negative selection of T cells in Hodgkin's disease antigen CD30-deficient mice. Cell **84**:551–562.
3. **Baker, S. J., and E. P. Reddy.** 1998. Modulation of life and death by the TNF receptor superfamily. Oncogene **17**:3261–3270.
4. **Banner, D. W., A. D'Arey, W. Janes, R. Gentz, H. J. Schoenfeld, C. Broger, H. Loetscher, and W. Lesslauer.** 1993 Crystal structure of the soluble human 55 kD TNF receptor-human TNF beta complex: implications for TNF receptor activation. Cell **73**:431–445.
5. **Bodmer, J.-L., K. Burns, P. Schneider, K. Hoffman, V. Steiner, M. Thome, T. Bornand, M. Hahne, M. Schroter, K. Becker, A. Wilson, L. E. French, J. L. Browning, H. Robson Macdonald, and J. Tschopp.** 1997. TRAMP, a novel apoptosis-mediating receptor with sequence homology to tumor necrosis factor receptor 1 and Fas (Apo-1/CD95). Immunity **6**:79–88.
6. **Boldin, M. P., E. E. Verfolomeev, C. Pancer, I. L. Mett, J. H. Carmonis, and D. Wallach.** 1995. A novel protein that interacts with the death domain of Fas/Apo1 contains a sequence motif related to the death domain. J. Biol. Chem. **270**:7795–7787.
7. **Boldin, M. P., T. M. Goncharov, Y. V. Goltsev, and D. Wallach.** 1996. Involvement of MACH, a novel MORT1/FADD-interacting protease, in Fas/APO-1- and TNF receptor-induced cell death. Cell **85**:803–815.
8. **Bowen, M. A., R. K. Lee, G. Miraglilotta, S. Y. Nam, and E. R. Podack.** 1996. Structure and expression of murine CD30 and its role in cytokine production. J. Immunol. **156**:442–449.
9. **Chiarle, R., A. Podda, G. Prolla, E. R. Podack, G. J. Thorbecke, and G. Inghirami.** 1999. CD30 overexpression enhances negative selection in the thymus and mediates programmed cell death via a Bcl-2 sensitive pathway. J. Immunol. **163**:194–205.
10. **Chicheportiche, Y., P. R. Bourdon, H. Xu, Y. M. Hsu, H. Scoyy, C. Hession, I. Garcia, and J. L. Browning.** 1997. TWEAK, a new secreted ligand in the tumor necrosis factor family that weakly induces apoptosis. J. Biol. Chem. **272**:32401–32410.
11. **Chinnaiyan, A. M., K. O'Rourke, G. L. Yu, R. H. Lyons, M. Garg, D. R. Duan, L. Xing, R. Gentz, J. Ni, and V. M. Dixit.** 1996. Signal transduction by DR3, a death domain-containing receptor related to TNFR-1 and CD95. Science **274**:990–992.
12. **Chinnaiyan, A. M., K. O'Rourke, M. Tewari, and V. M. Dixit.** 1995. FADD, a novel death domain-containing protein, interacts with the death domain of Fas and initiates apoptosis. Cell **81**:505–512.
13. **Dixit, V. M.** 1996. The cell-death machine. Curr. Biol. **6**:555–562.
14. **Doerfler, P., K. A. Forbush, and R. M. Perlmutter.** 2000. Caspase enzyme activity is not essential for apoptosis during thymocyte development. J. Immunol. **164**:4071–4079.
15. **Duan, H., and V. M. Dixit.** 1997. RAIDD is a new "death" adaptor molecule. Nature **385**:86–89.
16. **Grenet, J., V. Valentine, J. Kitson, H. Li, S. N. Farrow, and V. J. Kidd.** 1998. Duplication of the DR3 gene on human chromosome 1p36 and its deletion in human neuroblastoma. Genomics **49**:385–393.
17. **Henkart, P. A.** 1996. ICE family proteases: mediators of all apoptotic cell death? Immunity **4**:195–201.
18. **Hsu, H., S. B. Shu, M. G. Pan, and D. V. Goeddel.** 1996. TRADD-TRAF2 and TRADD-FADD interactions define two distinct TNF receptor 1 signal transduction pathways. Cell **84**:299–308.
19. **Hunter, T., and M. Karin.** 1992. The regulation of transcription by phosphorylation. Cell **70**:375–387.
20. **Itoh, N., S. Yonehara, A. Ishii, M. Yonehara, S. Mizushima, M. Sameshima, A. Hase, Y. Seto, and S. Nagata.** 1991. The polypeptide encoded by the cDNA for human cell surface antigen Fas can mediate apoptosis. Cell **66**: 233–243.
21. **Izquierdo, M., A. Grandien, L. M. Criado, S. Robles E. Leonardo, J. P. Albar, G. G. de-Buitrago, and A. C. Martinez.** 1999. Blocked negative selection of developing T cells in mice expressing the baculovirus p35 caspase inhibitor. EMBO J. **18**:156–166.
22. **Kieselow, P., H. Bluthmann, U. D. Staerz, M. Steinmetz, and H. von Boehmer.** 1988. Tolerance in T-cell-receptor transgenic mice involves deletion of nonmature $CD4^+8^+$ thymocytes. Nature **333**:742–746.
23. **Kishimoto, H., and J. Sprent.** 1999. Several different cell surface molecules control negative selection of medullary thymocytes. J. Exp. Med. **190**:65–73.
24. **Kitson, J., T. Raven, Y. P. Jiang, D. V. Goeddel, K. M. Giles, K. T. Pun, C. J. Grinham, R. Brown, and S. N. Farrow.** 1996. A death domain-containing receptor that mediates apoptosis. Nature **384**:372–375.
25. **Koni, P. A., and R. A. Flavell.** 1998. A role for tumor necrosis factor receptor type 1 in gut-associated lymphoid tissue development: genetic evidence of synergism with lymphotoxin β. J. Exp. Med. **187**:1977–1983.
26. **Koni, P. A., R. Sacca, P. Lawton, J. L. Browning, N. H. Ruddle, and R. A. Flavell.** 1997. Distinct roles in lymphoid organogenesis for lymphotoxins α and β revealed in lymphotoxin β-deficient mice. Immunity **6**:491–500.
27. **Kumar, S.** 1996. ICE-like proteases in apoptosis. Trends Biochem. Sci. **20**:198–202.
28. **Lucas, B., F. Vasseur, and C. Penit.** 1997. Normal sequence of phenotypic transitions in one cohort of 5-bromo-2'-deoxyuridine-pulse labeled thymocytes. J. Immunol. **151**:4574–4582.
29. **Marsters, S. A., J. P. Sheridan, C. J. Donahue, R. M. Pitti, C. L. Gray, A. D. Goddard, K. D. Bauer, and A. Ashkenazi.** 1996. Apo-3, a new member of the tumor necrosis factor receptor family, contains a death domain and activates apoptosis and NF-κB. Curr. Biol. **6**:1669–1676.
30. **Marsters, S. A., J. P. Sheridan, R. M. Pitti, J. Brush, A. Goddard, and A. Ashkenazi.** 1998. Identification of a ligand for the death-domain-containing receptor Apo3. Curr. Biol. **8**:525–528.
31. **Muzio, M., A. M. Chinnaiyan, F. C. Kischkel, K. O'Rourke, A. Shevchenko, J. Ni, C. Scaffidi, J. D. Bretz, M. Zhang, R. Gentz, M. Mann, P. H. Krammer, M. E. Peter, and V. M. Dixit.** 1996. FLICE, a novel FADD-homologous ICE/CED-3-like protease, is recruited to the CD95(Fas/APO-1) death-inducing signaling complex. Cell **85**:817–827.
32. **Neumann, B. A., K. Luz, K. Pfeffer, and B. Holzmann.** 1996. Defective Peyer's patch organogenesis in mice lacking the 55-kD receptor for tumor necrosis factor. J. Exp. Med. **184**:259–264.
33. **Newton, K., A. W. Harris, and A. Strasser.** 2000. FADD/MORT1 regulates the pre-TCR checkpoint and can function as a tumor suppressor gene. EMBO J. **19**:931–941.
34. **Newton, K., A. W. Harris, M. L. Bath, K. C. G. Smith, and A. Strasser.** 1998. A dominant interfering mutant of FADD/MORT1 enhances deletion of

autoreactive thymocytes and inhibits proliferation of mature T lymphocytes. EMBO J. **17**:706–718.
35. **Orlinick, J. R., and M. V. Chao.** 1998. TNF-related ligands and their receptors. Cell Signal. **10**:543–551.
36. **Park, Y. C., V. Burkitt, A. R. Villa, L. Tong, and H. Wu.** 1999. Structural basis for self-association and receptor recognition of human TRAF2. Nature **398**: 533–538.
37. **Pasparakis, M., L. Alexopoulou, M. Grell, K. Pfizenmaier, H. Bleuthmann, and G. Kollias.** 1997. Peyer's patch organogenesis is intact yet formation of B lymphocyte follicles is defective in peripheral lymphoid organs of mice deficient for tumor necrosis factor and its 55-kDa receptor. Proc. Natl. Acad. Sci. USA **94**:6319–6323.
38. **Rivera, R. R., C. P. Johns, J. Quan, R. S. Johnson, and C. Murre.** 2000. Thymocyte selection is regulated by the helix-loop-helix inhibitor protein, Id3. Immunity **12**:17–26.
39. **Roth, M., S. Wong, W. Henzel, and D. V. Goeddel.** 1994. A novel family of putative signal transducers associated with the cytoplasmic domain of the 75 kDa tumor necrosis factor receptor. Cell **78**:681–692.
40. **Schneider, P., R. Schwenzer, E. Haas, F. Muhlenbeck, G. Schubert, P. Scheurich, J. Tschopp, and H. Wajant.** 1999. TWEAK can induce cell death via endogenous TNF and TNF receptor 1. Eur. J. Immunol. **29**:1785–1792.
41. **Screaton, G., and X.-N. Xu.** 2000. T cell life and death signalling via TNF-receptor family members. Curr. Opin. Immunol. **12**:316–322.
42. **Screaton, G. R., X-N. Xu, A. L. Olsen, A. E. Cowper, R. Tan, A. J. McMichael, and J. I. Bell.** 1997. LARD, a new lymphoid-specific death domain containing receptor regulated by alternative pre-mRNA splicing. Proc. Natl. Acad. Sci. USA **94**:4615–4619.
43. **Sentman, C. L., J. R. Shutter, D. Hockenbery, O. Kanagawa, and S. J. Korsmeyer.** 1991. Bcl-2 inhibits multiple forms of apoptosis but not negative selection in thymocytes. Cell **67**:879–888.
44. **Smith, C. A., T. Farrah, and R. G. Goodwin.** 1994. The TNF receptor superfamily of cellular and viral proteins: activation, costimulation and death. Cell **76**:958–962.
45. **Strasser, A., A. W. Harris, H. von Boehmer, and S. Cory.** 1994. Positive and negative selection of T cells in T-cell receptor transgenic mice expressing a bcl-2 transgene. Proc. Natl. Acad. Sci. USA **91**:1376–1380.
46. **Takayama, E., T. Kina, Y. Katsura, and T. Tadakuma.** 1998. Enhancement of activation-induced cell death by fibronectin in murine $CD4^+$ $CD8^+$ thymocytes. Immunology **95**:553–558.
47. **Tan, K. B., J. Harrop, M. Reddy, P. Young, J. Terrett, J. Emery, G. Moore, and A. Truneh.** 1997. Characterization of a novel TNF-like ligand and recently described TNF ligand and TNF receptor superfamily genes and their constitutive and inducible expression in hematopoetic and non-hematopoietic cells. Gene **204**:35–46.
48. **Tartaglia, L. A., T. M. Ayers, G. H. W. Wong, and D. V. Goeddel.** 1993. A novel domain within the 55 kd TNF receptor signals cell death. Cell **74**:845–853.
49. **Teh, H. S., P. Kisielow, B. Scott, H. Kishi, Y. Uematsu, H. Bluthmann, and H. von Boehmer.** 1988. Thymic major histocompatibility complex antigens and the $\alpha\beta$ T-cell receptor determine the CD4/CD8 phenotype of T cells. Nature **335**:229–233.
50. **Walsh, C. M., B. G. Wen, A. M. Chinnaiyan, K. O'Rourke, V. M. Dixit, and S. M. Hedrick.** 1998. A role for FADD in T cell activation and development. Immunity **8**:439–449.
51. **Wang, E. C., J. Kitson, A. Thern, J. Williamson, S. N. Farrow, and M. J. Owen.** Genomic structure, expression and chromosome mapping of the murine homologue for the WSL-1 (DR3, Apo3, TRAMP, LARD, TR3, TNFRSF12) gene. Immunogenetics, in press.
52. **Ware, C. F., S. Vanarsdale, and T. L. Vanarsdale.** 1996. Apoptosis mediated by the TNF-related cytokine and receptor families. J. Cell Biochem. **60**:47–55.
53. **Warzocha, K., P. Ribeiro, C. Charlot, N. Renard, B. Coiffier, and G. Salles.** 1998. A new death receptor 3 isoform: expression in human lymphoid cell lines and non-Hodgkin's lymphomas. Biochem. Biophys. Res. Commun. **242**:376–379.
54. **Williams, O., T. Norton, M. Halligey, D. Kioussis, and H. J. M. Brady.** 1998. The action of Bax and bcl-2 on T cell selection. J. Exp. Med. **188**:1125–1133.
55. **Yang, X., R. Khosravi-far, H. Y. Chang, and D. Baltimore.** 1997. Daxx, a novel Fas-binding protein that activates JNK and apoptosis. Cell **89**:1067–1076.
56. **Zornig, M., A.-O. Huber, and G. Evan.** 1998. p53-dependent impairment of T-cell proliferation in FADD dominant-negative transgenic mice. Curr. Biol. **8**:467–470.

Signal Transduction by DR3, a Death Domain–Containing Receptor Related to TNFR-1 and CD95

Arul M. Chinnaiyan,* Karen O'Rourke,* Guo-Liang Yu,* Robert H. Lyons, Manish Garg, D. Roxanne Duan, Lily Xing, Reiner Gentz, Jian Ni,† Vishva M. Dixit†‡

Tumor necrosis factor receptor–1 (TNFR-1) and CD95 (also called Fas or APO-1) are cytokine receptors that engage the apoptosis pathway through a region of intracellular homology, designated the "death domain." Another death domain–containing member of the TNFR family, death receptor 3 (DR3), was identified and was shown to induce both apoptosis and activation of nuclear factor κB. Expression of DR3 appears to be restricted to tissues enriched in lymphocytes. DR3 signal transduction is mediated by a complex of intracellular signaling molecules including TRADD, TRAF2, FADD, and FLICE. Thus, DR3 likely plays a role in regulating lymphocyte homeostasis.

Apoptosis, or programmed cell death, is a physiologic process essential to the normal development and homeostasis of multicellular organisms (*1*). Derangements of apoptosis contribute to the pathogenesis of several human diseases including cancer, neurodegenerative disorders, and acquired immunodeficiency syndrome (*2*). CD95 and TNFR-1 (*3*) are both members of the TNFR family that also includes TNFR-2, low-affinity nerve growth factor receptor (NGFR), CD40, and CD30 (*4*). Family members are defined by the presence of cysteine-rich repeats in their extracellular domains, but CD95 and TNFR-1 also share a region of intracellular homology, designated the "death domain," which is distantly related to the *Drosophila* suicide gene *reaper* (*5*). Activation of CD95 recruits the Fas-associated death domain–containing molecule FADD (also called MORT1) (*6*), which in turn binds and presumably activates the FADD-like ICE (FLICE; also called MACH1), a member of the interleukin 1β-converting enzyme (ICE) family of proapoptotic proteases (*7*). Although the central role of CD95 is to trigger apoptosis, TNFR-1 can signal an array of diverse biological activities, many of which stem from its ability to activate nuclear factor κB (NF-κB) (*8*). Accordingly, TNFR-1 recruits the multivalent adapter molecule TRADD (TNFR-1–associated death domain protein), which like FADD also contains a death domain (*9*, *10*). Through its associations with a number of signaling molecules, including FADD, TRAF2 (TNFR-associated factor–2), and RIP (receptor interacting protein), TRADD can signal both apoptosis and NF-κB activation (*10*, *11*).

To identify additional receptors, we searched an expressed sequence tag (EST) database (*7*, *12*) for clones with homology to both the extracellular cysteine-rich domain and the intracellular death domain of TNFR-1 and CD95. A compilation of two clones fulfilled the search criteria: HTTBN61, from a human testes tumor library, had homology to the cysteine-rich domain, and HSAVO45, from a human anergic T cell library, had homology to the death domain. Clone HSAVO45 contained sequence identical to the 3′ end of HTTBN61, which was not full-length. To obtain a full-length coding sequence, we screened a human umbilical vein endothelial cell (HUVEC) library with a cDNA insert obtained from clone HTTBN61. Two independent clones were obtained containing an open reading frame encoding a protein of 417 amino acids that exhibited a predicted domain structure for a cell surface receptor (Fig. 1). Residues +1 to +201 constitute a cysteine-rich extracellular domain, with 28 cysteine residues and two potential sites for N-glycosylation (Asn-X-Ser/Thr). The middle of the molecule contains a stretch of 23 uncharged amino acids extending from Trp^{202} to Tyr^{224}, then a basic amino acid (Arg^{225}) characteristic of a transmembrane-spanning domain. The putative cytoplasmic domain comprises the remaining 192 amino acids.

Alignment of the predicted amino acid sequence of the clone with TNFR-1 and CD95 (Fig. 1) showed that the three molecules share significant homology in both the extracellular and intracellular domains. Like all members of the TNFR superfamily, the isolated clone contained characteristic cysteine repeats in its extracellular ligand-binding domain. The identity of the cysteine-rich subdomains of the clone with those of TNFR-1 and CD95 was 26% and 22%, respectively, consistent with the 20 to 30% identity reported for the known TNFR

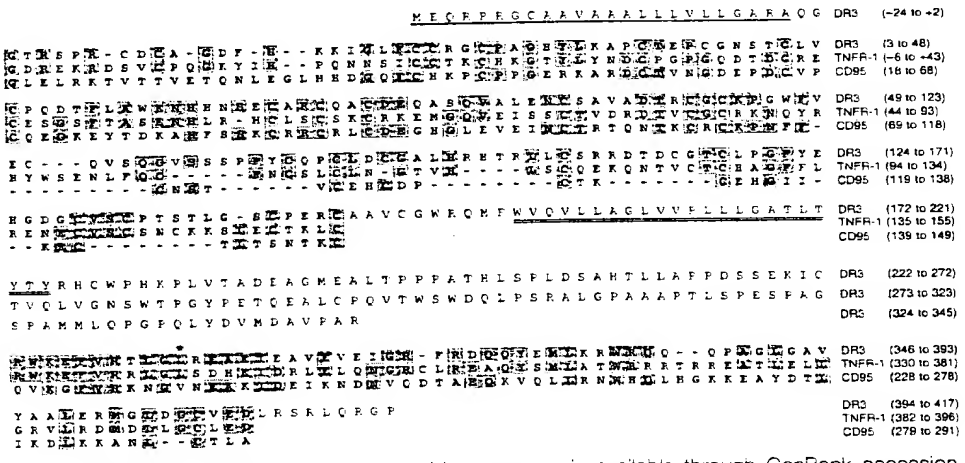

Fig. 1. Sequence analysis of DR3 (nucleotide sequence is available through GenBank accession number U72763) and sequence homology of the DR3 extracellular domain (residues 3 to 191) and intracellular death domain (residues 346 to 408) with the cell death receptors CD95 and TNFR-1. In the deduced amino acid sequence of the DR3 protein product, the putative signal peptide and transmembrane domain are single- and double-underlined, respectively. Alignments were done with Megalign (DNASTAR) software. Shading denotes consensus identical residues. The asterisk indicates a critical amino acid conserved in many death domains, mutation of which leads to inactivation of the receptor and the lpr phenotype in the case of CD95 (*21*). Abbreviations for the amino acid residues are as follows: A, Ala; C, Cys; D, Asp; E, Glu; F, Phe; G, Gly; H, His; I, Ile; K, Lys; L, Leu; M, Met; N, Asn; P, Pro; Q, Gln; R, Arg; S, Ser; T, Thr; V, Val; W, Trp; and Y, Tyr.

A. M. Chinnaiyan, K. O'Rourke, M. Garg, V. M. Dixit, Department of Pathology, University of Michigan Medical School, Ann Arbor, MI 48109, USA.
G.-L. Yu, D. R. Duan, L. Xing, R. Gentz, J. Ni, Human Genome Sciences Inc., 9620 Medical Center Drive, Suite 300, Rockville, MD 20850-3338, USA.
R. H. Lyons, Department of Biological Chemistry, University of Michigan Medical School, Ann Arbor, MI 48109, USA.

*These authors contributed equally to this report.
†These authors share senior authorship.
‡To whom correspondence should be addressed.

amily members. The clone contained significant homology to the death domains of TNFR-1 (47% identity) and CD95 (23% identity). Thus, the clone was designated death receptor 3 (DR3).

To determine the distribution of the DR3 transcript, we subjected various tissues to Northern (RNA) blot analysis. Expression of DR3 was detected in tissues enriched in lymphocytes, including peripheral blood leukocytes (PBLs), thymus, spleen, colon, and small intestine (Fig. 2). DR3 was not detected in any of the other tissues (Fig. 2). In contrast, TNFR-1 is ubiquitously expressed and CD95 is expressed in lymphocytes, liver, heart, lung, kidney, and ovary (13).

In vitro and in vivo binding studies were undertaken to investigate DR3 signaling pathways. As an initial screen, death domain–containing adapter molecules such as FADD, TRADD, and RIP were in vitro translated and precipitated with various glutathione-S-transferase (GST) fusion proteins immobilized on glutathione-Sepharose beads (Fig. 3A). As predicted (6, 9), FADD associated with the GST-Fas cytoplasmic domain, whereas TRADD associated with the GST–TNFR-1 cytoplasmic domain (Fig. 3A). GST–TNFR-1 also weakly interacted with RIP. GST-DR3 associated specifically with TRADD but not with FADD or RIP (Fig. 3A), and a truncated death domain mutant of DR3 (GST-ΔDR3) did not interact with TRADD. To demonstrate the association of DR3 and TRADD in vivo, we transiently transfected 293 human embryonic kidney cells with plasmids that direct the synthesis of Myc epitope–tagged TRADD (myc-TRADD) and Flag epitope–tagged DR3 (Flag-DR3), Flag–TNFR-1, or mutants (Fig. 3B). In a manner consistent with the in vitro binding results, TRADD specifically coprecipitated with DR3 and TNFR-1, but not with the death domain mutants, ΔDR3 and ΔTNFR-1 (Fig. 3B). Thus, DR3, like TNFR-1, may activate downstream signaling cascades by recruiting the adapter molecule TRADD. This result was expected because the death domains of DR3 and TNFR-1 have high homology (47% identity), whereas other death domain–containing molecules share 20 to 30% identity (3).

Overexpression of TRADD induces apoptosis and NF-κB activation, two of the most important activities signaled by TNFR-1 (9). Upon oligomerization of TNFR-1 by trimeric TNF, TRADD is recruited to the receptor signaling complex (10). TRADD can then bind TRAF2 (14), RIP (15), and FADD (6). Thus, we determined whether RIP, TRAF2, and FADD could be coimmunoprecipitated with DR3. In 293 cells expressing DR3 and RIP, only a weak association could be detected between the two molecules (Fig. 3C). However, in the presence of TRADD, RIP association with DR3 was enhanced (Fig. 3C). Likewise, little TRAF2 directly coprecipitated with DR3 in 293 cells. However, when DR3 and TRAF2 were expressed in the presence of both TRADD and RIP (both of which can bind TRAF2), enhanced binding of TRAF2 to DR3 could be detected (Fig. 3D). A similar association between FADD and DR3 was also observed. In the presence of TRADD, FADD efficiently coprecipitated with DR3 (Fig. 3E).

FADD can recruit the ICE-like protease FLICE to the CD95 death-inducing signaling complex (7). To determine whether FLICE can associate with TNFR-1 and DR3, we carried out coprecipitation experiments in 293 cells. FLICE formed complexes with TNFR-1 and DR3 (Fig. 3F). Cotransfection of TRADD, FADD, or both failed to enhance the FLICE–TNFR-1 or FLICE-DR3 interaction (16), which suggested that endogenous amounts of these adapter molecules were sufficient to maintain association.

Overexpression of CD95 and TNFR-1 in mammalian cells mimics receptor activation (7); thus, we used this approach to study the functional role of DR3. Ectopic expression of DR3 in MCF7 breast carcinoma cells and 293 cells induced rapid apoptosis (Fig. 4, A to C). The cells displayed morphological alterations typical of cells undergoing apoptosis, becoming rounded, condensed, and detaching from the dish (Fig. 4A). In MCF7 cells, plasmids encoding full-length DR3 or ΔDR3

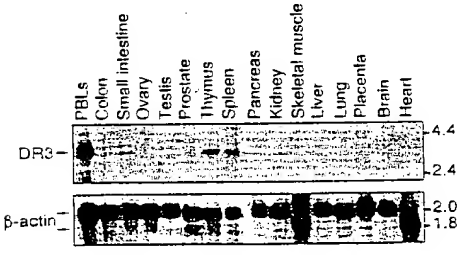

Fig. 2. Expression of DR3. Human adult tissue Northern blots (Clontech) containing 2 μg of polyadenylated RNA were probed with DR3 cDNA. PBLs, peripheral blood leukocytes. The blot was sequentially probed with β-actin cDNA. Heart skeletal muscle contain two forms of β-actin. Numbers at right denote kilobases.

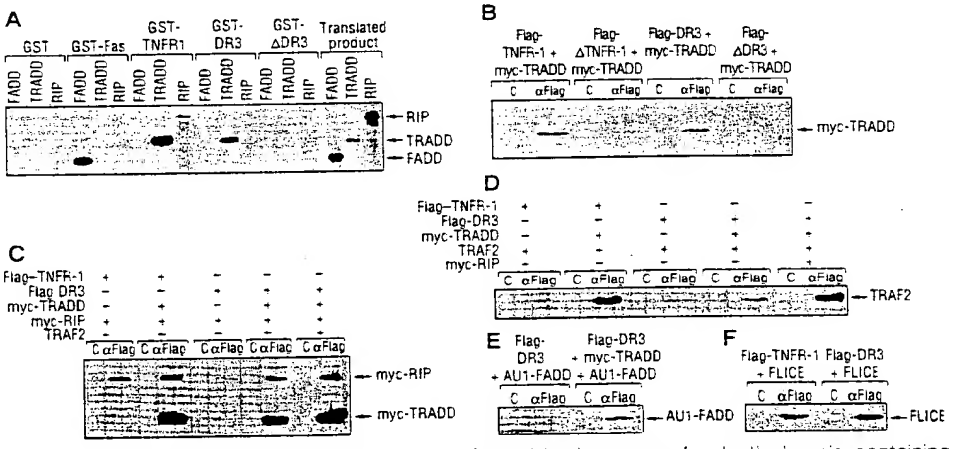

Fig. 3. Intracellular signaling molecules used by DR3. (**A**) In vitro screen for death domain–containing adapter molecules that bind to the cytoplasmic domain of DR3 (22). In vitro translated ^{35}S-labeled RIP, TRADD, and FADD were incubated with glutathione beads containing GST alone or GST fusions of the cytoplasmic domain of Fas, TNFR-1, DR3(215–393), or ΔDR3(215–321). After the beads were washed, retained proteins were analyzed by SDS-PAGE and autoradiography. The gel was Coomassie-stained to monitor equivalency of loading. (**B**) TRADD associates with DR3 in vivo. 293 cells were transfected with the indicated expression constructs for Flag-DR3, Flag-ΔDR3(1–321), Flag–TNFR-1, Flag–ΔTNFR-1, or myc-TRADD (23). After 24 to 32 hours, extracts were prepared and immunoprecipitated with a control mAb (C) or Flag mAb (αFlag) (IBI Kodak). Protein immunoblot analysis indicated that the amount of myc-TRADD and death receptor expression was similar in all samples. Coprecipitating myc-TRADD was detected by immunoblotting with horseradish peroxidase (HRP)–conjugated anti-Myc (Boehringer Mannheim). (**C**) TRADD enhances association of RIP with DR3. 293 cells were transfected and immunoprecipitated as in (B). Coprecipitating myc-RIP and myc-TRADD were detected by immunoblotting with HRP–conjugated anti-Myc. (**D**) TRADD enhances association of TRAF2 with DR3. 293 cells were transfected and immunoprecipitated as in (B). Coprecipitating TRAF2 was detected by immunoblotting with anti-TRAF2. (**E**) Coimmunoprecipitation of DR3-TRADD-FADD complexes. 293 cells were transfected and immunoprecipitated as in (B). Coprecipitating AU1 epitope–tagged FADD was detected by immunoblotting with anti-FADD. (**F**) FLICE coimmunoprecipitates with DR3 and TNFR-1. As in (B), except immunoblotted with anti–p10 subunit of FLICE.

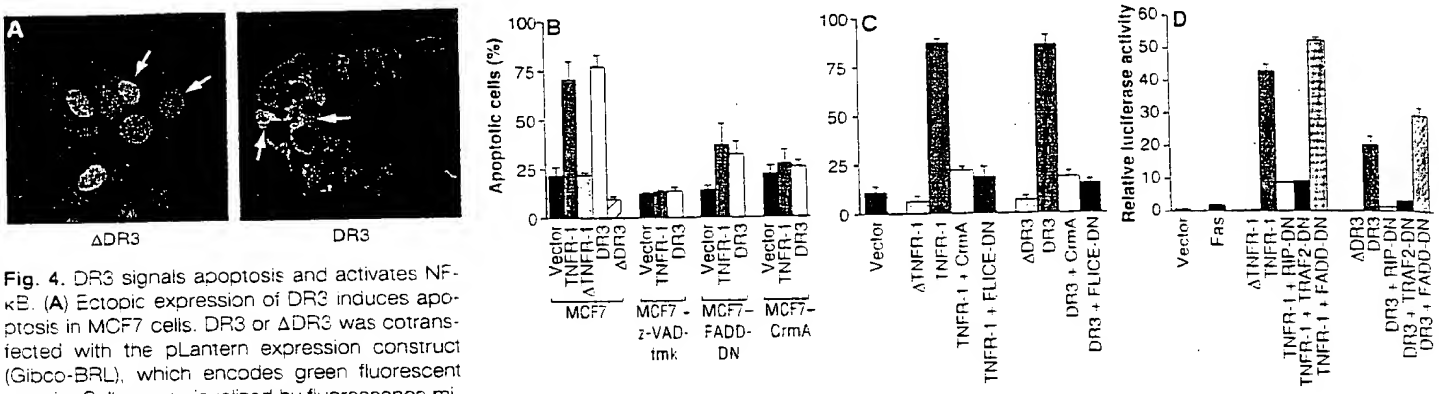

Fig. 4. DR3 signals apoptosis and activates NF-κB. (**A**) Ectopic expression of DR3 induces apoptosis in MCF7 cells. DR3 or ΔDR3 was cotransfected with the pLantern expression construct (Gibco-BRL), which encodes green fluorescent protein. Cells were visualized by fluorescence microscopy using a fluorescein isothiocyanate range barrier filter cube. Nuclei of transfected cells were visualized by DAPI staining and the image overlaid. Arrows indicate representative nuclei. (**B**) Apoptosis in MCF7 cells is inhibited by z-VAD-fmk (10 μM), FADD-DN (dominant negative), and CrmA. MCF7 cells or cells stably expressing CrmA (*17*) or FADD-DN (*18*) were transiently transfected with pCMV–β-galactosidase in the presence of a 10-fold excess of vector alone or expression constructs encoding DR3, ΔDR3, TNFR-1, or ΔTNFR-1 (*24*). The data (mean ± SD) are the percentage of round blue cells as a function of the total number of blue cells counted (n = 3). (**C**) DR3-induced apoptosis in 293 cells is blocked by FLICE-DN/MACHα1(C360S) (*7*) and CrmA. The data (mean ± SD) are the percentage of round blue cells as a function of the total number of blue cells counted (n = 3). (**D**) DR3 induces NF-κB activation, which is inhibitable by RIP-DN (*15*) and TRAF2-DN (*10, 14*). 293 cells were cotransfected with the indicated molecules and an NF-κB luciferase reporter plasmid (*14*), and luciferase activities were then determined (*25*). Results are from a representative experiment performed in duplicate three independent times (mean ± SD).

were cotransfected with the pLantern reporter construct encoding green fluorescent protein (Fig. 4A). Nuclei of cells transfected with DR3, but not with ΔDR3, exhibited apoptotic morphology as assessed by 4′,6′-diamidino-2-phenylindole (DAPI) staining (Fig. 4A). DR3-induced apoptosis was blocked by two inhibitors of ICE-like proteases, CrmA and z-VAD-fmk (Fig. 4, A to C), that also block apoptosis induced by TNFR-1 and CD95 (*7, 17*). Apoptosis induced by DR3 was also blocked by dominant negative versions of FADD (FADD-DN) or FLICE (FLICE-DN), which inhibit death signaling by CD95 and TNFR-1 (*7, 10, 18*). Thus, FADD and the ICE-like protease FLICE are likely necessary components of DR3-induced apoptosis.

Because DR3 activation recruits three molecules implicated in TNF-induced NF-κB activation, we examined whether DR3 could activate NF-κB. Transfection of a control vector or expression of CD95 did not induce NF-κB activation. In contrast, NF-κB was activated by ectopic expression of DR3 or TNFR-1, but not by the inactive signaling mutants ΔDR3 or ΔTNFR-1 (Fig. 4B). DR3-induced NF-κB activation was blocked by dominant negative derivatives of RIP (RIP-DN) and TRAF2 (TRAF2-DN), which block TNF-induced NF-κB activation (*10, 11*). As expected, FADD-DN did not interfere with DR3-mediated NF-κB activation (*10, 18*).

The identification of DR3 has added a third cell death receptor to the TNFR family. Its expression pattern suggests that DR3 may participate in lymphocyte homeostasis. None of the currently known ligands for these receptors [FasL, TNF, and TRAIL (TNF-related apoptosis-inducing ligand) (*19*)] bind to DR3 (*16*). In addition, it is unlikely that TRAIL serves as the ligand for DR3; TRAIL-induced apoptosis is not blocked by FADD-DN (*20*), which suggests that it uses an alternate death signaling pathway. It is also unclear whether TRAIL activates NF-κB. The identification of the DR3 ligand and targeted disruption of the DR3 gene will allow for a greater understanding of the physiologic role of DR3.

REFERENCES AND NOTES

1. H. Steller, *Science* **267**, 1445 (1995).
2. C. B. Thompson, *ibid.*, p. 1456.
3. J. L. Cleveland and J. N. Ihle, *Cell* **81**, 479 (1995); A. Fraser and G. Evan, *ibid.* **85**, 781 (1996); S. Nagata and P. Golstein, *Science* **267**, 1449 (1995).
4. C. A. Smith *et al.*, *Science* **248**, 1019 (1990).
5. P. Golstein, D. Marguet, V. Depraetere, *Cell* **81**, 185 (1995); K. White *et al.*, *Science* **264**, 677 (1994).
6. A. M. Chinnaiyan, K. O'Rourke, M. Tewari, V. M. Dixit, *Cell* **81**, 505 (1995); M. P. Boldin *et al.*, *J. Biol. Chem.* **270**, 7795 (1995); F. C. Kischkel *et al.*, *EMBO J.* **14**, 5579 (1995).
7. M. Muzio *et al.*, *Cell* **85**, 817 (1996); M. P. Boldin, T. M. Goncharov, Y. V. Goltsev, D. Wallach, *ibid.*, p. 803.
8. L. A. Tartaglia and D. V. Goeddel, *Immunol. Today* **13**, 151 (1992).
9. H. Hsu, J. Xiong, D. V. Goeddel, *Cell* **81**, 495 (1995).
10. H. Hsu, H.-B. Shu, M.-P. Pan, D. V. Goeddel, *ibid.* **84**, 299 (1996).
11. H. Hsu, J. Huang, H.-B. Shu, V. Baichwal, D. V. Goeddel, *Immunity* **4**, 387 (1996).
12. M. D. Adams *et al.*, *Nature* **377** (suppl.), 3 (1995); G. S. Feng *et al.*, *J. Biol. Chem.* **271**, 12129 (1996).
13. R. Watanabe-Fukunaga *et al.*, *J. Immunol.* **148**, 1274 (1992).
14. M. Rothe, S. C. Wong, W. J. Henzel, D. V. Goeddel, *Cell* **78**, 681 (1994); M. Rothe, V. Sarma, V. M. Dixit, D. V. Goeddel, *Science* **269**, 1424 (1995).
15. B. Z. Stanger, P. Leder, T. H. Lee, E. Kim, B. Seed, *Cell* **81**, 513 (1995).
16. A. M. Chinnaiyan, K. O'Rourke, V. M. Dixit, unpublished data.
17. M. Tewari and V. M. Dixit, *J. Biol. Chem.* **270**, 3255 (1995).
18. A. M. Chinnaiyan *et al.*, *ibid.* **271**, 4961 (1996).
19. R. Pitti *et al.*, *ibid.*, p. 12687; S. R. Wiley *et al.*, *Immunity* **3**, 673 (1995).
20. S. A. Marsters *et al.*, *Curr. Biol.* **6**, 750 (1996).
21. R. Watanabe-Fukunaga, C. I. Brannan, N. G. Copeland, N. A. Jenkins, S. Nagata, *Nature* **356**, 314 (1992); N. Itoh and S. Nagata, *J. Biol. Chem.* **268**, 10932 (1993).
22. In vitro binding experiments were done as described in (*6*).
23. The constructs encoding Flag–TNFR-1 and Flag–ΔTNFR-1 were described elsewhere (*18*). To facilitate epitope tagging, we cloned DR3 and ΔDR3(1–321) into the FLAG plasmid pCMV1FLAG (IBI Kodak) with the use of the signal peptide provided by the vector. Transfection of 293 cells was done by calcium phosphate precipitation with the constructs encoding the indicated proteins in combination with pcDNA3-CrmA (*17*) to prevent cell death and thus maintain protein expression. Cells were lysed in 1 ml of lysis buffer (50 mM Hepes, 150 mM NaCl, 1 mM EDTA, 1% NP-40, and a protease inhibitor cocktail). Lysates were immunoprecipitated with a control monoclonal antibody (mAb) or Flag mAb for at least 4 hours at 4°C, as described (*18*). The beads were washed three times with lysis buffer, but in the case of TRADD binding, the NaCl concentration was adjusted to 1 M. The precipitates were fractionated by 12.5% SDS–polyacrylamide gel electrophoresis (PAGE) and transferred to nitrocellulose. Subsequent protein immunoblotting was performed as described (*10, 18*).
24. Cell death assays were done as described (*6, 18*). The data (mean ± SD) are the percentage of round blue cells among the total number of blue cells counted. Data were obtained from at least three independent experiments.
25. NF-κB luciferase assays were performed as described (*11, 12, 14, 18*). The amounts of dominant negative inhibitors used were four times the amounts of the death receptors. Total DNA was kept constant.

26. Supported by the Medical Scientist Training Program (A.M.C.) and NIH grant GM-07863 (A.M.C.). The initial EST clones used in this study were discovered as part of a joint collaboration between scientists at The Institute for Genomic Research and at Human Genome Sciences. We thank D. Goeddel for the TRAF2 and RIP constructs, I. Jones for manuscript preparation, and H. Duan and C. Vincenz for helpful discussions.

9 September 1996; accepted 7 October 1996

BIOCHEMICAL AND BIOPHYSICAL RESEARCH COMMUNICATIONS 242, 376–379 (1998)
ARTICLE NO. RC977948

A New Death Receptor 3 Isoform: Expression in Human Lymphoid Cell Lines and Non-Hodgkin's Lymphomas

Krzysztof Warzocha, Patricia Ribeiro, Carole Charlot, Nathalie Renard, Bertrand Coiffier, and Gilles Salles

Department of Hematology, Centre Hospitalier Lyon-Sud, Hospices Civils de Lyon, and UPRES-JE 1879 "Hémopathies Lymphoïdes malignes", 69495 Pierre-Bénite, France

Received December 5, 1997

Two isoforms encoding the full-length transmembrane death receptor 3 (DR3) were isolated from mRNAs of a panel of human cell lines and tumor tissues obtained from patients with follicular non-Hodgkin's lymphoma. A new DR3 variant (DR3β) was characterized by 2 insertions of respectively 20- and 7-base pairs (bp) which result in a predictive translated polypeptide differing from the described DR3 molecule by a 28 amino-acid stretch in the extracellular domain. DR3 was shown to be expressed in all cell lines and lymphoma samples tested, whereas DR3β expression was restricted to lymphoid T-cell and immature B-cell lines and to selected cases with follicular lymphoma. These data provide new insight into the molecular heterogeneity of DR3, suggesting the presence of several receptor isoforms that can participate in lymphoid cell homeostasis. © 1998 Academic Press

The tumor necrosis factor (TNF) receptor family members are type I membrane molecules, structurally homologous, containing three to six cystein-rich repeats of 40 residues in its extracellular domain (1). The cytoplasmic domain generally lacks sequence homology, with the exception of a motif called the "death domain" found in type I TNF-receptor (p55), Fas, and death receptor (DR)-3, -4 and -5. The binding of ligands to their respective receptors induces oligomerization which initiates downstream signaling events resulting in NF-κB activation or apoptosis (2). Although DR3, also called WSL-1, Apo-3, TRAMP, or LARD, can signal both these cellular effects, it does not interact with any of the known apoptosis-inducing ligands of the TNF family (3-7). The expression of DR3, is more tightly regulated than the other death receptors as it was found predominantly on lymphocytes. This restricted expression pattern suggests that DR3 plays a specific role in lymphoid cells development and function. Alternative pre-mRNA splicing generated isoforms, including one membrane anchored and several soluble molecules, have been described and may participate in these functions (7).

In the present study we have cloned a new DR3 isoform, differing from the transcript encoding the full-length receptor by 20- and 7-bp insertions, that we have called DR3β. The predictive translated products of DR3β consisting in 426 amino-acids (aa) and DR3 consisting in 417 aa have identical intracytoplasmic and transmembrane domains but differ in their extracellular domain by 28-aa. Both transcripts are differently expressed in human cell lines and lymphoma tissues. This data provides new insight into the molecular heterogeneity of DR3 that may result in a complex regulating system of normal and malignant lymphocyte death.

MATERIAL AND METHODS

Cell samples. A panel of human cell lines, including two early pre-B acute lymphoblastic leukemia (Mieliki (8) and Reh from the American Type Culture Collection (ATCC), Rockville, MD), a mature B-cell lymphoma (RL, kindly provided by Dr. Walter J. Urba, Portland, OR), a T-cell leukemia (Jurkat, ATCC) and a histiocytic lymphoma (U-937, ATCC) as well as tumor tissue samples obtained from 11 newly diagnosed follicular lymphoma patients were tested for the expression of DR3 isoforms. Total RNA from cell line suspensions and lymph node homogenates was isolated by a single-step method of acid guanidium thiocyanate-phenol-chloroform extraction. Genomic DNA decontamination procedure and first strand cDNA synthesis were performed as previously described (9).

Cloning and sequencing of DR3 isoforms. PCR amplification with the use of primer pairs F4 (GCCCCTTGCACGGAGCCCTG) and R1 (GCGATCTCAGCCAAACTCCG) resulted in the amplification of several transcripts that corresponded in size to the full DR3 messenger and its directly spliced versions missing exon 3 and 2 in all samples whereas an additional band was present in some samples (not shown). Both the full-length DR3 and the variant DR3β were purified from the gel, cloned and sequenced, and were further characterized by the use of isoform-specific primers (Figure 1). The primer pairs F1 (CTGAAGGCGGAACCACGACG) and R2 (GGACCCAGAACATCTGCCTC), and F1 - R3 (GAACACACCTACTCTGCCTC) were used to amplify the 5′ terminus of both the original and DR3 variant sequences, respectively. The primer pairs F2 (GAGGCAGATGTTCTGGGTCC) and R1 (GCGATCTCAGCCAAACTCCG) and F3 (GAGG-

0006-291X/98 $25.00

CAGATGTTCTGGGTCC) - R1 were used to amplify respectively their 3' ends (Figure 1). After heating at 95°C for 10 min, PCR reactions were carried out for 36 cycles, each consisting in sequential steps of denaturation (95°C for 60 seconds), annealing (62°C for 60 seconds), and extension (72°C for 60 seconds). After the last cycle, extension phase was prolonged for 9 minutes at 72°C. Both overlapping 5' and 3' PCR-amplified fragments of each transcript were used as templates for cloning and sequencing as previously described (9). Three independent clones for each fragment were sequenced in both directions to avoid errors resulting from the possible mutations caused by *Taq* polymerase. Nucleotide sequence alignments and the computerization of protein characteristics were performed using BlastN and ProtParam tools of the National Center for Biotechnology Information and ExPASy Web servers.

PCR analysis of DR3 isoforms' expression. To determine the distribution of both DR3 isoforms, human cell lines and lymphoma tumor tissues were subjected to RT-PCR analysis. To normalize the amount of amplifiable cDNA in each sample, we used glyceraldehyde-3-phosphate dehydrogenase (G3PD) primers and primers specific for a given DR3 isoform in the same PCR reaction mixture (9). PCR was started with the primers specific for the original (F4-R2) or DR3 variant (F4-R3) sequence, and after the first 11 cycles of amplification, specific primers for G3PD were added. The PCR products were resolved on ethidium bromide-stained 1.5 % agarose gel, and UV-photographed.

RESULTS

Sequencing of DR3 and DR3β transcripts. RT-PCR performed with F4-R1 primers' pair showed the presence of cDNA fragments representing the full-length DR3 cDNA and its directly spliced versions missing exon 3 and 2 in all cell lines and lymphoma samples tested as well as an additional variant form expressed in several cases (not shown). PCR-amplified fragments representing the full-length transmembrane DR3 and additional transcripts were purified from the gel, cloned and sequenced, and were further characterized by the use of isoform-specific primers (Figure 1). The PCR-amplified products obtained by the use of F1-R2 and F2-R1 primers corresponded to the original cDNA sequence encoding the full-length transmembrane DR3, and shared identical expression pattern in the tested samples as previously demonstrated by the use of F4-R1 primers (not shown). The PCR-amplified product obtained by the use of F1-R3 primers' pair corresponded to the 5' cDNA terminus of DR3 differing from the original molecule by the presence of two insertions of respectively 20- and 7-bp (Figure 1). Sequence comparison showed that the 20-bp insertion in DR3 variant (DR3β) was localized between the nucleotide positions 612-613 of the original sequence, and did not correspond to any known sequences published in the GenBank database. In contrast, the 7-bp insertion in DR3β corresponded to the first 7 nucleotides of exon 3 which is usually skipped out from the original DR3 transcript. This insertion was localized between the nucleotide positions 667-668 of DR3 cDNA sequence (Figure 1). Following these insertions, the sequence of DR3β cDNA matched perfectly with that of the original DR3 molecule.

As a result, the predictive translated polypeptide of DR3β consists of 426-aa as compared to 417-aa for DR3. However, both 20- and 7-bp insertions caused a shift in the open reading frame which resulted downstream from the second insertion, in the conservation of the original DR3 reading frame until the 3'end, including the same stop codon (Figure 1). Therefore, both polypeptides have identical aa compositions within intracytoplasmic and transmembrane domains, but they differ by 28-aa (including the 9 newly encoded aa) in the proximal part of their extracellular domain.

Several PCR, cloning, and sequencing experiments from distinct cell lines and patients' samples were performed, and each showed the same nucleotide sequences. These results indicate the presence of two isoforms of the human DR3 encoding the full-length transmembrane receptors (Genbank accession numbers U72763 and AF026070).

Expression of DR3 and DR3β in human cell lines and lymphoma tumor tissue. Using internal control's primers in the same PCR reaction mixture containing specific primer pairs for DR3 (F4-R2) or DR3β (F4-R3), we determined the distribution of both transcripts in a panel of human lymphoid cell lines and tumor tissues obtained from patients with lymphoma (Figure 2). Whereas DR3 was abundantly expressed in all cell lines and lymphoma samples tested, DR3β expression had a more restricted expression pattern (Figure 2). DR3β-specific transcript was present in the early pre-B Mieliki and the pre-B Reh cell lines as well as in the Jurkat T-cell line, but it was not detectable in the mature B-cell RL and histiocytic U-937 cell lines. Only 6 out of 11 follicular lymphoma samples tested were found to be positive for DR3β. The PCR-amplified products obtained by the use of DR3 (F4-R2) and DR3β (F4-R3)-specific primers shared identical expression pattern in the tested samples as cDNAs amplified by the use of F4-R1 primers in preliminary studies (not shown). These results indicate that DR3 and DR3β transcripts show a distinct expression pattern in human cell lines and tumor tissues obtained from patients with lymphoma.

DISCUSSION

Recent findings of genomic organization of human DR3 demonstrated that alternative pre-mRNA splicing generates at least 12 distinct isoforms (7). The isoform missing exon 3 includes the transmembrane and death domains, whereas the other isoforms encode potentially secreted molecules. It has been also suggested that all but three DR3 isoforms are generated by the skipping of one or more complete exons. Two variants had 101- and 200-bp inserted sequences that matched to consensus splice sites at their 5' and 3' ends, therefore, they probably represented retained introns. The

FIG. 1. Nucleotide sequence of DR3 (upper line) and DR3β (lower line) (GenBank accession numbers U72763 and AF026070, respectively). Sequences marked by strikeout indicate missing nucleotides and bold underline marks stop codons. The arrowed lines indicate the positions and directions of primers used for the PCR and cloning procedures.

remaining DR3 variant contained three additional nucleotides probably corresponding to an alternative 3′ splice site proximal to the one used by the full-length DR3 cDNA (7). In the present study we characterized a new DR3 isoform (DR3β), homologous to the DR3 cDNA encoding the full-length transmembrane receptor. The sequence of DR3β differs from the original molecule by retaining the first seven nucleotides of the described exon 3 and by the insertion of new 20-bp. Although both nucleotide insertions result in a shift of the original reading frame, this frame is conserved after the second insertion until the 3′end of the messenger. The predictive translated polypeptide of DR3β corresponds therefore to a new transmembrane receptor (426 aa) differing from the original DR3 (417 aa) by 28-aa portion in the extracellular domain. Since the 20-bp insertion lacks consensus splice sites at its 5′ and 3′ ends and the 7-bp insertion represents a part of exon 3, the genomic organization as well as mechanisms involved in the processing of DR3 mRNAs are more complex than previously described (3-7).

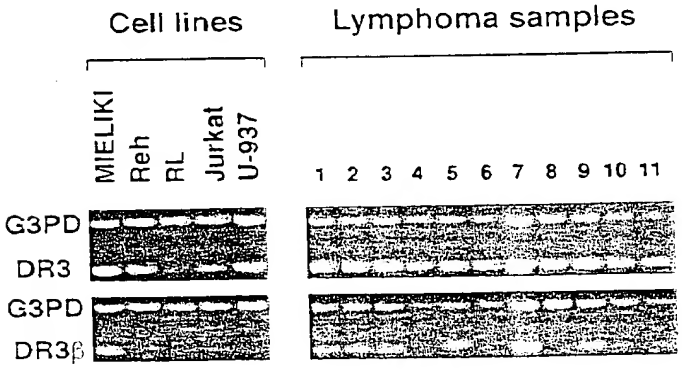

FIG. 2. RT-PCR analysis of DR3 and DR3β expression in a panel of human cell lines representing Mieliki, Reh, RL, Jurkat and U-937 (left panel), and in tumor tissues obtained from 11 newly diagnosed follicular lymphoma patients (right panel). To normalize the amount of amplifiable cDNA in each sample, we used G3PD primers and primers specific for a given isoform in the same PCR reaction mixture. The positions of PCR-amplified products are indicated on the left side of the figure.

Interestingly two DR4 isoforms were also recently identified as TRICK2a and TRICK2b. These transcripts were found to be expressed in a variety of tissues and to result from an alternative pre-mRNA splicing, differing by a 29-aa extension in the extracellular domain (10). It has been shown that DR4 and TRICK bind to the same ligand, TRAIL (TNF-related apoptosis inducing ligand). Since DR3 and DR3β show similar diversity, probably DR3β is another full-length transmembrane receptor for lymphocyte homeostasis regulation. DR3 ligand has not yet been identified and

whether DR3 and DR3β have either similar or distinct ligands, remains to be determined.

The close homology between DR3, Fas and TNFR1 indicate that they may share signaling pathways. In several recent reports (3-7) the intracellular interactions of DR3 have been found to resemble more TNFR1 than Fas, but in contrast to the latter, which are broadly expressed, DR3 has a restricted pattern of expression to lymphoid tissues. Our data indicates that DR3β may even have more restricted expression. Furthermore the alternative DR3 splicing on lymphocyte subsets and cell lines may set a balance between susceptibility and protection from apoptosis (7), since unstimulated B or T cells expressed abundantly DR3 truncated isoforms but very little of the full-length DR3 transcript. This splicing pattern reversed after cellular stimulation when the full-length DR3 predominated, while potentially secreted isoforms were reduced (7), indicating that alternative splicing plays a key role in the expression of the full-length DR3 receptor after lymphocyte activation. Our data shows that the expression of DR3 was detectable in all cell lines and lymphoma samples tested through RT-PCR analyses but DR3β expression was restricted to early B-lymphoid subsets and to some cases of follicular lymphoma. This suggests that the "programmed" change in DR3 alternative splicing may have functional effects not only in lymphocyte activation but also in lymphocyte differentiation and malignant transformation. The expression of a decoy receptor for TRAIL in normal tissues but not in tumor cell lines as well as the control of TRAIL-induced apoptosis by alternatively spliced receptors may confirm this notion (11).

In conclusion, our findings emphasize the molecular complexity of the DR3 death receptor which expression seems restricted to lymphoid cells and therefore may play a role in lymphoid cell differentiation and function.

ACKNOWLEDGMENTS

This study was supported by the Hospices Civils de Lyon - PHRC (96.044) and by INSERM (Paris). K.W. and P.R. were supported with grants founded respectively by the Fondation de France (Paris) and by the European Society for Medical Oncology (ESMO, Lugano).

REFERENCES

1. Bazzoni, F., and Beutler, B. (1996) *N. Eng. J. Med.* 334, 1717–1725.
2. Wallach, D. (1997) *Nature* 388, 123–126.
3. Chinnaiyan, A. M., O'Rourke, K., Yu, G. L., Lyons, R. H., Garg, M., Duan, D. R., Xing, L., Gentz, R., Ni, J., and Dixit, V. M. (1996) *Science* 274, 990–992.
4. Kitson, J., Raven, T., Jiang, Y. P., Goeddel, D. V., Giles, K. M., Pun, K. T., Grinham, C. J., Brown, R., and Farrow, S. N. (1996) *Nature* 384, 372–375.
5. Marsters, S. A., Sheridan, J. P., Donahue, C. J., Pitti, R. M., Gray, C. L., Goddard, A. D., Bauer, K. D., and Ashkenazi, A. (1996) *Curr. Biol.* 6, 1669–1676.
6. Bodmer, J. L., Burns, K., Schneider, P., Hofmann, K., Steiner, V., Thome, M., Bornand, T., Hahne, M., Schröter, M., Becker, K., Wilson, A., French, L. E., Browning, J. L., MacDonald, H. R., and Tschopp, J. (1997) *Immunity* 6, 79–88.
7. Screaton, G. R., Xu, X. N., Olsen, A. L., Cowper, A. E., Tan, R., McMichael, A. J., and Bell, J. I. (1997) *Proc. Natl. Acad. Sci. USA* 94, 4615–4619.
8. Renard, N., Duvert, V., Matthews, D. J., Pages, M-P., Magaud, J-P., Manel, A-M., Pandrau-Garcia, D., Philippe, N., Bancherau, J., and Saeland, S. (1995) *Leukemia* 9, 1219–1226.
9. Warzocha, K., Renard, N., Charlot, C., Bienvenu, J., Coiffier, B., and Salles, G. (1997) *Biol. Biochem. Res. Commun.* 238, 273–276.
10. Screaton, G. R., Mongkolsapaya, J., Xu, X. N., Cowper, A. E., McMichael, A. J., and Bell, J. I. (1997) *Curr. Biol.* 7, 693–696.
11. Sheridan, J. P., Marsters, S. A., Pitti, R. M., Gurney, A., Skubatch, M., Baldwin, D., Ramakrishnan, L., Gray, C. L., Baker, K., Wood, W. I., Goddard, A. D., Godowski, P., and Ashkenazi, A. (1997) *Science* 277, 818–821.

ISSN 0006-291X
Volume 242, Number 2, January 14, 1998

Biochemical and Biophysical Research Communications

Cell, Vol. 84, 299–308, January 26, 1996, Copyright ©1996 by Cell Press

TRADD–TRAF2 and TRADD–FADD Interactions Define Two Distinct TNF Receptor 1 Signal Transduction Pathways

Hailing Hsu, Hong-Bing Shu, Ming-Gui Pan, and David V. Goeddel
Tularik, Incorporated
270 East Grand Avenue
South San Francisco, California 94080

Summary

Tumor necrosis factor (TNF) can induce apoptosis and activate NF-κB through signaling cascades emanating from TNF receptor 1 (TNFR1). TRADD is a TNFR1-associated signal transducer that is involved in activating both pathways. Here we show that TRADD directly interacts with TRAF2 and FADD, signal transducers that activate NF-κB and induce apoptosis, respectively. A TRAF2 mutant lacking its N-terminal RING finger domain is a dominant-negative inhibitor of TNF-mediated NF-κB activation, but does not affect TNF-induced apoptosis. Conversely, a FADD mutant lacking its N-terminal 79 amino acids is a dominant-negative inhibitor of TNF-induced apoptosis, but does not inhibit NF-κB activation. Thus, these two TNFR1–TRADD signaling cascades appear to bifurcate at TRADD.

Introduction

Tumor necrosis factor (TNF) is a proinflammatory cytokine whose pleiotropic biological properties are signaled through two distinct cell surface receptors (reviewed by Tartaglia and Goeddel, 1992; Rothe et al., 1992). TNF receptor 1 (TNFR1; 55–60 kDa) and TNFR2 (75–80 kDa) are expressed on most cell types and are ~30% identical in their extracellular, cysteine-rich, ligand-binding regions (Loetscher et al., 1990; Schall et al., 1990; Smith et al., 1990). This extracellular domain architecture is characteristic of the larger TNFR superfamily, whose members include the Fas antigen, CD27, CD30, CD40, and several other receptors (reviewed by Smith et al., 1994). With the exception of TNFR1 and Fas, both of which can induce programmed cell death through a shared ~80 amino acid "death domain" of 28% identity (Tartaglia et al., 1993a; Itoh and Nagata, 1993), the cytoplasmic domains of receptors in this superfamily share no obvious sequence similarities.

Until recently, the molecular mechanisms utilized by members of the TNFR family to generate cellular responses have remained largely undefined. However, during the past year an improved understanding of these mechanisms has begun to emerge with the identification of two distinct classes of receptor-associated proteins, both of which appear to couple these receptors to downstream signaling cascades.

Three intracellular proteins that contain death domains were identified through yeast two-hybrid interaction cloning by virtue of their interactions with the death domains of TNFR1 and Fas. TRADD is a 34 kDa protein that interacts specifically with TNFR1 (Hsu et al., 1995), whereas the 23 kDa FADD (Boldin et al., 1995a; Chinnaiyan et al., 1995) and the 74 kDa RIP (Stanger et al., 1995) interact with Fas. In fact, death domains now appear to define interaction domains that are capable of both homotypic and heterotypic associations (Song et al., 1994; Boldin et al., 1995a, 1995b; Hsu et al., 1995; Chinnaiyan et al., 1995; Stanger et al., 1995). These observations suggest that death domains may function as adaptors to couple some members of the TNFR superfamily (at least TNFR1 and Fas) to other signaling proteins.

TRADD contains an N-terminal region of unknown function and a C-terminal death domain that is 23% identical to the death domain of TNFR1. TRADD may play an obligatory role in TNFR1 responses, since its overexpression activates TNFR1-like signaling pathways for both apoptosis and activation of the transcription factor NF-κB (Hsu et al., 1995). Similarly, overexpression of FADD (Boldin et al., 1995a; Chinnaiyan et al., 1995) or RIP (Stanger et al., 1995) mimics Fas activation, leading to programmed cell death. However, the mechanisms of signaling by TRADD, FADD, and RIP are not identical. Whereas the induction of cell death by TRADD or RIP requires only their death domains, apoptosis induced by FADD overexpression occurs independently of its C-terminal death domain. This suggests that FADD contains a "death effector" domain at its N-terminus, which may bind downstream apoptosis-signaling molecules for recruitment to Fas via death domain interactions.

The second family of signal transducing proteins utilized by the TNFR superfamily are the TNFR-associated factors (TRAFs). TRAF1 and TRAF2 were biochemically purified as TNFR2-associated proteins of 45 and 56 kDa, respectively (Rothe et al., 1994). TRAF1 and TRAF2 exist in a multimeric complex that interacts via TRAF2 with the signaling domains of both TNFR2 and CD40 (Rothe et al., 1994, 1995). TRAF3 was identified by two-hybrid interaction cloning as a CD40-associated protein of 64 kDa (Hu et al., 1994; Cheng et al., 1995; Mosialos et al., 1995; Sato et al., 1995). The three known TRAFs share a highly conserved C-terminal "TRAF domain" of about 150 amino acids, which is involved in oligomerization and receptor association (Rothe et al., 1994, 1995; Cheng et al., 1995; Sato et al., 1995). Overexpression of TRAF2, but not TRAF1 or TRAF3, activates NF-κB (Rothe et al., 1995). Furthermore, a truncated TRAF2 lacking its N-terminal RING finger acts as a dominant-negative inhibitor of NF-κB activation mediated by both TNFR2 and CD40 (Rothe et al., 1995). Therefore, TRAF2 is a common mediator of signal transduction by TNFR2 and CD40 and, perhaps, by other members of the TNFR superfamily.

Two of the most important activities of TNF, apoptosis and NF-κB activation, are signaled by TNFR1 following its oligomerization by the trimeric TNF (Tartaglia and Goeddel, 1992). We recently reported the molecular cloning and characterization of TRADD, a novel protein that specifically interacts with the death domain of TNFR1 and activates signaling pathways for both of these activities when overexpressed (Hsu et al., 1995).

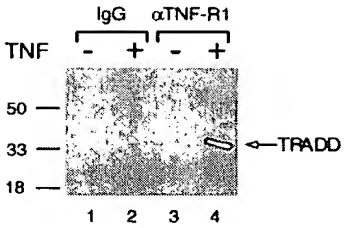

Figure 1. TNF Induces Association of TRADD with TNFR1

We treated U937 cells (5×10^7) with TNF for 15 min (lanes 2 and 4) or left them untreated (lanes 1 and 3). Cell lysates were immunoprecipitated with anti-TNFR1 monoclonal antibody 985 (lanes 3 and 4) or with mouse immunoglobulin G (IgG) control antibody (lanes 1 and 2). Coprecipitating TRADD was detected by immunoblot analysis using rabbit anti-TRADD antiserum. Positions of molecular mass standards (in kilodaltons) are shown.

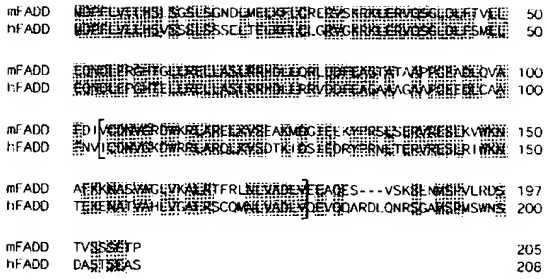

Figure 2. Predicted Amino Acid Sequence of Murine FADD

The amino acid sequences of murine and human FADD are aligned. Identical residues are stippled The death domain of FADD extends from amino acids 104–177, as indicated by the brackets.

Here we show that under normal conditions the association of TRADD with TNFR1 is TNF dependent. We also show that TRADD directly interacts with TRAF2 through its N-terminal half and with FADD through its C-terminal death domain. Furthermore, dominant-negative mutants of TRAF2 and FADD can block TNF-mediated NF-κB activation and cell death, respectively. Taken together, these data suggest that TNFR1 utilizes distinct TRADD-dependent mechanisms to activate signaling pathways for NF-κB activation and apoptosis.

Results

Interaction of TRADD with TNFR1 Is TNF Dependent

We previously demonstrated that TRADD specifically associates with TNFR1 when both proteins are overexpressed (Hsu et al., 1995). To determine whether the TRADD–TNFR1 interaction is physiologically relevant, we performed the following experiment using human U937 cells. Lysates from cells that had been treated with TNF for 15 min or left untreated were immunoprecipitated with a nonagonistic monoclonal antibody directed against the extracellular domain of TNFR1. Coprecipitating TRADD was detected by immuoblot analysis using a TRADD-specific polyclonal antiserum. TRADD coprecipitated with TNFR1 only in the TNF-treated cell lysates (Figure 1). Since TNF induces trimerization of TNFR1, this result suggests that the recruitment of TRADD to TNFR1 probably depends on a properly aggregated TNFR1 cytoplasmic domain.

Identification of TRAF2 and FADD as TRADD-Interacting Proteins

To identify potential downstream components of the TNFR1/TRADD signaling pathway, we used the yeast two-hybrid system (Fields and Song, 1989) to screen cDNA libraries for TRADD-interacting proteins. Multiple cDNA clones were obtained that encode several distinct proteins. As expected, two classes of clones encoded TRADD itself or portions of the intracellular region of TNFR1. Surprisingly, many of the cDNA clones were found to encode portions of TRAF2, a protein that interacts with TNFR2 and CD40 and transduces the signal for NF-κB activation by these two receptors (Rothe et al., 1994, 1995). The interaction of TRADD with TRAF2 was verified in yeast two-hybrid interaction assays using full-length TRAF2. TRADD was also found to interact strongly with TRAF1, and more weakly with TRAF3, in two-hybrid assays (data not shown).

The two-hybrid screen also yielded cDNA clones encoding full-length murine FADD and the C-terminal 126 amino acids of murine FADD. The 205 amino acid murine FADD shares 73% identity with human FADD throughout the region (amino acids 1–177) comprising the effector and death domains, whereas the C-terminal ~30 amino acids are very poorly conserved (Figure 2). Since FADD was originally identified owing to its interaction with Fas (Boldin et al., 1995a; Chinnaiyan et al., 1995), we compared the relative strength of the TRADD–FADD and Fas–FADD interactions in two-hybrid assays. These experiments indicated that FADD consistently interacts 10- to 20-fold more strongly with TRADD than with Fas (data not shown).

Since TRAF1, TRAF2, and FADD interact strongly with TRADD in two-hybrid tests, we performed coimmunoprecipitation assays to test whether these proteins might interact in human cells. An expression vector encoding TRADD was transfected alone or with expression vectors encoding Flag epitope–tagged TRAF1, TRAF2, or FADD into human embryonic kidney 293 cells. Cell extracts were immunoprecipitated using a monoclonal antibody against the Flag epitope, and coprecipitating TRADD was detected by Western blotting with anti-TRADD polyclonal antibody. TRAF1, TRAF2, and FADD were individually able to coprecipitate TRADD (Figure 3).

Mapping of TRADD–TRAF2 and TRADD–FADD Interaction Domains

To determine the region(s) of TRADD responsible for interaction with TRAF2 and FADD, a series of N-terminal and C-terminal TRADD truncation mutants were examined in two-hybrid assays (Figure 4A). A C-terminal deletion mutant of TRADD lacking its entire death domain retained TRAF2-binding activity. This demonstrated that the TRAF2-binding domain resides in the N-terminal half (amino acids 1–169) of TRADD. A further C-terminal deletion mutant (TRADD[1–106]) failed to interact with TRAF2. In contrast, TRADD interacts with FADD through its C-terminal death domain (amino acids 195–312). This

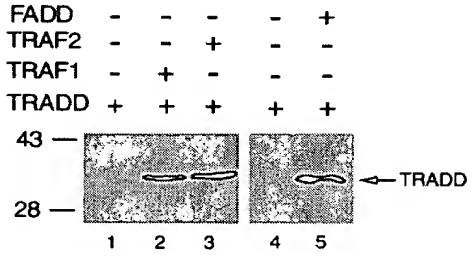

Figure 3. In Vivo Interaction of FADD and TRAF Proteins with TRADD

We transfected 293 cells (2×10^6) with the indicated combinations of expression vectors for TRADD and Flag epitope–tagged TRAF1, TRAF2, or FADD. After 24 hr, extracts were prepared and immunoprecipitated with an anti-Flag monoclonal antibody. Coprecipitating TRADD was detected by immunoblot analysis using polyclonal antibody against TRADD. Positions of molecular mass standards (in kilodaltons) are shown.

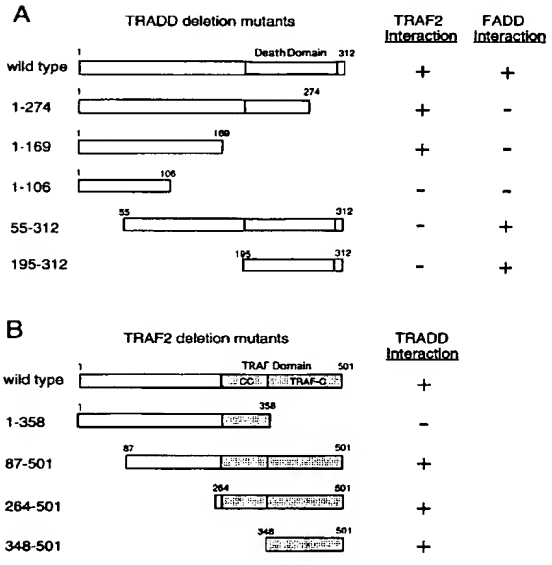

Figure 4. Mapping of TRADD–TRAF2 and TRADD–FADD Interaction Domains

(A) Interaction of TRAF2 and FADD with the N- and C-terminal domains of TRADD, respectively. Expression vectors encoding wild-type TRADD or the indicated deletion mutants fused to the GAL4 DNA-binding domain were cotransformed into yeast Y190 cells with a GAL4 activation domain–TRAF2 or GAL4 activation domain–FADD expression vector.

(B) The TRAF domain of TRAF2 interacts with TRADD. Expression vectors encoding wild-type TRAF2 or the indicated deletion mutants fused to GAL4 activation domain were cotransformed into yeast Y190 cells with a GAL4 DNA-binding domain–TRADD expression vector. The TRAF domain of TRAF2 can be subdivided into two parts, a coiled-coil (CC) region and a C-terminal (TRAF-C) region (Rothe et al., 1994). Transformation mixes were plated on synthetic dextrose plates lacking tryptophan and leucine. Filter assays were performed for β-galactosidase activity. Plus signs represent blue color development; minus signs indicate no color development.

is the same region of TRADD that is required for interaction with the death domain of TNFR1 (Hsu et al., 1995).

Deletion studies on TRAF2 indicate that its TRAF-C domain (amino acids 348–501) was sufficient for TRADD binding (Figure 4B). Previous studies had shown that the entire TRAF domain (amino acids 264–501) of TRAF2 can self-associate and interact with TRAF1, TNFR2, and CD40 (Rothe et al., 1994, 1995).

TRADD Recruits TRAF Proteins to TNFR1

The interaction of TRADD with TNFR1 and TRAFs occurs via its C-terminal death domain and N-terminal TRAF-binding domain, respectively. Therefore, TRADD might be able to bind simultaneously both TNFR1 and TRAFs, thereby recruiting TRAFs to the TNFR1 complex. To explore this possibility, we cotransfected 293 cells with plasmids that direct the synthesis of TNFR1, TRADD, and Flag-tagged TRAF1 or TRAF2. Cell extracts were immunoprecipitated with agonistic polyclonal antibodies against the extracellular domain of TNFR1, and coprecipitating TRAF proteins were detected by Western blotting with an anti-Flag monoclonal antibody. In lysates prepared from cells programmed for ectopic expression of TNFR1 and TRAF1 or TRAF2, antibody against TNFR1 failed to coprecipitate TRAF proteins (Figure 5A). This result, which suggests that no direct interaction occurs between the TNFR1 and TRAF1 or TRAF2, is in agreement with results obtained previously by yeast two-hybrid interaction assays (Rothe et al., 1995). However, when the same experiments were performed on lysates from cells that also expressed TRADD, both TRAF1 and TRAF2 were coimmunoprecipitated with TNFR1 (Figure 5A). These results provide evidence that TRADD can serve as an adaptor protein and recruit TRAF1, TRAF2, or both to TNFR1.

Since TRAF2 is capable of interacting with both TNFR2 and TRADD, we also considered the possibility that TRAF2 could recruit TRADD to the TNFR2 receptor complex. This was examined by cotransfection and immunoprecipitation experiments similar to those described above for TNFR1. However, no ternary TNFR2–TRADD–TRAF2 complex could be detected (data not shown), demonstrating that TRAF2 cannot simultaneously bind to both TNFR2 and TRADD. This finding suggests that TNFR2 and TRADD, both of which interact with the C-terminal TRAF domain of TRAF2 (see Figure 4B; Rothe et al., 1994), compete for the same, or an overlapping, binding site on TRAF2.

TRADD Enhances Association of FADD with TNFR1

The strong interaction between TRADD and FADD occurs via their death domains. TRADD also associates with TNFR1 through death domain interactions. To determine whether TRADD can simultaneously interact with both FADD and TNFR1 to recruit FADD to TNFR1, we performed coimmunoprecipitation experiments. FADD coprecipitated with Fas, consistent with previous results (Chinnaiyan et al., 1995), whereas no detectable FADD coprecipitated with TNFR1 (Figure 5B). In contrast, when TNFR1 and FADD were expressed in the

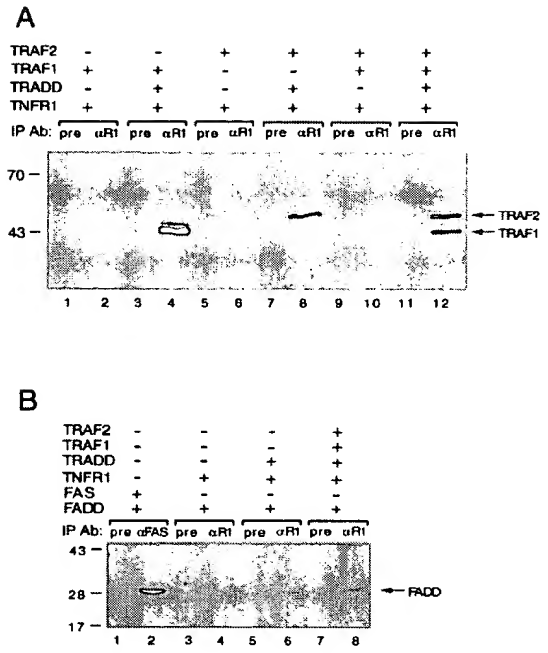

Figure 5. TRADD Recruits TRAF1, TRAF2, and FADD to TNFR1

(A) Coimmunoprecipitation of TNFR1–TRADD–TRAF complexes. We transfected 293 cells (2×10^6 per 100 mm plate) with the indicated combinations of expression vectors for TNFR1, TRADD, Flag–TRAF1, or Flag–TRAF2. After 24 hr, extracts were prepared and immunoprecipitated with preimmune serum (odd-numbered lanes) or with polyclonal antibody against the extracellular domain of TNFR1 (even-numbered lanes). Coprecipitating Flag–TRAF1 and Flag–TRAF2 were detected by immunoblot analysis with anti-Flag monoclonal antibody.

(B) Coimmunoprecipitation of TNFR1–TRADD–FADD complexes. We transfected 293 cells with the indicated combinations of expression vectors for Fas, TNFR1, TRADD, Flag–FADD, TRAF1, and TRAF2. Western blotting analysis indicated that Flag–FADD expression levels were similar in all samples (data not shown). Lysates were immunoprecipitated with preimmune (lanes 1, 3, 5, and 7), anti-Fas (lane 2), or anti-TNFR1 (lanes 4, 6, and 8) antiserum. Coprecipitating Flag–FADD was detected with anti-Flag monoclonal antibody.

presence of TRADD, FADD could be detected in the anti-TNFR1 immune complex. However, even under these conditions, the amount of FADD that coprecipitated with TNFR1 was less than with Fas. The addition of TRAF1 and TRAF2 did not inhibit, but rather slightly enhanced, the ability of TRADD to recruit FADD to TNFR1 (Figure 5B). This result shows that TRADD can simultaneously recruit TRAF proteins and FADD to TNFR1. Furthermore, these experiments suggest that, whereas TRADD–FADD and TRADD–TNFR1 complexes are relatively stable, trimeric TNFR1–TRADD–FADD complexes may exist only transiently or may require other proteins for their stabilization.

NF-κB Activation by TNFR1 Requires TRAF2

The activation of NF-κB by TNFR2 and CD40 is mediated by TRAF2 (Rothe et al., 1995). The presence of TRAF2 in the TNFR1 complex suggests that it may also be involved in signaling TNFR1 responses. However, our previous experiments using a dominant-negative mutation of TRAF2 lacking the N-terminal 86 amino acids that comprise the RING finger domain (TRAF2[87–501]) failed to demonstrate a role for TRAF2 in TNFR1-initiated NF-κB activation (Rothe et al., 1995). To examine further a potential role for TRAF2 in NF-κB activation by TNFR1, we selected the 293 cell line, since electrophoretic mobility shift assays have shown that TNF activates NF-κB exclusively through endogenous TNFR1 in these cells (Rothe et al., 1995).

We reasoned that our earlier failure to see an effect of TRAF2(87–501) on signaling through endogenous TNFR1 might be related to the stability of the TNFR1–TRADD–TRAF complex. In those experiments, TNF stimulation had been performed shortly after transfection, perhaps before the newly synthesized TRAF2(87–501) could displace endogenous TRAF1/TRAF2 from the complex. Therefore, we performed a time course experiment in which TNF was added at various times following TRAF2(87–501) transfection (Figure 6). We found that 293 cells transfected with a control expression vector responded to TNF with an approximately 20-fold increase in NF-κB reporter gene activity. When TNF stimulation was performed 16 hr after transfection with the TRAF2(87–501) expression vector, NF-κB activation was only partially compromised (approximately 7-fold activation). However, the inhibitory effect of TRAF2(87–501) increased with time. TRAF2(87–501) expression completely blocked TNF-induced NF-κB activation (1.2 ± 0.2-fold activation) when TNF treatment was performed 48 hr after transfection (Figure 6). Similar results were obtained using HeLa cells (data not shown).

TNF and interleukin-1 (IL-1) elicit many similar biological activities, including NF-κB activation in 293 cells. To determine the specificity of the observed TNF-inhibitory effect of TRAF2(87–501), we compared the effect of TRAF2(87–501) overexpression on NF-κB activation by these two cytokines. In a dose-response experiment, low levels (0.1 μg) of TRAF2(87–501) expression vector were sufficient to inhibit TNF-induced NF-κB-dependent reporter activity significantly, and high levels (3.2 μg) completely blocked activation. In contrast, overexpression of TRAF2(87–501) had no effect on IL-1-mediated NF-κB activation (Figure 7). These results provide strong evidence that the TRAF2(87–501) dominant-negative mutant is inhibiting NF-κB activation in a specific manner and that TRAF2 plays an important role in TNFR1 signaling.

The Apoptotic Pathway Activated by TNFR1 Does Not Require TRAF2

Two important activities of TNF signaled through TNFR1 are activation of NF-κB and induction of apoptosis. Overexpression of the TNFR1-associated protein TRADD can trigger both activities by activating two distinct signaling pathways (Hsu et al., 1995). However, overexpression of TRAF2 activates NF-κB (Rothe et al., 1995), but does not induce cell death (H. H. and D. V. G., unpublished data), suggesting that TRAF2 may not be an essential component of the TNFR1–TRADD apoptotic signaling cascade. To examine further whether TRAF2

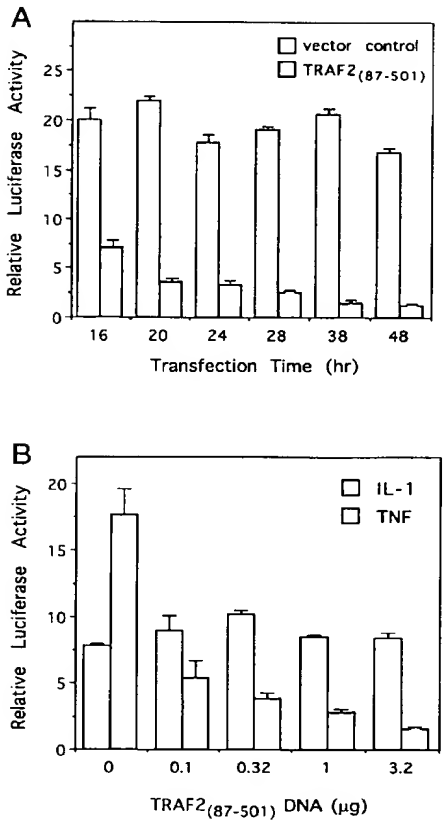

Figure 6. The TRAF2(87–501) Dominant-Negative Mutant Specifically Inhibits TNF-Induced NF-κB Activation

(A) Time-dependent effect of TRAF2(87–501) expression on TNF-induced NF-κB activation. We transfected 293 cells (2×10^5) with 1 μg of TRAF2(87–501) expression vector or 1 μg of pRK vector control, together with 1 μg of pELAM-luc reporter and 0.5 μg of pRSV-βgal plasmids. At the indicated times following transfection, cells were either treated with TNF (20 ng/ml) or left untreated for an additional 6 hr. The values indicated (shown as mean ± SEM) represent luciferase activities for TNF-treated cells relative to untreated cells for an experiment performed in duplicate.

(B) Dose response effect of TRAF2(87–501) expression on TNF-induced NF-κB activation. We transfected 293 cells (2×10^5) with 1 μg of pELAM-luc reporter, 0.5 μg of pRSV-βgal, and the indicated amounts of TRAF2(87–501) expression vector and supplemented them with pRK control vector for a total of 4.7 μg of DNA; 36 hr after transfection, cells were treated for 6 hr with 20 ng/ml of either TNF or IL-1. Values represent luciferase activities relative to the same cells without cytokine treatment and are shown as mean ± SEM for representative experiments performed in duplicate.

contributes to apoptosis, we studied the effect of the TRAF2 dominant-negative mutant on TNF-mediated killing of HeLa cells, a process which is signaled by TNFR1 (Tartaglia et al., 1993b). In this assay (Hsu et al., 1995), cells are cotransfected with a β-galactosidase expression plasmid. The cells are treated 36 hr later with TNF for 12 hr and then scored for cell death. Overexpression of TRAF2(87–501) had no protective effect in these assays, whereas CrmA, a known inhibitor of TNF-mediated apoptosis (Tewari and Dixit, 1995; Enari et al., 1995) completely blocked cell death (Table 1). Taken together, these observations strongly support a model for signaling by the TNFR1 complex in which TRAF2 is dispensable for apoptosis, but essential for NF-κB activation.

The Death Domain of FADD Inhibits TNF-Induced Apoptosis

Overexpression of FADD has been shown to induce programmed cell death (Boldin et al., 1995a; Chinnaiyan et al., 1995). This activity requires only amino acids 1–117 of FADD (Chinnaiyan et al., 1995). Futhermore, a FADD deletion mutant lacking amino acids 1–79 acts as a dominant-negative inhibitor of Fas-mediated apoptosis, demonstrating that the Fas apoptotic pathway requires FADD (V. M. Dixit, personal communication). Since FADD can directly associate with TRADD, we considered the possibility that FADD may also participate in TNF-induced cell death. We examined the effect of a deletion mutant of FADD lacking its 79 N-terminal amino acids (FADD[80–205]) on TNF-mediated killing of HeLa cells. Overexpression of wild-type FADD, but not FADD(80–205), was able to trigger cell death in these cells, in accordance with previous findings (Chinnaiyan et al., 1995). Importantly, FADD(80–205) was a potent inhibitor of TNF-mediated apoptosis, blocking cell death as effectively as CrmA (Table 1). Similar results were obtained using mouse NIH 3T3 cells (data not shown).

It has been shown previously that overexpression of either TRADD (Hsu et al., 1995) or TNFR1 (Boldin et al., 1995b) triggers cell death, presumably through an aggregation phenomenon that activates a TNFR1 signaling cascade. However, when 293 cells (Figure 7) or HeLa cells (data not shown) were cotransfected with the FADD(80–205) expression vector, neither TRADD nor TNFR1 overexpression induced cell death. The strong dominant-negative effect of FADD(80–205) on cell death induced by TNF, TNFR1, and TRADD suggests that FADD participates in the apoptotic pathway activated by TNF through TNFR1 and TRADD.

The Death Domain of FADD Does Not Inhibit TNF-Mediated NF-κB Activation

Since FADD(80–205) potently inhibits the TNFR1–TRADD pathway that triggers apoptosis, we asked whether it might also block the TNFR1–TRADD NF-κB activation pathway. In a dose-response experiment, FADD(80–205) overexpression failed to inhibit TNF-induced activation of an NF-κB-dependent reporter gene (Figure 8). In fact, when expressed at high levels, FADD(80–205) itself activates NF-κB. However, NF-κB activation mediated by TNF was still observed above these FADD(80–205)-induced levels. FADD(80–205) also failed to inhibit NF-κB activation triggered by overexpression of TRADD or TNFR1 (data not shown). These results suggest that FADD does not play a role in the TNFR1–TRADD signaling cascade leading to NF-κB activation.

Discussion

Recently, several novel proteins have been identified that interact with members of the TNFR superfamily to initiate intracellular signal transduction events (Rothe et

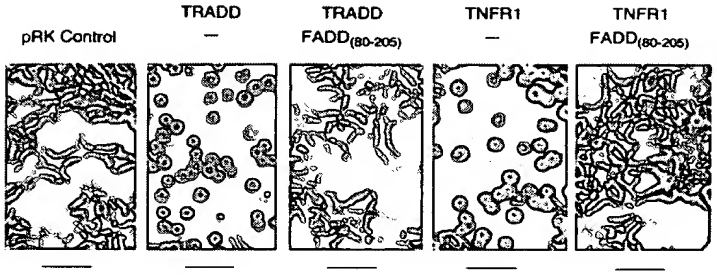

Figure 7. FADD(80–205) Inhibits Apoptosis Induced by Overexpression of TRADD and TNFR1

We transiently transfected 293 cells (2×10^5) with the indicated expression vectors (1 μg) and analyzed them 24 hr later by phase-contrast microscopy. Scale bar is 50 μm.

al., 1994; Hu et al., 1994; Boldin et al., 1995a; Cheng et al., 1995; Chinnaiyan et al., 1995; Hsu et al., 1995; Mosialos et al., 1995; Sato et al., 1995; Stanger et al., 1995). These signaling proteins fall into two structural classes, containing either death domains (TRADD, FADD, and RIP) or TRAF domains (TRAF1, TRAF2, and TRAF3). The death domain–containing proteins are involved in signaling by TNFR1 and Fas antigen, two receptors which themselves contain death domains. Therefore, death domains, in addition to their clear involvement in apoptotic signaling, appear to define sequences involved in protein–protein interactions. In contrast, the TRAF domain proteins interact with receptors (TNFR2 and CD40) that have no recognizable domains or motifs. The results of these initial cloning experiments seemed to confirm earlier predictions (Dembic et al., 1990; Lewis et al., 1991; Goodwin et al., 1991) that TNFR1 and TNFR2 would be found to activate independent and distinct signal transduction pathways.

TRADD interacts with the death domain of TNFR1 to initiate distinct signaling cascades for two of the most important biological activities of TNF, NF-κB activation and programmed cell death (Hsu et al., 1995). Our finding that this interaction is TNF dependent suggests that the death domains of TRADD and TNFR1 do not interact with each other as monomers. Instead, the trimeric TNF is likely to induce trimeric or perhaps higher order aggregates of TNFR1 (Banner et al., 1993) that are stabilized by the self-associating death domain of TNFR1 (Song et al., 1994; Boldin et al., 1995b). These aggregated TNFR1 death domains would then provide a high affinity binding site for TRADD, perhaps itself in a preassociated state (Figure 9).

A yeast two-hybrid screen was performed to identify TRADD-interacting proteins as candidate signal transducers for the NF-κB and apoptotic pathways. We isolated several clones encoding TRAF2, a 56 kDa protein originally purified through its association with TNFR2 (Rothe et al., 1994) and later shown to be a common mediator of NF-κB activation by TNFR2 and CD40 (Rothe et al., 1995). Thus, the two known classes of signal transducers for the TNFR family, TRAF domain and death domain proteins, are capable of direct interaction. We also isolated cDNAs encoding FADD, a death domain–containing protein previously shown to interact with Fas and to trigger cell death when overexpressed (Boldin et al., 1995a; Chinnaiyan et al., 1995).

Table 1. Inhibition of TNF-Induced Apoptosis of HeLa Cells by FADD(80–205), but Not by TRAF2(87–501)

Expression Vector	Number of Blue Cells per Well	
	Minus TNF	Plus TNF
pRK control	187 ± 25	0 ± 0
TRAF1	219 ± 12	0 ± 0
TRAF2	249 ± 4	0 ± 0
TRAF2(87–501)	226 ± 11	0 ± 0
FADD	9 ± 4	0 ± 0
FADD(80–205)	229 ± 22	237 ± 15
CrmA	266 ± 18	189 ± 39

HeLa cells (2×10^5 cells per well) were transiently cotransfected with pCMV-βgal (0.5 μg) and 2.5 μg of expression vector for TRAF1, TRAF2, TRAF2(87–501), FADD, FADD(80–205), or CrmA; 36 hr after transfection, cells were treated with 10 μg/ml cycloheximide with or without 20 μg/ml TNF for 12 hr. Data (± SEM) are shown as the number of blue cells per 35 mm dish for two independent transfections.

TRADD–TRAF2 Interaction and Activation of NF-κB

The identification of a TRADD–TRAF2 complex raised the possibility that TRAFs might associate indirectly with TNFR1 and TRADD might associate indirectly with

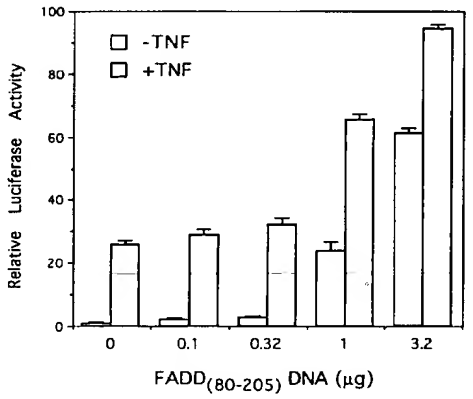

Figure 8. FADD(80–205) Is Not a Dominant-Negative Inhibitor of TNF-Induced NF-κB Activation

We transfected 293 cells (2×10^5) with 1 μg of pELAM-luc reporter, 0.5 μg of pRSV-βgal, and the indicated amounts of FADD(80–205) expression vector and supplemented them with pRK control vector for a total of 4.7 μg of DNA; 36 hr after transfection, cells were treated for 6 hr with 20 ng/ml TNF. Values represent luciferase activities relative to vector-transfected cells and are shown as mean ± SEM for representative experiments performed in duplicate.

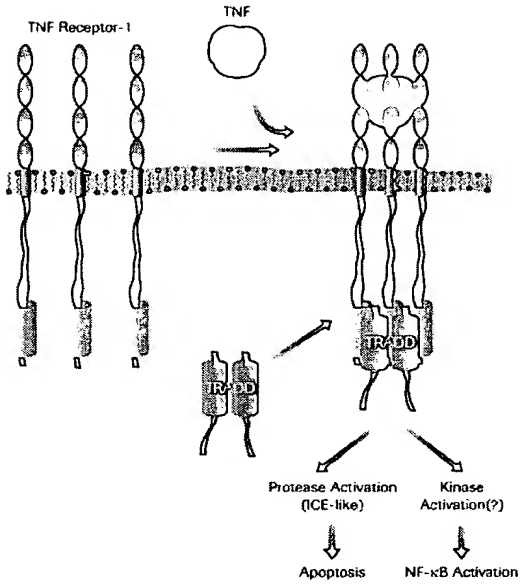

Figure 9. A Model for the Activation of Two Distinct TNFR1 Signal Transduction Pathways by TNF

The trimeric TNF induces TNFR1 aggregation, which is stabilized by homotypic interactions of the death domain of TNFR1. TRADD (perhaps as an oligomer) associates via its own death domain with the aggregated death domain of TNFR1 to initiate signaling cascades for both apoptosis and NF-κB activation. TRAF2 and FADD are TRADD-interacting proteins that define the NF-κB and cell death pathways, respectively (see text).

TNFR2. We found that TNFR1–TRAF–TRAF complexes can indeed exist. Conversely, TNFR2–TRADD–TRAF complexes cannot form, presumably because TNFR2 and TRADD compete for binding to similar sites in TRAF domains. These findings were conceptually appealing for two reasons. First, both TNFRs are independently capable of NF-κB activation (Wiegmann et al., 1992; L—greid et al., 1994; Rothe et al., 1994; Hsu et al., 1995) and association with TRAF2, a protein whose overexpression leads to NF-κB activation (Rothe et al., 1995). Second, of the two TNFRs, only TNFR1 interacts with the cell death–inducing protein TRADD (Hsu et al., 1995), and this receptor also exerts a far more dominant role in the signaling of apoptosis than does TNFR2 (Tartaglia et al., 1991, 1993b).

The role of TRAF2 in TNFR1 signaling was examined by expressing TRAF2(87–501), a truncated version of TRAF2 lacking its N-terminal RING finger domain. This dominant-negative TRAF2 mutant can inhibit NF-κB activation by TNFR2 and CD40 (Rothe et al., 1995). When overexpressed in 293 cells, TRAF2(87–501) blocked NF-κB activation by TNF, a process that is TNFR1 dependent. NF-κB activation by the cytokine IL-1 was unaffected by TRAF2(87–501), demonstrating that TRAF2 is not involved in IL-1 signaling. TRAF2(87–501) overexpression also had no effect on TNF-mediated apoptosis. This result is consistent with TRAF2 defining a point at which the two (or more) TNFR1–TRADD signal transduction pathways diverge. The TRAF2 pathway, which is shared with TNFR2, CD40, and probably other members of the TNFR superfamily, ultimately would result in NF-κB activation.

On the surface, the results described here would seem to contradict our earlier characterization of TRADD deletion mutants (Hsu et al., 1995). In those experiments we showed that a TRADD mutant (TRADD[195–312]) lacking amino acids 1–194 was capable of activating NF-κB when overexpressed. This result implied that the N-terminal 194 amino acids of TRADD, and by inference proteins such as TRAF2 that bind to this region of TRADD, would not be required for NF-κB activation. This apparent paradox can be explained by the following experimental result. We have found that the NF-κB activation pathway induced by TRADD(195–312) can be potently inhibited by overexpression of the TRAF2(87–501) dominant-negative mutant (data not shown) and is therefore TRAF2 dependent. To date, all TRAF2-dependent pathways for NF-κB activation appear to require TRAF2 aggregation (Rothe et al., 1995). Therefore, our current interpretation of these data is that TRADD(195–315) overexpression leads to aggregation of endogenous TRADD and its associated TRAF2.

Many details of the molecular mechanism(s) by which TRAF2 activates NF-κB remain a mystery. NF-κB consists of p50 and p65 subunits that are normally associated with the cytoplasmic inhibitor protein IκB (Liou and Baltimore, 1993; Beg and Baldwin, 1993). Activation of NF-κB by the proinflammatory cytokines IL-1 and TNF (Osborn et al., 1989) results in rapid serine phosphorylation and degradation of IκB, releasing NF-κB for translocation to the nucleus (Beg et al., 1993; Palombella et al., 1994). The phosphorylation of IκB is thought to be the cytokine-regulated step that targets IκB for degradation by the constitutive ubiquitin–proteasome pathway (Thanos and Maniatis, 1995). In this regard, TNF has been shown to activate a TNFR1-associated serine protein kinase activity (VanArsdale and Ware, 1994). If one assumes this kinase is required for NF-κB activation by TNF, then the essential role of the RING finger domain of TRAF2 in NF-κB activation might be to regulate kinase activity, recruit the kinase to the TNFR1 signaling complex, or both.

TRADD–FADD Interaction and Signaling of Apoptosis

The strong interaction observed between the death domains of TRADD and FADD suggested the possibility that TRADD might be able to recruit FADD to TNFR1. Indeed, low levels of FADD were found in the TNFR1 complex when FADD, TRADD, and TNFR1 were coexpressed, raising the question of whether FADD is involved in TNFR1-mediated signaling.

To address a possible role for FADD in signal transduction by TNFR1, we examined an N-terminal deletion mutant of murine FADD obtained in our two-hybrid screen. Expression of FADD(80–205) completely blocked cell death induced by TNF treatment, or by overexpression of TNFR1 or TRADD, without affecting NF-κB activation. The anti-apoptotic activity of FADD(80–205) in

these assays was as potent as that of CrmA and much more potent than Bcl-2 (Hsu et al., 1995). A similarly truncated human FADD acts as a dominant-negative inhibitor of Fas-mediated apoptosis (V. M. Dixit, personal communication). Therefore, FADD may be a component of the cell death pathways triggered by both TNFR1 and Fas. Alternatively, FADD(80–205) may exert its dominant-negative effect through titration of an unidentified component of the TNFR1 cell death pathway. However, high level expression of FADD(80–205) did not appear to interfere with TRADD binding to TNFR1 (data not shown).

The signaling of cell death by TNFR1 and Fas is not well understood, but considerable evidence suggests the apoptotic pathway requires activation of a protease cascade that ultimately leads to cleavage of cell death substrates (reviewed by Martin and Green, 1995). CrmA expression blocks this pathway by directly binding to cysteine proteases of the CED-3/interleukin-1β-converting enzyme (ICE) family (Tewari and Dixit, 1995; Enari et al., 1995; Los et al., 1995). Presumably, FADD(80–205) blocks the cell death pathway at a receptor-proximal step that precedes protease activation, either by displacing FADD or by tying up other components required to execute the death signal(s). As such, FADD(80–205) should be a useful reagent for dissecting apoptotic cascades initiated by other events.

Apoptosis mediated by TNFR1 and Fas are similar in that both signaling cascades are initiated by death domains and end in activation of ICE-like protease(s). However, clear differences in these two cell death pathways have been observed (Wong and Goeddel, 1994; Schulze-Osthoff et al., 1994). For example, Fas-mediated cell death occurs much more rapidly than that triggered by TNFR1 (Clement and Stamenkovic, 1994; Abreu-Martin et al., 1995). These differences might be due to differential contributions from other, non-FADD components of the receptor complexes. It is also possible that the greater affinity of FADD for Fas than for TNFR1–TRADD observed in our coimmunoprecipitation experiments might reflect affinity differences under physiological conditions. In turn, the amount of FADD present in the respective receptor complexes might correlate with potency of the death signal.

Conclusions

The demonstration that TRADD interacts with TRAF2 and FADD, and can recruit both to TNFR1, suggested that TRAF2 and FADD may be involved in TNFR1–TRADD-mediated signaling. That these interactions define two distinct signaling pathways emanating from TRADD (Figure 9) is supported by the ability of TRAF2 and FADD to activate NF-κB and induce apoptosis, respectively. This hypothesis is further strengthened by the effectiveness of dominant-negative mutants at selectively inhibiting one pathway or the other: TRAF2(87–501) blocks NF-κB activation by TNFR1 and FADD(80–205) blocks apoptosis. It will now be of great interest to identify downstream events in these signaling cascades that connect TRAF2 to IκB phosphorylation and FADD to cysteine protease activation.

Experimental Procedures

Reagents and Cell Lines

Recombinant human TNF and IL-1 were provided by Genentech. The rabbit anti-TNFR1, anti-Fas, and anti-TRADD antisera and the monoclonal antibody against the Myc epitope tag have been described previously (Tartaglia et al., 1991; Wong and Goeddel, 1994; Hsu et al., 1995). Monoclonal antibody 985 against the extracellular domain of TNFR1 was provided by Genentech. The monoclonal antibody against the Flag epitope was purchased from Kodak International Biotechnologies. The human 293 embryonic kidney (R. Tjian), human HeLa derivative HtTA-1 (H. Bujard), human U937 histiocytic lymphoma (G. Wong), and murine NIH 3T3 fibroblast (American Type Culture Collection) cell lines were obtained from the indicated sources.

Expression Vectors

Mammalian cell expression vectors encoding TNFR1, TRADD, TRAF1, TRAF2, TRAF2(87–501), and CrmA have been described previously (Hsu et al., 1995; Rothe et al., 1995). The expression vectors for Fas were provided by Dr. V. Dixit. The full-length FADD and FADD(80–205) expression plasmids was prepared by inserting a SalI–NotI fragment from the two-hybrid *FADD* cDNA clones in-frame with an N-terminal Flag epitope in the vector pRK5. The control expression plasmid pRK5, the NF-κB reporter plasmid pELAM-luc, and pCMV-βgal were also described previously (Hsu et al., 1995). Restriction sites in the *TRADD* cDNA (StuI, SmaI, and NotI) were used to obtain deletion mutants of TRADD (amino acids 1–274, 1–169, and 1–106, respectively). Wild-type and deletion mutants of TRADD were cloned into the yeast GAL4 DNA-binding domain vector pGBT9 (Clontech). Plasmids containing the GAL4 activation domain fused with TRAF2, TRAF2(87–501), and TRAF2(264–501) were as described previously (Rothe et al., 1994, 1995). TRAF2(348–501)/GAL4ad was generated by cloning the appropriate coding sequence into pPC86. TRAF2(1–358)/GAL4ad was provided by Dr. H. Y. Song.

Yeast Two-Hybrid Cloning

The plasmid GAL4bd–TRADD (Hsu et al., 1995), which encodes the GAL4 DNA-binding domain fused to full-length TRADD, was used as bait in two-hybrid screens of HeLa (Clontech) and mouse fetal liver stromal cell (provided by L. Lasky) cDNA libraries. The isolation of positive clones and subsequent two-hybrid interaction analyses were carried out as described elsewhere (Hsu et al., 1995). DNA sequencing was performed on an Applied Biosystems model 373A automated DNA sequencer.

Transfections and Reporter Assays

The 293, NIH 3T3, and HtTA-1(HeLa) cell lines were maintained in high glucose Dulbecco's modified Eagle's medium containing 10% fetal calf serum, 100 μg/ml penicillin G, and 100 μg/ml streptomycin (GIBCO). For reporter and apoptosis assays, $\sim 2 \times 10^5$ cells per well were seeded on 6-well (35 mm) dishes. For coimmunoprecipitations, $\sim 2 \times 10^6$ cells per well were seeded on 100 mm plates. Cells were transfected the following day by the calcium phosphate precipitation method (Ausubel et al., 1994). Luciferase reporter assays were performed as described elsewhere (Hsu et al., 1995).

Coimmunoprecipitation and Western Blot Analysis

We grew U937 cells (5×10^7) in RPMI medium containing 10% fetal calf serum and 100 μg/ml each of penicillin G and streptomycin, washed them in warm PBS, and incubated them for 15 min in the presence or absence of TNF (100 ng/ml). Cells were lysed in 1 ml of lysis buffer (20 mM Tris [pH 7.5], 150 mM NaCl, 1% Triton X-100, 1 mM EDTA, 30 mM NaF, 2 mM sodium pyrophosphate, 10 μg/ml aprotinin, 10 μg/ml leupeptin). Lysates were incubated with 25 μg of monoclonal antibody 985 or mouse IgG for 2 hr at 4°C, then mixed with 25 μl of a 1:1 slurry of protein GammaBind G–Sepharose, and incubated for another 2 hr. The Sepharose beads were washed twice with 1 ml of lysis buffer, twice with 1 ml of high salt (1 M NaCl) lysis buffer, and twice more with lysis buffer. Transfected 293 cells from each 100 mm dish were lysed in 1 ml of E1A buffer (50 mM HEPES [pH 7.6], 250 mM NaCl, 0.1% NP-40, 5 mM EDTA). For each immunoprecipitation, 0.5 ml aliquots of lysates were incubated with

1 μl of anti-TNFR1 or anti-Fas antibody or with 2 μl of anti-Flag antibody at 4°C for at least 1 hr. The lysates were mixed with 20 μl of a 1:1 slurry of protein A- or protein G-Sepharose (Pharmacia) and incubated for another hour. The Sepharose beads were washed twice with 1 ml of E1A buffer, twice with 1 ml of high salt (1 M NaCl) E1A buffer, and twice again with E1A buffer. The precipitates were fractionated on 10% SDS-PAGE and transferred to Immobilon-P membrane (Millipore). Subsequent Western blotting analyses were performed as described elsewhere (Hsu et al., 1995).

Apoptosis Assays

Transfected HeLa cells were washed with PBS, fixed in PBS containing 2% paraformaldehyde, 0.2% glutaraldehyde for 5 min at 4°C, and washed again with PBS. Fixed cells were stained overnight with PBS containing 1 mg/ml X-Gal, 5 mM potassium ferricyanide, 5 mM potassium ferrocyanide, 2 mM $MgCl_2$, 0.02% NP-40, 0.01% SDS. The number of blue-staining cells was determined microscopically. We analyzed 293 cells for apoptosis by phase-contrast microscopy 24 hr after transfection.

Acknowledgments

We thank Keith Williamson for DNA sequencing, Carl Ware and Todd VanArsdale for advice on the U937 immunoprecipitations, Vishva Dixit for communication of unpublished data, and Mike Rothe for stimulating discussions and for providing various TRAF reagents. We also thank Steve McKnight and Mike Rothe for helpful comments on the manuscript.

Received September 1, 1995; revised December 1, 1995.

References

Abreu-Martin, M.T., Vidrich, A., Lynch, D.H., and Targan, T.R. (1995). Divergent induction of apoptosis and IL-8 secretion in HT-29 cells in response to TNF-α and ligation of Fas antigen. J. Immunol. *155*, 4147–4154.

Ausubel, F.M., Brent, R., Kingston, R.E., Moore, D.D., Seidman, J.G., Smith, J.A., and Struhl, K. (1994). Current Protocols in Molecular Biology (New York: Greene Publishing Associates/Wiley & Sons).

Banner, D.W., D'Arcy, A., Janes, W., Gentz, R., Schoenfeld, H.-J., Broger, C., Loetscher, H., and Lesslauer, W. (1993). Crystal structure of the soluble human 55 kd TNF receptor-human TNFβ complex: implications for TNF receptor activation. Cell *73*, 431–445.

Beg, A.A., and Baldwin, A.S. (1993). The IκB proteins: multifunctional regulators of Rel/NF-κB transcription factors. Genes Dev. *7*, 2064–2070.

Beg, A.A., Finco, T.S., Nantermet, P.V., and Baldwin, A.S. (1993). Tumor necrosis factor and interleukin-1 lead to phosphorylation and loss of IκBα: a mechanism for NF-κB activation. Mol. Cell. Biol. *13*, 3301–3310.

Boldin, M.P., Varfolomeev, E.E., Pancer, Z., Mett, I.L., Camonis, J.H., and Wallach, D. (1995a). A novel protein that interacts with the death domain of Fas/APO1 contains a sequence motif related to the death domain. J. Biol. Chem. *270*, 7795–7798.

Boldin, M.P., Mett, I.L., Varfolomeev, E.E., Chumakov, I., Shemer-Avni, Y., Camonis, J.H., and Wallach, D. (1995b). Self-association of the "death domains" of the p55 tumor necrosis factor (TNF) receptor and Fas/APO1 prompts signaling for TNF and Fas/APO1 effects. J. Biol. Chem. *270*, 387–391.

Cheng, G., Cleary, A.M., Ye, Z., Hong, D.I., Lederman, S., and Baltimore, D. (1995). Involvement of CRAF2, a relative of TRAF, in CD40 signaling. Science *267*, 1494–1498.

Chinnaiyan, A.M., O'Rourke, K., Tewari, M., and Dixit, V.M. (1995). FADD, a novel death domain-containing protein, interacts with the death domain of Fas and initiates apoptosis. Cell *81*, 505–512.

Clement, M.-V., and Stamenkovic, I. (1994). Fas and tumor necrosis factor receptor-mediated cell death: similarities and distinctions. J. Exp. Med. *180*, 557–567.

Dembic, Z., Loetscher, H., Gubler, U., Pan, Y.-C.E., Lahm, H.W., Genz, R., Brockhaus, M., and Lesslauer, W. (1990). Two human TNF receptors have similar extracellular, but distinct intracellular, domain sequences. Cytokine *2*, 231–237.

Enari, M., Hug, H., and Nagata, N. (1995). Involvement of an ICE-like protease in Fas-mediated apoptosis. Nature *375*, 78–81.

Fields, S., and Song, O.-k. (1989). A novel genetic system to detect protein-protein interactions. Nature *340*, 245–246.

Goodwin, R.G., Anderson, D., Jerzy, R., Davis, T., Brannan, C.I., Copeland, N.G., Jenkins, N.A., and Smith, C.A. (1991). Molecular cloning and expression of the type I and type II murine receptors for tumor necrosis factor. Mol. Cell. Biol. *11*, 3020–3026.

Hsu, H., Xiong, J., and Goeddel, D.V. (1995). The TNF receptor 1-associated protein TRADD signals cell death and NF-κB activation. Cell *81*, 495–504.

Hu, M.H., O'Rourke, K., Boguski, M.S., and Dixit, V.M. (1994). A novel RING finger protein interacts with the cytoplasmic domain of CD40. J. Biol. Chem. *269*, 30069–30072.

Itoh, N., and Nagata, S. (1993). A novel protein domain required for apoptosis. J. Biol. Chem. *268*, 10932–10937.

Lægreid, A., Medvedev, A., Nonstad, U., Bombara, M.P., Ranges, G., Sundan, A., and Espevik, T. (1994). Tumor necrosis factor receptor p75 mediates cell-specific activation of nuclear factor κB and induction of human cytomegalovirus enhancer. J. Biol. Chem. *269*, 7785–7791.

Lewis, M., Tartaglia, L.A., Lee, A., Bennett, G.L., Rice, G.C., Wong, G.H.W., Chen, E.Y., and Goeddel, D.V. (1991). Cloning and expression of cDNAs for two distinct murine tumor necrosis factor receptors demonstrate one receptor is species specific. Proc. Natl. Acad. Sci. USA *88*, 2830–2834.

Liou, H.-C., and Baltimore, D. (1993). Regulation of the NF-κB/rel transcription factor and IκB inhibitor system. Curr. Biol. *5*, 477–487.

Loetscher, H., Pan, Y.-C.E., Lahm, H.-W., Gentz, R., Brockhaus, M., Tabuchi, H., and Lesslauer, W. (1990). Molecular cloning and expression of the human 55 kd tumor necrosis factor receptor. Cell *61*, 351–359.

Los, M., van de Craen, M., Penning, L.C., Schenk, H., Westendorp, M., Baeuerle, P.A., Droge, W., Krammer, P.H., Fiers, W., and Schulze-Osthoff, K. (1995). Requirement of an ICE/CED-3 protease for Fas/APO-1-mediated apoptosis. Nature *375*, 81–83.

Martin, S.J., and Green, D.R. (1995). Protease activation during apoptosis: death by a thousand cuts? Cell *82*, 349–352.

Mosialos, G., Birkenbach, M., Yalamanchili, R., VanArsdale, T., Ware, C., and Kieff, E. (1995). The Epstein-Barr virus transforming protein LMP1 engages signaling proteins for the tumor necrosis factor receptor family. Cell *80*, 389–399.

Osborn, L., Kunkel, S., and Nabel, G.J. (1989). Tumor necrosis factor a and interleukin 1 stimulate the human immunodeficiency virus enhancer by activation of the nuclear factor κB. Proc. Natl. Acad. Sci. USA *86*, 2336–2340.

Palombella, V.J., Rando, O.J., Goldberg, A.L., and Maniatis, T. (1994). The ubiquitin-proteasome pathway is required for processing the NF-κB1 precursor protein and the activation of NF-κB. Cell *78*, 773–785.

Rothe, J., Gehr, G., Loetscher, H., and Lesslauer, W. (1992). Tumor necrosis factor receptors: structure and function. Immunol. Rev. *11*, 81–90.

Rothe, M., Wong, S.C., Henzel, W.J., and Goeddel, D.V. (1994). A novel family of putative signal transducers associated with the cytoplasmic domain of the 75 kDa tumor necrosis factor receptor. Cell *78*, 681–692.

Rothe, M., Sarma, V., Dixit, V.M., and Goeddel, D.V. (1995). TRAF2-mediated activation of NF-κB by TNF receptor 2 and CD40. Science *269*, 1424–1427.

Sato, T., Irie, S., and Reed, R.C. (1995). A novel member of the TRAF family of putative signal transducing proteins binds to the cytosolic domain of CD40. FEBS Lett. *358*, 113–118.

Schall, T.J., Lewis, M., Koller, K.J., Lee, A., Rice, G.C., Wong, G.H.W., Gatanaga, T., Granger, G.A., Lentz, R., Raab, H., Kohr, W.J., and

Goeddel, D.V. (1990). Molecular cloning and expression of a receptor for human tumor necrosis factor. Cell *61*, 361–370.

Schulze-Osthoff, K., Krammer, P.H., and Droge, W. (1994). Divergent signalling via APO-1/Fas and the TNF receptor, two homologous molecules involved in physiological cell death. EMBO J. *13*, 4587–4596.

Smith, C.A., Davis, T., Anderson, D., Solam, L., Beckmann, M.P., Jerzy, R., Dower, S.K., Cosman, D., and Goodwin, R.G. (1990). A receptor for tumor necrosis factor defines an unusual family of cellular and viral proteins. Science *248*, 1019–1023.

Smith, C.A., Farrah, T., and Goodwin, R.G. (1994). The TNF receptor superfamily of cellular and viral proteins: activation, costimulation, and death. Cell *76*, 959–962.

Song, H.Y., Dunbar, J.D., and Donner, D.B. (1994). Aggregation of the intracellular domain of the type 1 tumor necrosis factor receptor defined by the two-hybrid system. J. Biol. Chem. *269*, 22492–22495.

Stanger, B.Z., Leder, P., Lee, T.-H., Kim, E., and Seed, B. (1995). RIP: a novel protein containing a death domain that interacts with Fas/APO-1 (CD95) in yeast and causes cell death. Cell *81*, 513–523.

Tartaglia, L.A., and Goeddel, D.V. (1992). Two TNF receptors. Immunol. Today *13*, 151–153.

Tartaglia, L.A., Weber, R.F., Figari, I.S., Reynolds, C., Palladino, M.A., and Goeddel, D.V. (1991). The two different receptors for tumor necrosis factor mediate distinct cellular responses. Proc. Natl. Acad. Sci. USA *88*, 9292–9296.

Tartaglia, L.A., Ayres, T.M., Wong, G.H.W., and Goeddel, D.V. (1993a). A novel domain within the 55 kd TNF receptor signals cell death. Cell *74*, 845–853.

Tartaglia, L.A., Rothe, M., Hu, Y.-F., and Goeddel, D.V. (1993b). Tumor necrosis factor's cytotoxic activity is signaled by the p55 TNF receptor. Cell *73*, 213–216.

Tewari, M., and Dixit, V.M. (1995). Fas- and TNF-induced apoptosis is inhibited by the poxvirus crmA gene product. J. Biol. Chem. *270*, 3255–3260.

Thanos, A.M., and Maniatis, T. (1995). NF-κB: a lesson in family values. Cell *80*, 529–532.

VanArsdale, T.L., and Ware, C.F. (1994). TNF receptor signal transduction: ligand-dependent stimulation of a serine protein kinase activity associated with (CD120a) $TNFR_{60}$. J. Immunol. *153*, 3043–3050.

Wiegmann, K., Schütze, S., Kampen, E., Himmler, A., Machleidt, T., and Krönke, M. (1992). Human 55-kDa receptor for tumor necrosis factor coupled to signal transduction cascades. J. Biol. Chem. *267*, 17997–18001.

Wong, G.H.W., and Goeddel, D.V. (1994). Fas antigen and p55 TNF receptor signal apoptosis through distinct pathways. J. Immunol. *152*, 1751–1755.

GenBank Accession Number

The accession number for the murine FADD sequence reported in this paper is U43184.

B Cells from p50/NF-κB Knockout Mice Have Selective Defects in Proliferation, Differentiation, Germ-Line C_H Transcription, and Ig Class Switching

Clifford M. Snapper,[1]* Piotr Zelazowski,* Fabio R. Rosas,* Marilyn R. Kehry,† Ming Tian,‡ David Baltimore,§ and William C. Sha§

To better understand the role of NF-κB in normal B cell physiology, we used a purified population of resting B cells from p50/NF-κB knockout ($p50^{-/-}$) mice to determine their ability to proliferate, secrete Ig, express germ-line C_H RNA, and undergo Ig isotype switching in vitro in response to a number of distinct stimuli. $p50^{-/-}$ B cells proliferated normally in response to dextran-anti-IgD Abs (αδ-dex) and membrane-bound, but not soluble, CD40 ligand (CD40L), and they were virtually unresponsive to LPS when compared with control B cells. $p50^{-/-}$ B cells secreted markedly reduced Ig in response to αδ-dex or mCD40L in the presence of IL-4 + IL-5, despite their relatively normal proliferative rates, whereas normal Ig secretion was restored by the combination of αδ-dex and CD40L. $p50^{-/-}$ B cells expressed normal steady-state levels of germ-line $C_H\gamma1$ and $C_H\alpha$ RNA but markedly reduced germ-line $C_H\gamma3$ and $C_H\epsilon$ RNA upon appropriate stimulation. Although $p50^{-/-}$ B cells underwent substantial switching to IgG1, a marked reduction in the switch to IgG3 and IgE, as well as IgA, was observed. These data are the first to demonstrate key, independent roles for p50/NF-κB in normal B cell maturation to Ig secretion, germ-line C_H gene activation, and Ig class switching, as well as mitogenesis, and provide a powerful and well-defined in vitro model system for studying the role of p50/NF-κB in a wide range of normal cellular functions. *The Journal of Immunology,* **1996, 156: 183–191.**

NF-κB is a heterodimeric transcription factor composed of a p50 and p65 subunit, which is constitutively present as an inactive complex in the cytoplasm of numerous cell types because of its linkage to an inhibitor, IκB (for review see Refs. 1 and 2). Cellular activation with a wide range of stimuli involved in inflammation and immunity, including LPS, Ag receptor cross-linkers, CD40 activation, and cytokines, leads to phosphorylation and degradation of the IκB component of the NF-κB complex, resulting in translocation of the p50/p65 dimer to the nucleus. Subsequent binding of NF-κB in the nucleus to decameric κB sequence motifs (5′ GGGRNNYYCC 3′) associated with the promoters/enhancers of a wide array of genes, including Igκ light chain, cytokines, and MHC class I and class II, is believed to play a key role in regulating their transcription in a positive manner. The cloning of p50 and p65 led to the identification of the NF-κB/rel family of transcription factor subunits (3, 4), which also includes c-Rel, RelB, and p52. These polypeptides can interact with each other to create different heterodimeric forms with resulting differences in binding specificity, function, and interactions with other promoter/enhancer binding factors. Utilizing normal B cells and B cell tumors, a patterned expression of NF-κB/*rel* family members during ontogeny and upon activation was reported (5). Thus, pre-B cells express mainly p50 and p65, mature B cells express p50 and c-Rel, and plasmacytoma lines or LPS-activated B cells express p52 and RelB along with the others.

Recent studies from Kenter and colleagues demonstrated p50 binding sites within the murine switch (S)γ3, Sγ1, and Sγ2b regions and showed that these sites were nonrandomly associated with switch recombination breakpoints (6–8). Thus, the potential role of p50 in regulating switch recombination was suggested. Further, p50 binding sites have been demonstrated in the germ-line promoters of the $C_H\epsilon$ gene (Iε) (9), Iγ3 (10), Iγ1, and Iα,[2] suggesting that p50 could play a role in regulating germ-line C_H transcription and hence the ability to undergo C_H gene rearrangement.

Despite great advances in elucidating the genetics and biochemistry of NF-κB/*rel* family members, little is certain about their role in cellular activation, proliferation, and differentiation in normal B cells. Nevertheless, NF-κB/Rel family members may play a critical role in modulating B cell responses based on their induction following activation through the membrane Ig or CD40 signaling pathways (11–13). Recently, mice with a targeted disruption of the p50 subunit of NF-κB ($p50^{-/-}$) were generated (14). B cells from such mice developed normally and expressed equivalent levels of membrane-bound (m)[3]IgM and mIgD, as well as MHC class I and II molecules, relative to wild-type controls, with normal, preferential usage of κ light chain. However, B cells from $p50^{-/-}$ mice showed a defective proliferative response to LPS, although not

*The Department of Pathology, Uniformed Services University of the Health Sciences, Bethesda, MD 20814; †Boehringer Ingelheim Pharmaceuticals, Ridgefield, CT 06877; ‡Howard Hughes Medical Institute at Children's Hospital, Boston, MA 02115; and §Department of Biology, Massachusetts Institute of Technology, Cambridge, MA 02139

Received for publication August 7, 1995. Accepted for publication October 26, 1995.

The costs of publication of this article were defrayed in part by the payment of page charges. This article must therefore be hereby marked *advertisement* in accordance with 18 U.S.C. Section 1734 solely to indicate this fact.

[1] Address correspondence and reprint requests to Dr. Clifford M. Snapper, Department of Pathology, USUHS, 4301 Jones Bridge Road, Bethesda, MD 20814-4799.

[2] Lin, S. C., and J. Stavnezer. *Submitted for publication.*

[3] Abbreviations used in this paper: m, membrane-bound (e.g., mIgM); αδ-dex, dextran-conjugated anti-IgD Abs; C_H, constant heavy (gene); CD40L, CD40 ligand; SN, supernatant; FBS, fetal bovine serum; RT-PCR, reverse transcriptase-PCR; s, soluble (e.g., sCD40L); cIgM, cytoplasmic IgM.

0022-1767/96/$02.00

anti-Ig, in vitro. Further, unimmunized $p50^{-/-}$ mice showed variable reductions in their serum levels of multiple Ig isotypes, although not IgM, and demonstrated defective production of all Ig isotypes in response to immunization with a T cell-dependent Ag. Because these in vivo responses reflect interactions between multiple immune cell types, and in vitro abnormalities had been identified in both B and T lymphocyte responses, we sought to clarify the cellular basis for these abnormalities by examining the ability of purified resting B cells to undergo B cell maturation and Ig class switching under defined in vitro conditions.

The resting B lymphocyte represents an ideal and extensively studied model for determining parameters that regulate all aspects of the cellular functional program including activation, proliferation, differentiation, and genetic rearrangements. Snapper, Mond, and colleagues have developed an in vitro polyclonal system for studying B cell Ig synthesis and class switching in response to mIg-mediated B cell activation, utilizing dextran-conjugated anti-IgD Abs (αδ-dex) (for reviews see Refs. 15, 16). With the use of this novel conjugate, these investigators completed a series of studies that indicated unique interrelationships between distinct B cell activators and various cytokines for induction of B cell proliferation, differentiation to Ig secretion, Ig class switching, and germline constant heavy gene (C_H) transcription. In particular, they demonstrated that different B cell activators such as LPS, αδ-dex, and CD40L, either alone or in various combinations, engaged functionally as well as biochemically distinct signaling pathways and furthermore often played a determining role in the functional response of the B cell to a given set of cytokines (17–21). To gain a better understanding of the role of p50/NF-κB in cellular activation, we utilized these distinct in vitro systems to compare purified resting B cells from $p50^{-/-}$ mice with control B cells from wild-type and heterozygous littermates for their ability to undergo proliferation, differentiation to Ig secretion, germ-line C_H gene expression, and Ig class switching. In this report, p50/NF-κB is shown for the first time to play key selective and independent roles in normal B cell maturation to Ig secretion, C_H gene activation, and Ig class switching, in addition to mitogenesis.

Materials and Methods

Mice

Mice lacking the p50 subunit of NF-κB were originally established from $p50^{+/-}$ mice of (129/Ola × C57BL/6J)F1 background and were subsequently maintained by intercrosses in a specific pathogen-free environment (14). To minimize potential contributions from differences in background genes between C57BL/6J and 129/Ola strains, small resting $p50^{-/-}$ and control $p50^{+/-}$ or $p50^{+/+}$ B cells were purified from splenocytes pooled from multiple littermates derived from the same matings. Because no differences in B cell responses were observed between $p50^{+/+}$ and $p50^{+/-}$ cells in our initial experiments, $p50^{+/-}$ B cells, derived from $p50^{+/-}$ × $p50^{-/-}$ matings, were used as control populations in subsequent experiments.

Culture medium

RPMI 1640 (Biofluids, Rockville, MD) supplemented with 10% fetal bovine serum (Sigma Chemical Co., St. Louis, MO), L-glutamine (2 mM), 2-ME (0.05 mM), penicillin (Life Technologies, Grand Island, NY; 50 μg/ml), and streptomycin (Life Technologies; 50 μg/ml) were used for culturing cells.

Reagents

Hδ^a/1 (monoclonal mouse IgG2b (b allotype) anti-mouse IgD (a allotype)) and AF3 (monoclonal mouse IgG2a (a allotype) anti-mouse IgD (b allotype)) Abs were purified from ascites. Dextran-conjugated Hδ^a/1 and AF3 Abs (αδ-dex) were prepared by conjugation of the respective mAbs, to high m.w. dextran (2×10^6 m.w.), as previously described (22). The concentration of dextran-conjugated Abs that is noted in the text reflects only the anti-Ig Ab concentrations and not that of the entire dextran conjugate. Recombinant CD8-CD40L fusion protein was constructed and expressed in a soluble form as previously described (23) and partially purified from culture supernatants by precipitation with ammonium sulfate, and chromatography over a CM-Sepharose column. Endotoxin levels in purified CD8-CD40L were <0.02 ng/ml. mCD40L was prepared from Sf9 insect cells infected with a CD40L-containing recombinant baculovirus vector. LPS W, extracted from *Escherichia coli* 0111:B4, was obtained from Difco Laboratories, Inc. (Detroit, MI). Recombinant murine IL-4, IL-5, IFN-γ, and human TGF-β2 were kind gifts from Alan Levine (Searle, St. Louis, MO), Richard Hodes (National Institutes of Health, Bethesda, MD), Genentech, Inc. (South San Francisco, CA), and Wendy Waegell (Celtrix Pharmaceuticals, Santa Clara, CA), respectively. The following FITC-labeled mAbs were used for flow cytometric analysis: rat IgG1 anti-mouse IgG1 (Zymed Laboratories, South San Francisco, CA), rat IgG1 anti-mouse IgA and rat IgG2a anti-mouse IgG3 (PharMingen, San Diego, CA). Rat IgG1 anti-IgE mAb (R1.E4) (24) was purified from ascites and conjugated to FITC by a standard protocol. R1.E4 recognizes an epitope of the IgE molecule that is masked when IgE is bound to FcεRII; thus R1.E4 recognizes intrinsic, but not cytophilic, IgE and can be used without further treatment of cells to quantitate the percentage of B cells switching to IgE. Monoclonal rat IgG2b anti-mouse FcγRII (2.4G2) was purified from ascites. Propidium iodide was purchased from Sigma Chemical Co. Percoll was obtained from Pharmacia (Piscataway, NJ).

Preparation of B cells

Spleens from age-matched $p50^{-/-}$ and control $p50^{+/-}$ or $p50^{+/+}$ mice were removed asceptically and single-cell suspensions were made. T cells were depleted by incubating spleen cells at 4°C in a mixture of monoclonal rat anti-mouse Thy-1 (clone 3H11; ascites), anti-mouse CD4 (clone GK1.5, culture SN), and anti-mouse CD8 (clone 53-6.7, culture SN) Abs, followed by treatment at 37°C with guinea pig complement (Life Technologies) in the presence of monoclonal mouse anti-rat Igκ Ab (clone MAR 18.5, culture SN). Cells were then fractionated into high and low density populations by centrifugation on a discontinuous Percoll gradient consisting of 70, 65, 60, and 50% Percoll solutions (with densities of 1.086, 1.081, 1.074, and 1.062 g/ml, respectively). The high density cells were collected from the 70 to 65% interface and consisted of 90 to 95% B cells and <1% T cells. These cells were small and resting and were used in all experiments reported herein. Cells were cultured in 96-well and 24-well flat-bottom plates, or 25-cm^2 flasks (Corning, Inc., Corning, NY) at 37°C in a humidified incubator containing 6% CO_2. Cultures containing mCD40L were established at 2×10^4 cells/ml due to subsequent extensive expansion of B cells. All other cultures were established at 1×10^5 cells/ml.

Measurement of DNA synthesis by [^{3}H]TdR incorporation

B cells were cultured for 48 h in a final volume of 0.2 ml in complete RPMI in flat-bottom 96-well trays (Costar, Cambridge, MA). [^{3}H]TdR (1 μCi) (Amersham Corp., Arlington Heights, IL), sp. act. 20 Ci/mmol, was added to the cultures for an additional 18 h. Cultured cells were then harvested onto glass fiber filter paper with an LKB-Wallac (Turku, Finland) 1295-001 cell harvester. Specific incorporation of [^{3}H]TdR was analyzed by scintillation spectroscopy and results are expressed as the arithmetic mean ± SEM of triplicate cultures.

Flow cytometric analysis

All steps were performed on ice. Cultured cells were harvested, washed twice in cold HBSS without phenol red (Bio Whittaker, Walkersville, MD) + 3% FBS ("staining buffer"), and then resuspended in 100 μl of cold staining buffer. Cells were incubated for 15 min with rat IgG2b anti-FcγRII (2.4G2) (final concentration 5 μg/ml) to prevent cytophilic binding of the FITC-labeled mAbs which were subsequently added at a final concentration of 10 μg/ml for an additional 30 min. Fluorescence analysis was conducted utilizing a FACScan (Becton Dickinson, Mountain View, CA) set for logarithmic amplification. Only viable cells, which were identified on the basis of their characteristic forward and side scatter profiles and their exclusion of propidium iodide, were analyzed.

Quantitation of secreted Ig isotype concentrations in culture SN

Ig isotype concentrations were measured by ELISA. For determination of concentrations of secreted IgM, IgG3 (IgG1, IgG2b, IgG2a), and IgA in culture SN, Immulon 2, 96-well flat-bottom ELISA plates (Dynatech Laboratories, Inc., Alexandria, VA) were coated with unlabeled affinity-purified polyclonal goat anti-mouse IgM, IgG3, IgG, and IgA Abs (Southern Biotechnology Associates, Birmingham, AL), respectively. Plates were then washed, blocked with FBS-containing buffer, and incubated with various dilutions of culture SN and standards. After washing, plates were

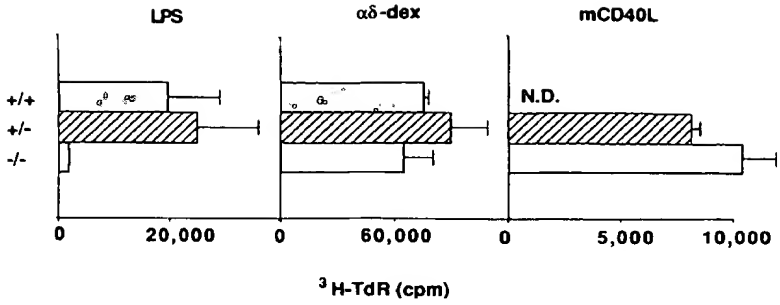

FIGURE 1. $p50^{-/-}$ B cells show intact proliferative responses to mCD40L and αδ-dex, but not to LPS. $p50^{-/+}$, $p50^{+/-}$, and $p50^{-/-}$ B cells were stimulated with LPS (20 μg/ml), mCD40L (1/1000 v/v), or αδ-dex (3 ng/ml). [^{3}H]TdR incorporation during the period 48 to 66 h after initiation of culture was measured. Data are expressed as the mean of triplicate cultures ± SEM. Cells cultured in medium alone had <300 cpm of [^{3}H]TdR incorporation.

incubated with alkaline phosphatase-conjugated affinity-purified, polyclonal goat anti-mouse IgM, IgG3, IgG1, IgG2b, IgG2a, and IgA Abs (Southern Biotechnology Associates) as indicated, washed again, and a fluorescent product was generated by cleavage of exogenous 4-methylumbilliferyl phosphate (Sigma Chemical Co.) by the plate-bound alkaline phosphatase-conjugated Abs. For determination of IgE concentrations, a similar procedure was followed except that plates were coated with monoclonal rat IgG2a anti-mouse IgE (clone EM95) (purified from ascites, and a kind gift of Dr. Fred Finkelman, Uniformed Services University of the Health Sciences, Bethesda, MD), followed by samples and standards, then affinity-purified polyclonal rabbit anti-mouse IgE (kind gift of Dr. Ildy Katona, Uniformed Services University of the Health Sciences, Bethesda, MD), then alkaline phosphatase-conjugated affinity-purified polyclonal goat anti-rabbit IgG (Southern Biotechnology Associates). Fluorescence was quantitated on a 3M FluoroFAST 96 fluorometer (Becton Dickinson), and fluorescence units were converted to Ig concentrations by interpolation from standard curves that were determined with known concentrations of purified myeloma Ig. Each assay system showed no significant cross-reactivity or interference from other Ig isotypes (IgM, IgD, IgG3, IgG1, IgG2b, IgG2a, IgE, and IgA) found in the culture supernatants.

Fluorescence microscopy for determination of cIgM$^+$ cells

Cultured B cells were harvested, and 5×10^4 viable cells were spun onto glass slides, air-dried, and then fixed for 1 h at 4°C in methanol. FITC-polyclonal goat anti-mouse IgM Abs at 50 μg/ml in cold HBSS without phenol red + 3% FBS was applied directly to the fixed cells for 30 min in a humidified chamber. The cells were then subjected to three rounds of washing using PBS, followed by a final round of washing with distilled H_2O.

Measurement of steady-state levels of germ-line C_H RNA by RT-PCR

Isolation of RNA. RNA was extracted from cultured B cells using RNAzol (Tel-Test, Inc., Friendswood, TX) according to manufacturers' instructions. RNA was separated according to size by electrophoresis in a 2% agarose gel and the 18S and 28S bands were visualized by ethidium bromide staining to assess RNA quality.

Reverse transcriptase reaction. Three micrograms of RNA in 25 μL of diethyl pyrocarbonate (DEPC)-treated double distilled H_2O were reverse-transcribed using SUPERSCRIPT RNase H$^-$ reverse transcriptase (Life Technologies) as previously described (25). Subsequent calculations were based on the assumption that 100% of RNA was reverse-transcribed to cDNA.

Polymerase chain reaction. The primer pairs for amplification of germline γ3, γ1, ε, and α RNA were chosen, based on published sequences, to complement specific sequences in the corresponding I and C_H exons, respectively (26–31). Likewise, probes were constructed to specifically recognize the amplified PCR products. The sequences of the primers and probes are as follows:

Germ-line γ3: sense, 5′ CAAGTGGATCTGAACACA 3′ (860–877); antisense, GGCTCCATAGTTCCATT (2125–2141); probe, 5′ GATATAT CAGGATACCT 3′ (939–955); amplified product, 350 bp.

Germ-line γ1: sense, 5′ CAGCCTGGTGTCAACTAG 3′ (448–465); antisense, CTGTACATATGCAAGGCT (767–784); probe, 5′ ATGTA GAGCTGCACACCCCA 3′ (509–528); amplified product, 532 bp.

Germ-line ε: sense,: 5′ ACTAGAGATTCACAACG 3′ (771–778); antisense, AGCGATGAATGGAGTAGC (991–1008); probe, 5′ AGC CACTCACTTATCAGAGG 3′ (842–861); amplified product, 423 bp.

Germ-line α: sense, 5′ CTACCATAGGGGAAGATAGCCT 3′ (13–33); antisense, TAATCGTGAATCAGGCAG (200–217); probe, 5′ TTC CCCTATGAAGGACA 3′ (93–109); amplified product, 225 bp.

GAPDH (housekeeping gene control): sense, 5′ CCATGGAGAAG GCTGGGG 3′; antisense, CAAAGTTGTCATGGATGACC; probe, 5′ CTAAGCATGTGGTGGTGCA 3′; amplified product, 188 bp.

The PCR reaction mix contained 200 μM concentrations of each of the four deoxyribonucleotide triphosphates and 10 × PCR reaction buffer II (100 mM Tris-HCl, pH 8.3; 500 mM KCl). $MgCl_2$ concentrations were varied according to the germ-line transcript being amplified as follows: γ3 and GAPDH (2 mM), γ1 (4 mM), ε (1 mM), and α (2.5 mM). Two hundred nanomolar concentrations each of the primer pairs, 2.5 U of Taq polymerase, 20 to 100 ng of cDNA for germ-line γ1, ε, and α, and 150 to 500 ng of cDNA for γ3 amplification were added. Amounts of cDNA for GAPDH were matched for each group. All reagents except primers and probes were purchased from Perkin-Elmer Corp. (Branchburg, NJ).

The number of PCR cycles performed to yield an optimal signal was established experimentally as follows: γ3 and γ1 (30 cycles), ε (28 cycles), α (25 cycles), and GAPDH (15 cycles). Each cycle consisted of 1 min at 95°C for DNA denaturation, 1.5 min at 53°C for primer annealing, and 2 min at 72°C for primer extension. The PCR reaction for the various germline transcripts was performed in parallel with GAPDH to normalize the cDNA concentrations within each set of samples.

Southern blot analysis of amplified PCR products. Following PCR amplification, 10 μL of reaction mix were electrophoresed in a 2% agarose gel for 1 h at 100 V. The cDNA was denatured, neutralized, and then transferred to a nylon membrane and fixed according to standard procedures. The Southern blots were prehybridized at 42°C in a buffer containing 5 × SSPE, 10X Denhardt's solution, 1% SDS, and 100 μg/ml of salmon sperm DNA. After 2 h, the ^{32}P-end-labeled-specific oligonucleotide probe was added and hybridized at 42°C overnight. The blots were washed twice in 2 × SSPE plus 0.1% SDS for 20 min, once in 0.5 × SSPE plus 0.1% SDS for 20 min, and twice in 0.2 × SSPE plus 0.1% SDS for 20 min. The Southern blots were then placed into PhosphorImager cassettes for various time periods, and the relative intensity of the bands was measured by densitometry using a PhosphorImager (Molecular Dynamics, Sunnyvale, CA). In each case, single bands of the predicted size were generated. The specificity of the PCR was further supported by demonstrating specific induction of γ3 with LPS or IFN-γ, γ1 and ε with IL-4, and α by TGF-β. The semiquantitative nature of the PCR was established in each case as indicated in Figure 5.

Results

B cells from $p50^{-/-}$ mice proliferate normally in response to αδ-dex and CD40L, but not to LPS

In a previous study, it was demonstrated that resting B cells from $p50^{-/-}$ mice proliferated poorly in response to LPS, but showed almost normal responses to unconjugated anti-IgM Ab (14). To better define the role of p50 in regulating the cell cycle, we determined the level of DNA synthesis of $p50^{-/-}$ B cells, relative to $p50^{+/+}$ or $p50^{+/-}$ B cells, in response to signaling through the CD40 activation pathway, using mCD40L. We further determined the ability of $p50^{-/-}$ B cells to proliferate in response to dextran-conjugated anti-IgD Abs (αδ-dex) (22, 32). We confirmed the relatively poor proliferative response of $p50^{-/-}$ B cells to LPS activation (14) (Fig. 1). By contrast, proliferation of $p50^{-/-}$ B cells in response to mCD40L or αδ-dex was comparable to that observed in the $p50^{+/+}$ and $p50^{+/-}$ B cell population.

The combination of LPS- and mIg-mediated signaling has been shown to be synergistic for B cell proliferation (33, 34). Whereas

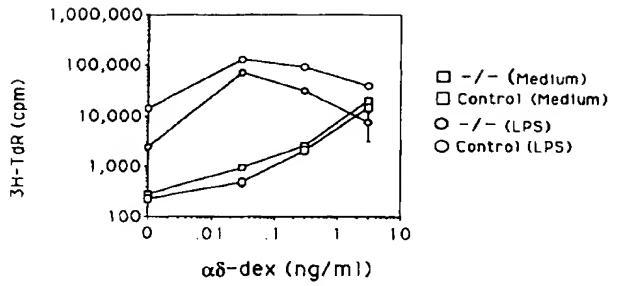

FIGURE 2. LPS synergizes with αδ-dex for induction of proliferation in $p50^{-/-}$ B cells. Control and $p50^{-/-}$ B cells were stimulated with 0.03, 0.3, or 3 ng/ml of αδ-dex in the presence or absence of LPS (20 μg/ml). [^{3}H]TdR incorporation during the period 48 to 66 h after initiation of culture was measured. Data are expressed as the mean of triplicate cultures ± SEM.

LPS by itself induced a poor proliferative response by $p50^{-/-}$ B cells, it strongly synergized with suboptimal concentrations of αδ-dex for induction of mitogenesis (Fig. 2), indicating that some aspect of the LPS mitogenic pathway remained intact in the absence of p50/NF-κB. Nevertheless, activation with LPS plus αδ-dex still led to lower levels of DNA synthesis in $p50^{-/-}$ compared with control B cells. Proliferation of $p50^{-/-}$ and control B cells in response to αδ-dex alone was comparable over a wide range of αδ-dex concentrations (Fig. 2). Thus, these data demonstrate a p50-independent, as well as -dependent, component to the LPS-mediated mitogenic pathway.

$p50^{-/-}$ B cells respond normally to the mitogenic effects of IL-4 + IL-5, but show defective proliferative responses to sCD40L

IL-4 and IL-5 each augment B cell proliferation in response to LPS, αδ-dex, and CD40L. Further, IL-4 and IL-5 exert substantially greater effects when acting in combination. We thus determined the functional status of the IL-4 + IL-5 pathway for induction of mitogenesis in $p50^{-/-}$ B cells. Furthermore, in the presence of these cytokines, we compared the proliferative responses of $p50^{-/-}$ B cells to activation with mCD40L vs soluble (s)CD40L. mCD40L has been shown to be a more potent mediator of CD40 signaling than sCD40L, most likely due to the multivalent nature of the former reagent (35, 36). Thus, in contrast to mCD40L, which induced a significant proliferative response in the absence of exogenous cytokines, sCD40L required the concerted action of IL-4 to induce proliferation by resting B cells. The combination of IL-4 + IL-5 alone failed to induce a significant proliferative response by resting B cells from either $p50^{-/-}$ or control mice (data not shown). The combination of IL-4 + IL-5 augmented proliferation by αδ-dex- and mCD40L-activated $p50^{-/-}$ and control B cells to a comparable degree (Fig. 3). By contrast, sCD40L co-stimulated a substantially lower proliferative response in $p50^{-/-}$ B cells in the presence of IL-4 + IL-5, indicating a quantitative role for p50/NF-κB in the CD40 signaling pathway. Finally, IL-4 + IL-5 partially restored the defective proliferative response of $p50^{-/-}$ B cells to LPS.

$p50^{-/-}$ B cells show a marked defect in B cell maturation to IgM secretion despite normal levels of proliferation

To assess a role for p50 in B cell maturation to Ig synthesis, we compared $p50^{-/-}$ and control B cells for their IgM secretory responses under conditions in which proliferation was comparable between the two populations. Thus, B cells were stimulated with either αδ-dex or mCD40L in the presence of IL-4 + IL-5. Both IL-4 and IL-5 are required for inducing maximal Ig secretion by αδ-dex or mCD40L-activated cells (17, 36). Despite relatively comparable levels of proliferation, $p50^{-/-}$ B cells secreted 32-fold less IgM in response to 3 ng/ml of αδ-dex plus IL-4 + IL-5 relative to control B cells (Table I). This defect became even more pronounced when the αδ-dex concentration was lowered from 3 to 0.3 ng/ml, suggesting some role for p50 in mIg-mediated co-stimulation of Ig synthesis. Likewise, $p50^{-/-}$ B cells secreted 41-fold less IgM than control B cells in response to mCD40L + IL-4 + IL-5 (Table II). Consistent with their poor proliferative responses, $p50^{-/-}$ B cells secreted substantially lower amounts of IgM in response to sCD40L + IL-4 + IL-5 or LPS (Table I), although the defects in IgM secretion in the $p50^{-/-}$ population appeared to be even greater than those observed for proliferation (Table I, Fig. 1, Fig. 3).

The combination of mIg and CD40 signaling restores B cell maturation to IgM secretion in $p50^{-/-}$ B cells

Combined signaling through mIg and CD40 is synergistic for B cell proliferation (37, 38) and Ig secretion and class switching (36, 39). Although $p50^{-/-}$ B cells were markedly deficient in IgM secretion in response to αδ-dex or CD40L in the presence of IL-4 + IL-5, the combination of 3 or 0.3 ng/ml of αδ-dex plus sCD40L restored the ability of $p50^{-/-}$ B cells to secrete IgM to levels comparable to that observed in the control B cell population (Table I). This result of combined αδ-dex and CD40L action on IgM secretion mostly reflected an effect on B cell maturation, not on proliferation (data not shown). When the concentration of αδ-dex was lowered from 0.3 to 0.03 ng/ml in the presence of sCD40L + IL-4 + IL-5, IgM secretion by $p50^{-/-}$ B cells dropped by over 13-fold, whereas IgM synthesis was maintained in the control population (Table I). Once again, this suggested a relative role for p50/NF-κB in mIg-mediated co-stimulation of B cell maturation to Ig synthesis.

To confirm that the differences and changes observed in secreted IgM in the $p50^{-/-}$ and control B cell cultures truly reflected differences in B cell maturation to IgM secretion, and not simply alterations in transport of IgM out of the cell, we enumerated the percentages of cytoplasmic (c)IgM^+ cells by fluorescence microscopy 4 days after stimulation of $p50^{-/-}$ and control B cells with αδ-dex and/or sCD40L in the presence of IL-4 + IL-5. Cells with distinctly positive staining for cIg are considered to be actively secreting cells. Replicate cultures were established to determine IgM concentrations in culture SN on day 6. As indicated in Table III, $p50^{-/-}$ B cells showed greatly reduced percentages of $cIgM^+$ cells, compared with control cells, after stimulation with αδ-dex or sCD40L in the presence of IL-4 + IL-5, consistent with the data obtained for secreted IgM concentrations. Indeed, only dull-staining $cIgM^+$ cells were observed in the $p50^{-/-}$ population. The combination of sCD40L plus αδ-dex in the presence of IL-4 + IL-5 led to a marked increase in the percentages of $cIgM^+$ cells, as well as IgM secretion, in the $p50^{-/-}$ population, with many cells staining brightly for cIgM. The control population showed approximately twofold higher percentage of $cIgM^+$ cells and IgM secretion, compared with $p50^{-/-}$ cells, in response to the combined actions of αδ-dex plus sCD40L.

IL-4 is well-known for its ability to induce IgG1 (40, 41) and IgE (42) class switching. Since the combination of sCD40L and αδ-dex in the presence of IL-4 + IL-5 stimulates comparable amounts of IgM in the $p50^{-/-}$ and control B cell populations, any differences observed in IgG1 and/or IgE secretion would suggest

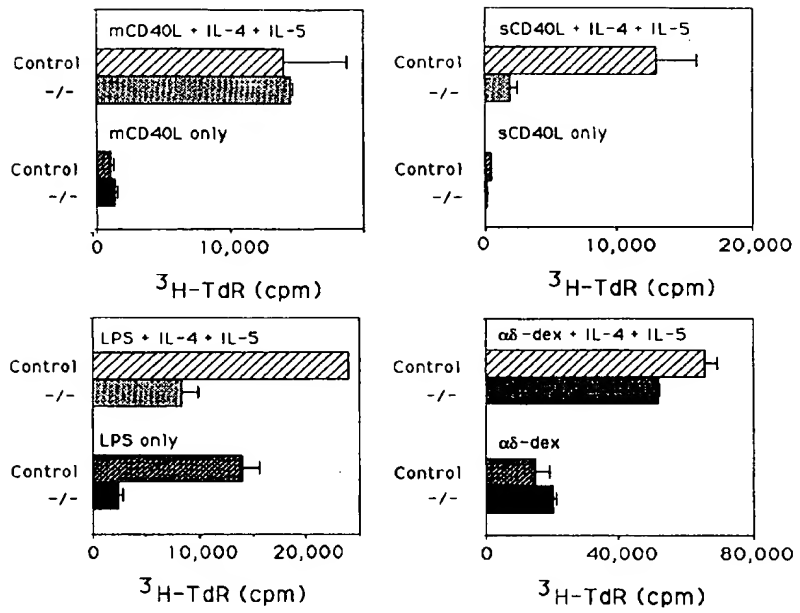

FIGURE 3. IL-4 + IL-5 enhance proliferation of control and $p50^{-/-}$ B cells to a comparable degree. Control and $p50^{-/-}$ B cells were stimulated with mCD40L (1/1000 v/v), sCD40L (10 μg/ml), LPS (20 μg/ml), or αδ-dex (3 ng/ml) in the presence or absence of IL-4 (4.2 ng/ml) + IL-5 (150 U/ml). [^{3}H]TdR incorporation during the period 48 to 66 h after initiation of culture was measured. Data are expressed as the mean of triplicate cultures ± SEM.

Table I. *$p50^{-/-}$ B cells show defective maturation to Ig secretion that can be restored through the combined action of αδ-dex and CD40L*[a]

	Medium		sCD40L		LPS	
	Control	−/−	Control	−/−	Control	−/−
IgM secretion (ng/ml):						
Medium	<60	<60	<60	<60	162,000	200
IL-4 + IL-5	1475	<60	24,375	1,100	200,000	1,025
αδ-dex (3.0) + 4,5	256,000	8,050	103,000	106,000	57,500	7,750
αδ-dex (0.3) + 4,5	356,000	275	134,000	184,000	169,000	5,250
αδ-dex (0.03) + 4,5	20,900	212	207,000	13,700	250,000	1,350
IgG1 secretion (ng/ml):						
IL-4 + IL-5	<62	<62	9,250	65	87,500	<62
αδ-dex (3.0) + 4,5	37,500	650	16,250	53,750	3,625	625
αδ-dex (0.3) + 4,5	35,000	<62	50,000	27,500	6,000	<62
αδ-dex (0.03) + 4,5	525	<62	187,000	1,000	18,700	<62
IgE secretion (ng/ml):						
IL-4 + IL-5	5	5	338	5	1,500	<4
αδ-dex (3.0) + 4,5	<4	<4	787	9	27	<4
αδ-dex (0.3) + 4,5	<4	<4	762	18	67	<4
αδ-dex (0.03) + 4,5	5	5	5,250	5	162	<4

[a] Control and $p50^{-/-}$ B cells were stimulated with 3, 0.3, or 0.03 ng/ml of αδ/dex in the presence of IL-4 (4.2 ng/ml) + IL-5 (150 U/ml) and in the presence or absence of sCD40L (10 μg/ml) or LPS (20 μg/ml). Concentrations of secreted IgM, IgG1, and IgE were measured in culture SN by ELISA 6 days after initiation of culture. The values represent the mean of triplicate cultures.

differences in the ability of these cells to switch to the production of these Ig isotypes and not simply differences in their ability to mature into Ig-secreting cells. $p50^{-/-}$ and control B cells secreted comparable amounts of IgG1 in response to 3 or 0.3 ng/ml of αδ-dex in the presence of sCD40L, IL-4, and IL-5 (Table I). Reducing the concentration of αδ-dex from 0.3 to 0.03 ng/ml of αδ-dex, to assess the relative requirements for decreasing levels of mIg-mediated stimulation, led to a 27-fold reduction in IgG1 secretion by $p50^{-/-}$ B cells, but a 3.7-fold increase by control cells, thus revealing a relative defect in the mIg signaling pathway in the $p50^{-/-}$ B cells. $p50^{-/-}$ B cells, in marked contrast to control cells, secreted virtually undetectable amounts of IgE under all conditions (Table I), suggesting a selective defect of $p50^{-/-}$ B cells for secretion of this Ig isotype. $p50^{-/-}$ B cells were defective in both IgG1 and IgE secretion in response to LPS + IL-4 + IL-5, consistent with that observation for IgM. Furthermore, as reported

Table II. *mCD40L-activated $p50^{-/-}$ B cells are defective in maturation to Ig secretion in response to IL-4 + IL-5*[a]

	Medium		mCD40L	
	Control	−/−	Control	−/−
IgM secretion (ng/ml):				
Medium	<60	<60	<60	<60
IL-4 + IL-5	<60	<60	16,250	400
IgG1 secretion (ng/ml):				
IL-4 + IL-5	<62	<62	10,700	1,675
IgE secretion (ng/ml):				
IL-4 + IL-5	<4	<4	1,120	15

Control and $p50^{-/-}$ B cells were stimulated with mCD40L (1/1000 v/v) and/or IL-4 (4.2 ng/ml) + IL-5 (150 U/ml) for 6 days. Concentrations of secreted IgM, IgG1, and IgE were measured in culture SN by ELISA. The values represent the mean of triplicate cultures.

Table III. *Fluorescence microscopic analysis of cIgM$^+$ cells after stimulation with αδ-dex and/or sCD40L in the presence of IL-4 + IL-5 directly demonstrates defective B cell maturation to Ig secretion in the p50$^{-/-}$ B cell population*[a]

	Total Cells	cIgM$^+$ Cells	% cIgM$^+$ Cells	IgM Secretion (ng/ml)
−/−				
αδ-dex + 4,5	365	3 (dull)	0.8	130
sCD40L + 4,5	141	8 (dull)	5.7	1,950
sCD40L + αδ-dex + 4,5	254	80	32	37,500
Control:				
αδ-dex + 4,5	183	79	43	53,100
sCD40L + 4,5	528	112	21	31,200
sCD40L + αδ-dex + 4,5	138	83	60	87,500

Control and p50$^{-/-}$ B cells were stimulated with αδ-dex (3 ng/ml) and/or sCD40L (10 μg/ml) in the presence of IL-4 (4.2 ng/ml) + IL-5 (150 U/ml) for 4 days. The percentages of cIgM$^+$ cells were then determined by fluorescence microscopy after staining fixed cells with FITC-labeled polyclonal goat anti-mouse IgM Abs. Replicate cultures were also established to determine the concentration of secreted IgM in culture SN by ELISA performed 6 days after initiation of culture.

previously (43) for normal B cells, the combination of αδ-dex and LPS was mutually antagonistic for IL-4 + IL-5-dependent Ig-secretion by control cells, and likewise failed to restore Ig-secretory responses in p50$^{-/-}$ cells (Table I).

p50$^{-/-}$ B cells are defective in IgG3, IgE, and IgA class switching but undergo substantial switching to IgG1

The ability to induce substantial levels of proliferation by p50$^{-/-}$ B cells in response to αδ-dex and/or CD40L allowed us to determine whether p50 played a role in the process of Ig class switching, as assessed by flow cytometric analysis of mIg$^+$ cells stimulated with one or both of these activators in the presence of cytokine switch factors. We used IFN-γ to induce the switch to IgG3 (18), TGF-β to stimulate IgA class switching (20, 28, 44), and IL-4 to induce both IgG1 and IgE switching (36, 45). Substantial, although reduced, switching to IgG1 was observed for p50$^{-/-}$ relative to control B cells under all conditions tested (Fig. 4). By contrast, the generation of mIgG3$^+$, mIgE$^+$, and mIgA$^+$ cells was markedly reduced in the p50$^{-/-}$ population. mIgE$^+$ cells represented cells switching to IgE, and not cells with cytophilic IgE (see *Materials and Methods*).

p50$^{-/-}$ B cells express normal steady-state levels of germ-line γ1 and α RNA but markedly reduced germ-line γ3 and ε RNA

Cytokines, as well as B cell activators, are believed to regulate Ig class switching, in part through selectively inducing transcriptional activation or inhibition of C_H genes *prior* to switch rearrangement. Transcriptional activity, as reflected by the steady-state levels of germ-line C_H RNA, is thought to make C_H genes accessible to the binding of regulatory factors that mediate their rearrangement (46, 47). Germ-line C_H RNA transcripts are known to initiate at a specific promoter (I region), which is located 5′ to every switch (S) region. After splicing of the initial germ-line RNA, which consists of I, S, and C_H sequences, a final germ-line RNA is generated consisting only of I and C_H sequences. Productive C_H RNA, generated subsequent to switch rearrangement, lacks the specific I region sequence due to its deletion during the switching process (for review see Ref. 48).

To better define the defects in class switching in p50$^{-/-}$ B cells, we developed a semiquantitative PCR assay, using specific primers to I and C_H, to measure the levels of germ-line C_H RNA. Initial studies were performed to establish the assay as semiquantitative. Conditions were determined whereby the addition of increasing amounts of substrate generated increased signal in a linear relationship after binding of the PCR product with specific ^{32}P-labeled probe (Fig. 5). The specificity of each assay was also confirmed (see *Materials and Methods*). Germ-line C_H RNA was measured in response to IL-4, IFN-γ, or TGF-β, 48 h after activation with CD40L and/or αδ-dex (Fig. 6). Induction of germ-line $C_H\gamma 1$ in response to IL-4 was comparable between p50$^{-/-}$ and control B cells. By contrast, germ-line $C_H\epsilon$ RNA was virtually undetectable in the p50$^{-/-}$ population, whereas it was highly expressed in control B cells. These data were consistent with the findings from flow cytometric analyses of mIgG1$^+$ and mIgE$^+$ cells (Fig. 4). Although p50$^{-/-}$ B cells generated markedly reduced percentages of mIgA$^+$ cells (Fig. 4), p50$^{-/-}$ and p50$^{+/-}$ cells expressed comparable levels of germ-line $C_H\alpha$ RNA (Fig. 6), either at low levels in the absence of TGF-β or at substantially higher levels in the presence of TGF-β. Finally, consistent with flow cytometric analysis of mIgG3$^+$ cells (Fig. 4), p50$^{-/-}$ B cells expressed markedly reduced levels of germ-line $C_H\gamma 3$ RNA after activation with αδ-dex + IL-5 + IFN-γ (Fig. 6). All observations on steady-state levels of germ-line C_H RNA were confirmed in a second, similar set of studies.

Discussion

These data demonstrate that murine B cells have different degrees of dependence upon p50/NF-κB activity for their functional responses to three distinct modes of B cell activation, which are mediated by LPS, CD40L, and αδ-dex, despite the fact that all three modes of activation induce NF-κB in resting B cells (11–13, 49, 50). The functional integration of NF-κB-mediated events, in a given activational milieu, with those elicited by other transcription factors, including other Rel family members, probably determines the ultimate impact of NF-κB on the B cell response. Indeed, the patterned expression of different NF-κB/Rel family members seen during terminal B cell differentiation (5) is consistent with the interpretation that the selective defects we have observed with B cells lacking p50/NF-κB represent the disruption of a larger developmental program in which different NF-κB/Rel complexes participate in terminal B cell differentiation. In this light, it will be intriguing to examine the responses of B cells that lack other individual and multiple subunits of the NF-κB/Rel family of transcription factors.

A striking synergy between the mIg and CD40 signaling pathways for induction of proliferation, maturation to Ig secretion, and Ig class switching has been demonstrated (36–39). The synergistic interplay of these two pathways appeared to circumvent the requirement for p50/NF-κB for induction of B cell maturation to Ig secretion. Indeed, the only condition under which relatively normal levels of Ig secretion could be obtained by p50$^{-/-}$ B cells was through combined activation with αδ-dex and CD40L. The fact that B cells could generate substantial percentages of mIgG1$^+$ cells in response to mCD40L + IL-4 + IL-5, in the absence of αδ-dex while failing to secrete significant amounts of IgG1, further indicated that the process of class switching could be separated from B cell maturation to Ig secretion. A similar segregation between these two processes was observed previously in a different system (51). The ability of mIg and CD40 signaling pathways to

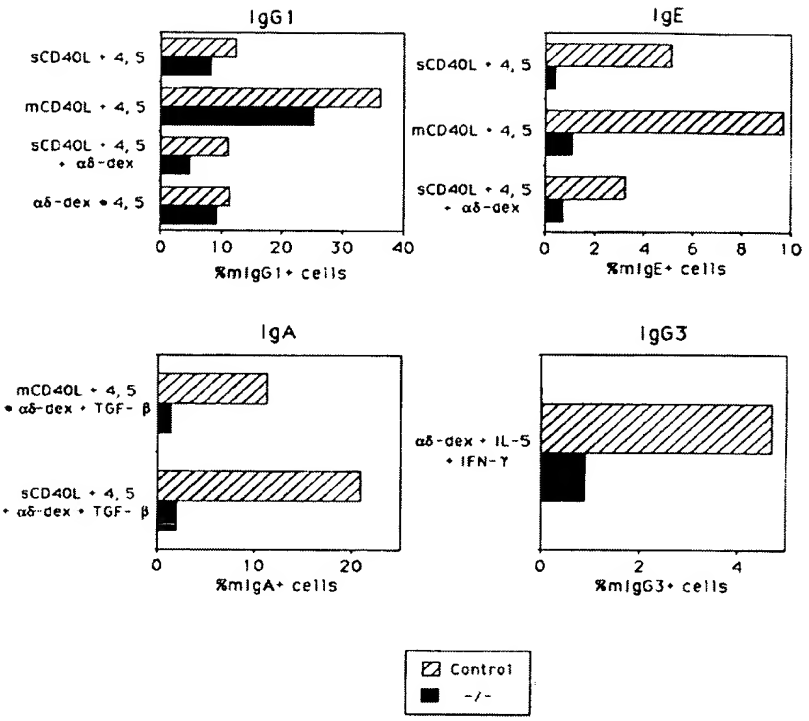

FIGURE 4. $p50^{-/-}$ B cells are defective in class switching to IgG3, IgE, and IgA, but demonstrate substantial switching to IgG1. Control and $p50^{-/-}$ B cells were stimulated as indicated. Concentrations of reagents were as follows: sCD40L (10 μg/ml), mCD40L (1/1000 v/v), αδ-dex (3 ng/ml), IL-4 (4.2 ng/ml), IL-5 (150 U/ml), TGF-β (3 ng/ml), and IFN-γ (10 U/ml). Flow cytometric analysis was performed 4 days after initiation of culture for determination of the percentages of $mIgG3^+$, $mIgG1^+$, $mIgE^+$, and $mIgA^+$ cells using FITC-labeled rat anti-mouse mAbs specific for the respective Ig isotypes.

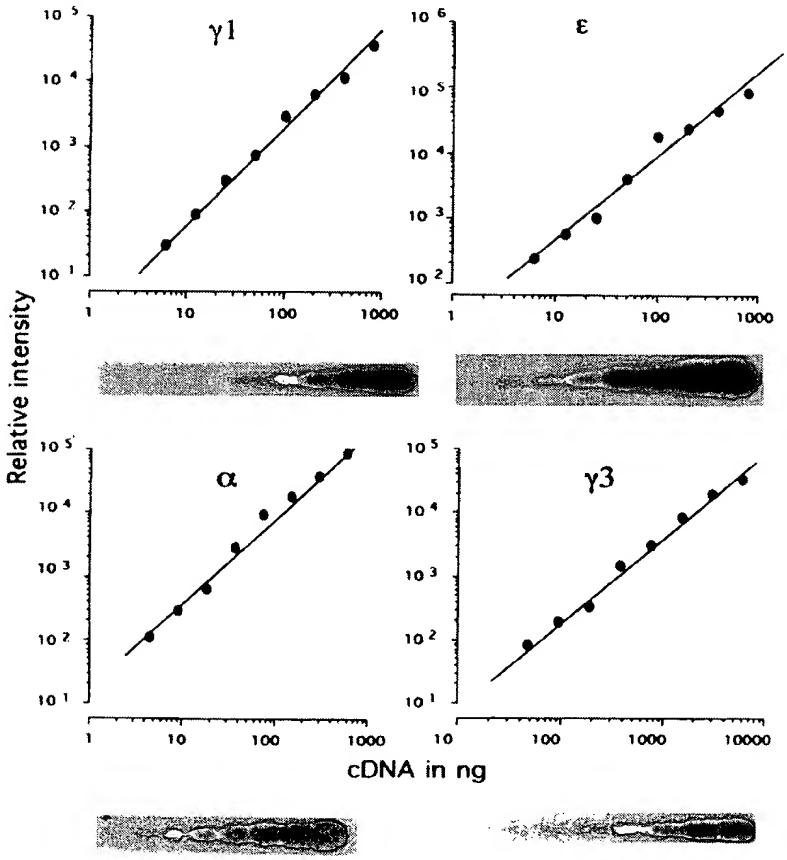

FIGURE 5. The RT-PCR assay for detection of germ-line γ3, γ1, ε, α RNA is semiquantitative. The number of cycles required to give an optimal signal for each RT-PCR assay was first established as indicated in *Materials and Methods*. To establish the semiquantitative nature of each assay, serial twofold dilutions of cDNA templates were prepared as follows: γ1, ε, α, and GAPDH (800 ng-6.25 ng) and γ3 (6000 ng-46.8 ng). RT-PCR was then performed at the fixed cycle number established for each assay, and the products were hybridized to the respective ^{32}P-labeled specific probes.

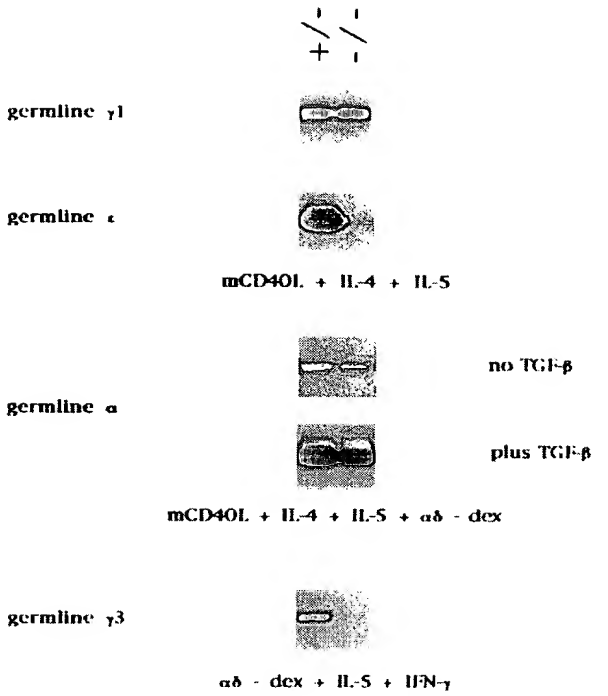

FIGURE 6. $p50^{-/-}$ B cells show defective expression of germ-line γ3 and ε RNA, but normal expression of germ-line γ1 and α RNA. Control $p50^{+/-}$ and $p50^{-/-}$ B cells were stimulated as indicated. Concentrations of reagents are the same as in Figure 4. RNA was purified 48 h after initiation of culture for determination of steady-state levels of C_H-specific germ-line RNA by RT-PCR.

synergize to allow $p50^{-/-}$ B cells to undergo terminal B cell differentiation raises the intriguing issue of whether this synergy results from the activation of other, NF-κB-independent, signaling pathways, which can also result in terminal B cell differentiation, or results from the activation of non-p50 containing NF-κB/Rel complexes, which are present in lower concentrations and may have more complex inductive requirements.

The inability of $p50^{-/-}$ B cells to induce germ-line RNA for $C_H\gamma3$ and $C_H\epsilon$ while expressing normal levels of $C_H\gamma1$ and $C_H\alpha$ is reminiscent of recent observations by Cogne et al. with B cells from mice made genetically deficient in expression of an enhancer located 3′ to the $C_H\alpha$ gene ($3'E_H$) (52). B cells from these mice were defective in their induction of germ-line RNA for $C_H\gamma3$ and $C_H\gamma2b$ in response to LPS, and for $C_H\epsilon$ upon stimulation with LPS + IL-4, but expressed normal levels of germ-line $C_H\gamma1$ RNA upon LPS + IL-4 induction and germ-line $C_H\alpha$ RNA after stimulation with LPS + TGF-β. The level of induction of germ-line C_H RNA in $3'E_H^{-/-}$ B cells correlated with the ability of these cells to undergo switching to these respective Ig isotypes. These data raise the interesting possibility that p50/NF-κB acts either directly or indirectly as a key positive regulator of $3'E_H$ activity. Indeed, a p50/NF-κB binding site was recently demonstrated in the $3'E_H$.[3]

The reports of NF-κB binding sites in murine Iε (9) and murine Iγ3 (10) also suggest the possibility of a more direct effect of p50/NF-κB on the activity of the germ-line $C_H\epsilon$ and $C_H\gamma3$ promoters, respectively. However, a p50/NF-κB binding site has also been observed both in the murine Iγ1 and murine Iα promoters,[2] both of which appear to be intact in $p50^{-/-}$ B cells. It should be noted that the knockout of the $3'E_H$ region involved the introduction within the $3'E_H$ locus of a selectable marker. Thus, the effects observed in these B cells could involve selectable marker-mediated promoter/enhancer competition of other regulatory loci. Indeed, additional enhancers have been identified within the region 3′ to Cα (53–57), but their role in regulating germ-line C_H transcription, and perhaps other aspects of switch recombination, is unknown. One of these regions, designated HS-4, has also recently been shown to contain a p50/NF-κB binding site.[4]

The $p50^{-/-}$ and $3'E_H^{-/-}$ model systems also demonstrate distinct functional differences, in that LPS stimulated $3'E_H^{-/-}$, but not $p50^{-/-}$, B cells to proliferate and secrete IgM at normal levels. $3'E_H^{-/-}$ B cells also generated substantial percentages of $mIgA^+$ cells in response to LPS or CD40L in combination with αδ-dex, IL-4, IL-5, and TGF-β (C. M. Snapper and F. W. Alt, unpublished observations), whereas $p50^{-/-}$ B cells were strikingly deficient in this regard, despite expressing normal levels of germ-line $C_H\alpha$ RNA. This latter observation suggested an additional role for NF-κB in class switching beyond its effect on germ-line C_H transcription. Work by Kenter and colleagues (6–8) demonstrated the presence of p50/NF-κB binding sites in the switch regions for IgG3, IgG1, and IgG2b. These motifs appeared to be nonrandomly located at sites of switch recombination, suggesting a possible role for p50/NF-κB in the switch rearrangement event. Our data demonstrating substantial IgG1 switching in $p50^{-/-}$ B cells did not rule out an important role for p50/NF-κB binding for switch rearrangement, but indicated that p50/NF-κB was not absolutely required, at least for the IgM to IgG1 switch. Whether the defect in IgA class switching in $p50^{-/-}$ B cells, which was associated with normal levels of germ-line $C_H\alpha$ RNA, involved an p50/NF-κB-dependent event at the α switch region remains to be determined.

In a previous report, a defective proliferative response of $p50^{-/-}$ B cells to LPS, but not anti-Ig stimulation was demonstrated (14). The data presented here significantly extend those in vitro observations by demonstrating independent defects in other B cell functions including maturation to Ig secretion, germ-line C_H gene activation, and Ig class switching, as well as by utilizing additional stimuli. This establishes a powerful and well-defined model system for studying the role of p50/NF-κB over a wide range of normal cellular functions. The in vivo defects in Ig isotype production previously observed in $p50^{-/-}$ mice cannot be readily compared with our in vitro observations, which utilized purified populations of resting B cells, since the in vivo setting involves a far more complex activational milieu with interactions and functional cascades occurring between multiple cell types, all of which may be affected by the absence of p50/NF-κB.

Acknowledgments

We thank Drs. James Mond, Fred Alt, Janet Stavnezer, and Barbara Birshtein for helpful discussions.

References

1. Liou, H.-C., and D. Baltimore. 1993. Regulation of the NF-κB/rel transcription factor and IκB inhibitor system. *Curr. Opin. Cell Biol. 5:477.*
2. Baeuerle, P. A., and T. Henkel. 1994. Function and activation of NF-κB in the immune system. *Annu. Rev. Immunol. 12:141.*
3. Ghosh, S., A. M. Gifford, L. R. Rivere, P. Tempest, G. P. Nolan, and D. Baltimore. 1990. Cloning of the p50 DNA binding subunit of NF-κB: homology to *rel* and *dorsal*. *Cell 62:1019.*
4. Nolan, G. P., S. Ghosh, H.-C. Liou, P. Tempest, D. Baltimore. 1991. DNA binding and IκB inhibition of the cloned p65 subunit of NF-κB, a *rel*-related polypeptide. *Cell 64:961.*

[3] Michaelson, J. S., M. Singh, C. M. Snapper, W. C. Sha, D. Baltimore, and B. K. Birshtein. 1995. Regulation of 3′IgH enhancers by a set of common factors, including κB-binding proteins. *Submitted for publication.*

5. Liou, H.-C., W. C. Sha, M. L. Scott, and D. Baltimore. 1994. Sequential induction of NF-kB/Rel family proteins during B-cell terminal differentiation. *Mol. Cell. Biol. 14:5349.*
6. Kenter, A. L., R. Wuerffel, R. Sen, C. E. Jamieson, and G. V. Merkulov. 1993. Switch recombination breakpoints occur at nonrandom positions in the Sγ tandem repeat. *J. Immunol. 151:4718.*
7. Wuerffel, R., C. E. Jamieson, L. Morgan, G. V. Merkulov, R. Sen, and A. L. Kenter. 1992. Switch recombination breakpoints are strictly correlated with DNA recognition motifs for immunoglobulin Sγ3 DNA-binding proteins. *J. Exp. Med. 176:339.*
8. Wuerffel, R. A., A. T. Nathan, and A. L. Kenter. 1990. Detection of an immunoglobulin switch region-specific DNA-binding protein in mitogen-stimulated mouse splenic B cells. *Mol. Cell. Biol. 10:1714.*
9. Delphin, S., and J. Stavnezer. 1995. Characterization of an interleukin 4 (IL-4) responsive region in the immunoglobulin heavy chain germline ε promoter: regulation by NF-IL-4, a C/EBP family member and NF-κB/p50. *J. Exp. Med. 181: 181.*
10. Gerondakis, S., C. Gaff, D. J. Goodman, R. J. Grumont. 1991. Structure and expression of mouse germline immunoglobulin γ3 heavy chain transcripts induced by the mitogen lipopolysaccharide. *Immunogenetics 34:392.*
11. Rooney, J. W., P. M. Dubois, and C. H. Sibley. 1991. Crosslinking of surface IgM activates NF-κB in B lymphocytes. *Eur. J. Immunol. 21:2993.*
12. Lalmanach-Girard, A.-C., T. C. Chiles, D. C. Parker, and T. L. Rothstein. 1993. T cell-dependent induction of NF-κB in B cells. *J. Exp. Med. 177:1215.*
13. Berberich, I. G., L. Shu, and E. A. Clark. 1994. Cross-linking CD40 on B cells rapidly activates nuclear factors-κB1. *J. Immunol. 153:4357.*
14. Sha, W. C., H.-C. Liou, E. I. Tuomanen, and D. Baltimore. 1995. Targeted disruption of the p50 subunit of NF-κB leads to multifocal defects in immune responses. *Cell 80:321.*
15. Snapper, C. M., and J. J. Mond. 1993. Towards a comprehensive view of immunoglobulin class switching. *Immunol. Today 14:15.*
16. Mond, J. J., A. Lees, and C. M. Snapper. 1995. T cell independent antigens type 2. *Annu. Rev. Immunol. 13:655.*
17. Snapper, C. M., L. M. T. Peçanha, A. D. Levine, and J. J. Mond. 1991. IgE class switching is critically dependent upon the nature of the B cell activator, in addition to the presence of IL-4. *J. Immunol. 147:1163.*
18. Snapper, C. M., T. M. McIntyre, R. Mandler, L. M. T. Peçanaha, F. D. Finkelman, A. Lees, and J. J. Mond. 1992. Induction of IgG3 secretion by interferon γ: a model for T cell-independent class switching in response to T cell-independent type 2 antigens. *J. Exp. Med. 175:1367.*
19. McIntyre, T. M., D. R. Klinman, P. Rothman, M. Lugo, J. R. Dasch, J. J. Mond, and C. M. Snapper. 1993. Transforming growth factor β1 selectively stimulates immunoglobulin G2b secretion by lipopolysaccharide-activated murine B cells. *J. Exp. Med. 177:1031.*
20. McIntyre, T. M., M. R. Kehry, C. M. Snapper. 1995. Novel in vitro model for high-rate immunoglobulin-A class switching. *J. Immunol. 154:3156.*
21. Zelazowski, P., J. T. Collins, W. Dunnick, and C. M. Snapper. 1995. Antigen receptor cross-linking differentially regulates germ-line C_H ribonucleic acid expression in murine B cells. *J. Immunol. 154:1223.*
22. Brunswick, M., F. D. Finkelman, P. F. Highet, J. K. Inman, H. M. Dintzis, and J. J. Mond. 1988. Picogram quantities of anti-Ig antibodies coupled to dextran induce B cell proliferation. *J. Immunol. 140:3364.*
23. Lane, P., T. Brocker, S. Hubele, E. Padovan, A. Lanzavecchia, and F. McConnell. 1993. Soluble CD40 ligand can replace the normal T cell-derived CD40 ligand signal to B cells in T cell-dependent activation. *J. Exp. Med. 177:1209.*
24. Baniyash, M., M. Kehry, and Z. Eshhar. 1988. Anti-IgE monoclonal antibodies directed at the Fcε receptor binding site. *Mol. Immunol. 25:705.*
25. Svetic, A., F. D. Finkelman, Y. C. Jian, C. W. Dieffenbach, D. E. Scott, K. F. McCarthy, A. D. Steinberg, and W. C. Gause. 1991. Cytokine gene expression after in vivo primary immunization with goat antibody to mouse IgD antibody. *J. Immunol. 147:2391.*
26. Thyphronitis, G., I. M. Katona, W. C. Gause, and F. D. Finkelman. 1993. Germline and productive Cε gene expression during in vivo IgE responses. *J. Immunol. 151:4128.*
27. Noelle, R. J., D. M. Sheperd, and H. P. Fell. 1992. Cognate interaction between T helper cells and B cells. VII. Role of contact and lymphokines in the expression of germ-line and mature γ1 transcripts. *J. Immunol. 149:1164.*
28. Lebman, D. A., D. Y. Nomura, R. L. Coffman, and F. D. Lee. 1990. Molecular characterization of germ-line immunoglobulin A transcripts produced during transforming growth factor type β-induced isotype switching. *Proc. Natl. Acad. Sci. USA 87:3962.*
29. Rothman, P., S. Lutzker, B. Gorham, V. Stewart, R. Coffman and F. W. Alt. 1990. Structure and expression of germline immunoglobulin γ3 heavy chain gene transcripts: implications for mitogen and lymphokine directed class-switching. *Int. Immunol. 2:621.*
30. Diamond, S. L., J. B. Sharefkin, C. Dieffenbach, K. Frasier-Scott, L. V. McIntire, and S. G. Eskin. 1990. Tissue plasminogen activator messenger RNA levels increase in cultured human endothelial cells exposed to laminar shear stress. *J. Cell. Physiol. 143:364.*
31. Wels, J. A., C. J. Word, D. Rimm, G. P. Der-Balan, H. M. Martinez, P. W. Tucker, and F. R. Blattner. 1984. Structural analysis of the murine IgG3 constant region gene. *EMBO J. 3:2041.*
32. Peçanha, L. M. T., C. M. Snapper, F. D. Finkelman, and J. J. Mond. 1991. Dextran-conjugated anti-Ig antibodies as a model for T cell-independent type 2 antigen-mediated stimulation of Ig secretion in vitro. I. Lymphokine dependence. *J. Immunol. 146:833.*
33. Kearney, J. F., M. D. Cooper, and A. Lawton. 1976. B lymphocyte differentiation induced by lipopolysaccharide. III. Suppression of B cell maturation by anti-mouse immunoglobulin antibodies. *J. Immunol. 116:1664.*
34. Kearney, J. F., J. Klein, D. E. Bockman, M. D. Cooper, and A. R. Lawton. 1978. B cell differentiation induced by lipopolysaccharide. V. Suppression of plasma cell maturation by anti-μ: mode of action and characterics of suppressed cells. *J. Immunol. 120:158.*
35. Kehry, M. R., and B. E. Castle. 1994. Regulation of CD40 ligand expression and use of recombinant CD40 ligand for studying B cell growth and differentiation. *Semin. Immunol. 6:287.*
36. Snapper, C. M., M. R. Kehry, B. E. Castle, and J. J. Mond. 1995. Multivalent, but not divalent, antigen receptor cross-linkers synergize with CD40 ligand for induction of Ig synthesis and class switching in normal murine B cells. *J. Immunol. 154:1177.*
37. Clark, E. A., and J. A. Ledbetter. 1986. Activation of human B cells mediated through two distinct cell surface differentiation antigens, Bp35 and Bp50. *Proc. Natl. Acad. Sci. USA 83:4494.*
38. Ledbetter, J. A., G. Shu, M. Gallagher, and E. A. Clark. 1987. Augmentation of normal and malignant B cell proliferation by monoclonal antibody to the B cell-specific antigen BP50 (CDW40). *J. Immunol. 138:788.*
39. Splawski, J. B., S. M. Fu, and P. E. Lipsky. 1993. Immunoregulatory role of CD40 in human B cell differentiation. *J. Immunol. 150:1276.*
40. Isakson, P. C., E. Pure, E. S. Vitetta, and, P. H. Krammer. 1982. T cell-derived B cell differentiation factor(s): effect on the isotype switch of murine B cells. *J. Exp. Med. 155:734.*
41. Severinson, E., S. Bergstedt-Lindqvist, W. van der Loo, and C. Fernandez. 1982. Characterization of the IgG response induced by polyclonal B cell activators. *Immunol. Rev. 67:73.*
42. Coffman, R. L., and J. Carty. 1986. A T cell activity that enhances polyclonal IgE production and its inhibition by interferon-γ. *J. Immunol. 136:949.*
43. Peçanha, L. M. T., H. Yamaguchi, A. Lees, R. J. Noelle, J. J. Mond, and C. M. Snapper. 1993. Dextran-conjugated anti-IgD antibodies inhibit T cell-mediated IgE production but augment the synthesis of IgM and IgG. *J. Immunol. 150:2160.*
44. Coffman, R. L., D. A. Lebman, and B. Shrader. 1989. Transforming growth factor β specifically enhances IgA production by lipopolysaccharide-stimulated murine B lymphocytes. *J. Exp. Med. 170:1039.*
45. Mandler, R., C. C. Chu, W. E. Paul, E. E. Max, and C. M. Snapper. 1993. Interleukin 5 induces Sμ-Sγ1 DNA rearrangement in B cells activated with dextran-anti-IgD antibodies and interleukin 4: a three component model for Ig class switching. *J. Exp. Med. 178:1577.*
46. Stavnezer-Nordgren, J., and S. Sirlin. 1986. Specificity of immunoglobulin heavy chain switch correlates with activity of germline heavy chain genes prior to switching. *EMBO J. 5:95.*
47. Yancopoulos, G. D., R. A. DePinho, K. A. Zimmerman, S. G. Lutzker, N. Rosenberg, and F. W. Alt. 1986. Secondary genomic rearrangement events in pre-B cells: V_HDJ_H replacement by a LINE-1 sequence and directed class switching. *EMBO J. 5:3259.*
48. Snapper, C. M., and F. D. Finkelman. 1993. Immunoglobulin class switching. In *Fundamental Immunology*, 3rd Ed. W. E. Paul ed. Raven Press, New York, pp. 837–863.
49. Liu, J., T. C. Chiles, R. Sen, and T. L. Rothstein. 1991. Inducible nuclear expression of NF-κB in primary B cells stimulated through the surface Ig receptor. *J. Immunol. 146:1685.*
50. Sen, R., and D. Baltimore. 1986. Inducibility of κ immunoglobulin enhancer-binding protein NF-κB by a post-tranlational mechanism. *Cell 47:921.*
51. Purkerson, J. M., and P. C. Isakson. 1991. Isotype switching in anti-immunoglobulin-activated B lymphoblasts: differential requirements for interleukin 4 and other lymphokines to elicit membrane vs. secreted IgG1. *Eur. J. Immunol. 21: 707.*
52. Cogne, M., R. Lansford, A. Boaro, J. Zhang, J. Gorman, F. Young, C. Hwei-Ling, and F. W. Alt. 1994. A class switch control region at the 3' end of the immunoglobulin heavy chain locus. *Cell 77:1.*
53. Madisen, L., and M. Groudine. 1994. Identification of a locus control region in the immunoglobulin heavy-chain locus that deregulates c-*myc* expression in plasmacytoma and Burkitt's lymphoma cells. *Genes Dev. 8:2212.*
54. Dariavach, P., G. T. Williams, K. Campbell, S. Pettersson, and M. Neuberger. 1991. The mouse IgH 3'-enhancer. *Eur. J. Immunol. 21:499.*
55. Lieberson, R., S. L. Giannini, B. K. Birshtein, and L. A. Eckhardt. 1991. An enhancer at the 3' end of the mouse immunoglobulin heavy chain locus. *Nucleic Acids Res. 19:933.*
56. Matthias, P., and D. Baltimore. 1993. The immunoglobulin heavy chain locus contains another B-cell-specific 3' enhancer close to the α constant region. *Mol. Cell. Biol. 13:1547.*
57. Pettersson, S., G. P. Cook, M. Bruggemann, G. T. Williams, and M. S. Neuberger. 1990. A second B-cell-specific enhancer 3' of the immunoglobulin heavy chain locus. *Nature 344:165.*

THE JOURNAL OF BIOLOGICAL CHEMISTRY
Vol. 270, No. 1, Issue of January 6, pp. 387–391, 1995
Printed in U.S.A.

Self-association of the "Death Domains" of the p55 Tumor Necrosis Factor (TNF) Receptor and Fas/APO1 Prompts Signaling for TNF and Fas/APO1 Effects*

(Received for publication, October 4, 1994, and in revised form, November 4, 1994)

Mark P. Boldin‡, Igor L. Mett‡, Eugene E. Varfolomeev, Irina Chumakov, Yonat Shemer-Avni, Jacques H. Camonis§, and David Wallach¶

From the Department of Membrane Research and Biophysics, The Weizmann Institute of Science, Rehovot 76100, Israel and §Denis Diderot University, INSERM Unit 248, 75010 Paris, France

Signaling by the p55 tumor necrosis factor (TNF) receptor and by the structurally related receptor Fas/APO1 is initiated by receptor clustering. Data presented here and in other recent studies (Wallach, D., Boldin, M., Varfolomeev, E. E., Bigda, Y., Camonis, H. J. and Mett, I. (1994) *Cytokine* 6, 556; Song, H. Y., Dunbar, J. D., and Bonner, D. B. (1994) *J. Biol. Chem.* 269, 22492–22495) indicate that part of that region within the intracellular domains of the two receptors that is involved in signaling for cell death, as well as for some other effects (the "death domain", specifically self-associates. We demonstrate also the expected functional consequence of this association; a mere increase in p55 TNF receptor expression, or the expression just of its intracellular domain, is shown to trigger signaling for cytotoxicity as well as for interleukin 8 gene induction, while expression of the intracellular domain of Fas/APO1 potentiates the cytotoxicity of co-expressed p55 TNF receptor. These findings indicate that the p55 TNF and Fas/APO1 receptors play active roles in their own clustering and suggest the existence of cellular mechanisms that restrict the self-association of these receptors, thus preventing constitutive signaling.

Many cell surface receptors are triggered upon clustering. Unless restricted, this mode of triggering may result in their spontaneous signaling due to receptor chance encounters. The implications with regard to regulation of receptor function are underscored by the findings in the present study regarding the mechanisms of signaling by the p55 tumor necrosis factor (TNF)[1] receptor (p55-R) and Fas/APO1. These two structurally related receptors provide signals that can cause the death of cells expressing them, via structurally related sequence motifs in their intracellular domains (the "death domains"; Refs. 2, 5, and 6). Dominant negative effects of mutations in these domains (2) and mimetic effects of antibodies against the two receptors (1, 7, 8) indicate that their signaling is initiated as a consequence of their clustering and self-interaction. TNF, and quite likely also the closely similar Fas ligand (9), occur as homotrimeric molecules (see, *e.g.*, Refs. 10 and 11) and thus can induce clustering of receptors merely by binding to them. Data presented here (see also Ref. 33) and in another recent study (4) show, however, that the intracellular domains of p55-R and of Fas/APO1 can aggregate even in the absence of their ligands, prompted by the ability of their death domains to self-associate. Additionally, we show that an increase in expression of these receptors, or even just of their death domain, can result in the induction of TNF and Fas/APO1-like effects, suggesting that the self-association of the death domain suffices to trigger signaling. These findings emphasize the need to elucidate how spontaneous signaling as a consequence of chance encounters between receptors normally is prevented.

EXPERIMENTAL PROCEDURES

Two-hybrid Screen and Two-hybrid β-Galactosidase Expression Test—cDNA inserts were cloned by polymerase chain reaction, either from the full-length cDNAs cloned previously in our laboratory, or from purchased cDNA libraries. β-Galactosidase expression in yeasts (SFY526 reporter strain; Ref. 12) transformed with these cDNAs in the pGBT-9 and pGAD-GH vectors (DNA binding domain (DBD) and activation domain (AD) constructs, respectively) was assessed by a liquid test (13), as well as by a filter assay, which yielded qualitatively the same results (not shown). Two-hybrid screening (14) of a Gal4 AD-tagged HeLa cell cDNA library (Clontech, Palo Alto, CA) for proteins that bind to the intracellular domain of the p55-R (p55-IC), was performed using the *HF7c* yeast reporter strain. Positivity of the isolated clones was assessed by (*a*) prototrophy of the transformed yeasts for histidine when grown in the presence of 5 mM 3-aminotriazole, (*b*) β-galactosidase expression, and (*c*) specificity tests (interaction with SNF4 and lamin fused to Gal4 DBD).

In Vitro Self-association of Bacterially Produced p55-IC Fusion Proteins—Glutathione *S*-transferase (GST) and glutathione *S*-transferase-p55-IC fusion protein (GST-p55-IC) were produced as described elsewhere (15, 16). Maltose-binding protein (MBP) fusion proteins were obtained using the pMalcRI vector (New England Biolabs) and purified on an amylose resin column. The interaction of the MBP and GST fusion proteins was investigated by incubating glutathione-agarose beads sequentially with the GST and MBP fusion proteins (5 μg of protein/20 μl of beads), first for 15 min and then for 2 h, at 4 °C. Incubation with MBP fusion proteins was carried out in a buffer solution containing 20 mM Tris-HCl, pH 7.5, 100 mM KCl, 2 mM $CaCl_2$, 2 mM $MgCl_2$, 5 mM dithiothreitol, 0.2% Triton X-100, 0,5 mM phenylmethylsulfonyl fluoride, and 5% (v/v) glycerol or, when indicated, in that same buffer containing 0.4 M KCl or 5 mM EDTA instead of $MgCl_2$. Association of the MBP fusion proteins was assessed by SDS-polyacrylamide gel electrophoresis of the proteins associated with the glutathione-agarose beads, followed by Western blotting. The blots were probed with rabbit antiserum against MBP (produced in our laboratory) and with horseradish-peroxidase-linked goat anti-rabbit immunoglobulin.

* This work was supported in part by grants from Inter-Lab Ltd. (Ness-Ziona, Israel), from Ares Trading S.A. (Switzerland), and from the Israeli Ministry of Arts and Sciences. The costs of publication of this article were defrayed in part by the payment of page charges. This article must therefore be hereby marked "*advertisement*" in accordance with 18 U.S.C. Section 1734 solely to indicate this fact.

‡ Equivalent contributions were made by these two authors.

¶ To whom correspondence should be addressed. Tel: 972-8-343941. Fax: 972-8-343165.

[1] The abbreviations used are: TNF, tumor necrosis factor; AD, activation domain; DBD, DNA binding domain; GST, glutathione *S*-transferase; IC, intracellular domain; IL-8, interleukin 8; MBP, maltose-binding protein; p55-IC, intracellular domain of the p55-R; p55-R, p55 tumor necrosis factor receptor; ELISA, enzyme-linked immunosorbent assay.

TABLE I

Self-association of the intracellular domains of p55-R and Fas/APO1 within transformed yeasts: assessment by a two-hybrid β-galactosidase expression test

Quantitative assessment of the interaction of Gal4 hybrid constructs encompassing the following proteins: the intracellular domain of human p55-R and its various deletion mutants, the intracellular domains of mouse p55-R (residues 334-454), mouse Fas/APO1 (Fas-IC, residues 166-306), human CD40 (CD40-IC, residues 216-277), and human p75 TNF receptor (p75-IC, residues 287-461; for residue numbering see Refs. 22, 23, and 30–32). SNF1 and SNF4 were used as positive (14), and lamin as a negative control (12). Proteins encoded by the Gal4 DBD constructs (pGBT9) are listed vertically; those encoded by the Gal4 AD constructs (pGAD-GH), horizontally. The two deletion mutants denoted by asterisks were cloned in a two-hybrid screen of a HeLa cell cDNA library (Clontech, Palo Alto, CA), using p55-IC cloned in pGBT9 as "bait." Four of about 4×10^6 cDNA clones were positive, of which three were found to correspond to parts of human p55-R cDNA (two were identical, encoding residues 328-426, and one encoded residues 278-426). The fourth encoded an unknown protein. The β-galactosidase expression data are averages of assays of two independent transformants and are presented as amount of β-galactosidase product (a unit of activity being defined as $OD_{420} \times 10^3$ divided by OD_{600} of the yeast culture and reaction time, in minutes). The detection limit of the assay was 0.05 units. Variation between duplicate samples were in all cases less than 25% of the average. —, not tested.

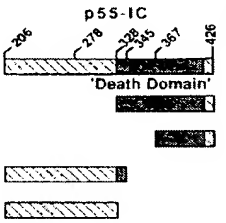

	HUMAN p55-IC & DELETION MUTANTS								OTHER PROTEINS					
	206-426	278-426*	328-426*	328-414	328-404	328-373	344-414	206-326	mouse p55-IC	mouse Fas-IC	human CD40-IC	human p75-IC	SNF4	pGAD-GH
HUMAN p55-IC &DELETION MUTANTS														
206-426 (p55-IC)	5.0	3.6	44.5	30.3	3.5	0	0	0	—	—	—	—	—	0
328-426*	5.2	—	63.5	—	—	—	—	—	—	—	—	—	—	0
367-426	0	—	—	—	—	—	—	—	—	—	—	—	—	—
206-345	0	—	0	—	—	—	—	—	—	—	—	—	—	—
206-326	0	—	0	—	—	—	—	0	—	—	—	—	—	—
OTHER PROTEINS														
mouse p55-IC	0.17	0.38	3.0	—	—	—	—	—	2.5	—	—	—	—	0
mouse Fas-IC	0	0	0.14	—	—	—	—	—	0	38.8	—	0	0	0
hu CD40-IC	0	0	0	—	—	—	—	—	0	0	0	—	—	0
human p75-IC	0	—	—	—	—	—	—	—	—	0	—	0	—	0
SNF1	—	—	—	—	—	—	—	—	—	—	—	—	2.7	0
Lamin	0	0	0	—	—	—	—	—	—	0	—	—	—	0
pGBT9	0	0	0	—	—	—	—	—	0	0	—	—	—	—

Induced Expression in HeLa Cells of the p55-R, Fragments Thereof, and Fas-IC—HeLa cells expressing the tetracycline-controlled transactivator (the HtTA-1 clone; Ref. 17) were grown in Dulbecco's modified Eagle's medium, containing 10% fetal calf serum, 100 units/ml penicillin, 100 μg/ml streptomycin, and 0.5 mg/ml neomycin. cDNA inserts encoding the p55-R or parts thereof were introduced into a tetracycline-controlled expression vector (pUHD10–3, provided by H. Bujard). The cells were transfected with the expression construct (5 μg of DNA/6-cm plate) by the calcium phosphate precipitation method (16). Effects of transient expression of the transfected proteins were assessed at the indicated times after transfection in the presence or absence of tetracycline (1 μg/ml). Clones of cells stably transfected with the human p55-IC cDNA in the pUHD10–3 vector were established by transfecting the cDNA to HtTA-1 cells in the presence of tetracycline together with a plasmid conferring resistance to hygromycin, followed by selection for clones resistant to hygromycin (200 μg/ml). Expression of the cDNA was obtained by removal of tetracycline, which was otherwise maintained constantly in the cell growth medium.

Assessment of TNF-like Effects Triggered by Induced Expression of the p55-R, Fragments Thereof, or Fas-IC—Effects of induced expression of the receptors and of TNF on cell viability were assessed by the neutral-red uptake method (18). Induction of interleukin 8 (IL-8) gene expression was assessed by Northern analysis. RNA was isolated using TRI Reagent (Molecular Research Center, Inc.), denatured in formaldehyde/formamide buffer, electrophoresed through an agarose/formaldehyde gel, and blotted to a GeneScreen Plus membrane (DuPont) in 10 × SSPE buffer, using standard techniques. Filters were hybridized with an IL-8 cDNA probe (19), nucleotides 1–392), radiolabeled by random primed DNA labeling kit (Boehringer, Mannheim, Germany), and washed stringently.

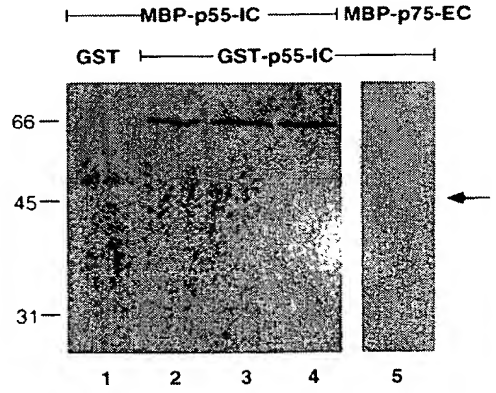

FIG. 1. **Self-association of the intracellular domain of p55-R *in vitro*: specific association of bacterially-produced fusion proteins containing the intracellular domain.** Interaction between fusion of human p55-IC to MBP (MBP-p55-IC) and to GST (*lane 2*) and the effect of EDTA (*lane 3*) and increased salt concentration (0.4 M KCl, *lane 4*) on this interaction. Interaction of MBP-p55-IC with GST (*lane 1*) and of GST-p55-IC with the fusion product of MBP and an irrelevant peptide (residues 195–229 in the mouse p75 TNF-R, MBP-p75-EC, *lane 5*; position indicated by an *arrow*) were also tested. SDS-polyacrylamide gel electrophoresis (10% acrylamide) of the interacting proteins, followed by Western blotting, using anti-MBP antiserum, was performed as described under "Experimental Procedures."

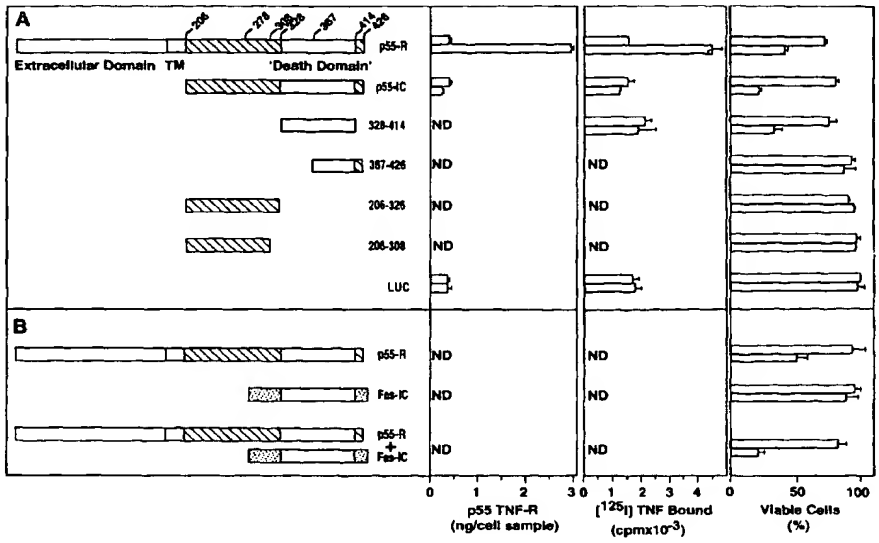

FIG. 2. **Ligand-independent triggering of a cytocidal effect in HeLa cells transfected with p55-R, or parts thereof, or with Fas-IC.** TNF receptor expression (*left* and *middle*) and viability (*right*) in: *A*, HeLa cells expressing transiently the full-length p55-R (p55-R), p55-IC or parts thereof or, as a control, luciferase (*LUC*); and *B*, in cells expressing Fas-IC, alone or together with the p55-R, using a tetracycline-controlled expression vector. □, cells transfected in the presence of tetracycline (1 μg/ml), which inhibits expression; ■, cells transfected in the absence of tetracycline. TNF receptor expression was assessed 20 h after transfection, both by ELISA, using antibodies against the receptor's extracellular domain (*left*), and by determining the binding of radiolabeled TNF to the cells (*middle*). The cytocidal effect of the transfected proteins was assessed 48 h after transfection. Data shown are from one of three experiments with qualitatively similar results, in which each construct was tested in duplicate. *ND*, not determined.

Assessment of TNF Receptor Expression—TNF receptor expression in samples of 1×10^6 cells was assessed by measuring the binding of TNF, labeled with ^{125}I by the chloramine-T method, as described previously (20). It was also assessed by ELISA, performed as described for the quantification of the soluble TNF receptors (21), except for the use of radioimmune precipitation buffer (10 mM Tris-HCl, pH 7.5, 150 mM NaCl, 1% Nonidet P-40, 1% deoxycholate, 0.1% SDS, 1 mM EDTA, and 1 mM phenylmethylsulfonyl fluoride) to lyse the cells (70 μl/10^6 cells) and to dilute the tested samples. The soluble form of the p55-R, purified from urine, served as the standard.

RESULTS

Self-association of the death domain in the p55-R was observed by happenstance, on screening a HeLa cell cDNA library by the two-hybrid system technique (14) for proteins that bind to the intracellular domain of this receptor. Among the cDNAs whose products bound specifically to the intracellular domain-GAL4 DBD fusion-protein, several clones encoded parts of the p55-R intracellular domain (p55-IC; marked with asterisks in Table I).

The extent of specificity in the self-association of p55-IC and the particular region involved was evaluated by the two-hybrid test. Table I shows the following. (*a*) The self-association of p55-IC is confined to a region within the death domain. Its N terminus is located between residues 328 and 344; its C terminus, close to residue 404, is somewhat upstream of the reported C terminus of this domain (residue 414). (*b*) Deletion of the membrane-proximal part of p55-IC upstream of the death domain enhanced self-association, suggesting that this region has an inhibitory effect. (*c*) Mouse p55-IC self-associates and also associates with the death domain of human p55-R. (*d*) Examination of the self-association of the intracellular domains of three other receptors of the TNF/NGF receptor family: Fas/APO1, CD40 (22), and the p75 TNF receptor (23), showed that Fas-IC, which signals for cell death by a sequence motif related to the p55-R death domain, self-associates and associates to some extent with the p55-IC. However, CD40-IC, which provides growth stimulatory signals (even though also containing a sequence resembling the death domain), and p75-IC, which bears no structural resemblance to p55-IC, do not self-associate, nor do they bind p55-IC or Fas-IC.

An *in vitro* test of the interaction of a p55-IC-GST bacterial fusion protein with a p55-IC-MBP fusion protein confirmed that p55-R self-associates and ruled out involvement of yeast proteins (Fig. 1). The association was not affected by increased salt concentration or by EDTA (Fig. 1, *lanes 3* and *4*).

To evaluate the functional implications of the self-association of the death domain, we examined the way in which induced expression of p55-R, or of parts of it, affects cells sensitive to TNF cytotoxicity. Using an expression vector that permits strictly controlled expression of transfected cDNAs by a tetracycline regulated transactivator (17), we found that merely increasing p55-R expression in HeLa cells by expression of transiently transfected cDNA for the full-length receptor resulted in quite extensive cell death. Even greater cytotoxicity was observed when expressing just p55-IC (Figs. 2 and 3, *A* and *B*). Significant cytotoxicity was also observed when expressing just the death domain. In contrast, expression of parts of the p55-IC that lacked the death domain or contained only part of it (or expression of the luciferase gene, used as an irrelevant control) had no effect on cell viability. Expression of Fas-IC did not result in cytotoxicity, yet significantly enhanced the cytotoxicity of co-expressed p55-R (Fig. 2). The cytotoxicity of p55-IC was further confirmed using cells stably transfected with its cDNA; these cells continued to grow when p55-IC expression was not induced but died when p55-IC was expressed (Fig. 3*C*).

We examined also the effects of increased expression of p55-R and expression of just the intracellular domain of the receptor on the transcription of IL-8, known to be activated by TNF (19). As shown in Fig. 4, transfection of HeLa cells with a tetracycline-controlled construct encoding the p55-R cDNA induced IL-8 transcription. An even stronger induction was observed in cells transfected with the cDNA for p55-IC. In both cases, the induction occurred only when tetracycline was excluded from the cell growth medium, indicating that it occurs as a consequence of expression of the transfected p55-R or p55-IC. Transfection with luciferase cDNA, as a control, had no effect on IL-8 transcription.

DISCUSSION

Studies employing the two-hybrid technique suggested that the intracellular domain of the p55-R self-associates and located this self-association to a part of a region found to be critical for signaling by this receptor (Ref. 4 and the present report; see also Ref. 33). Further tests confirmed that this association is not artifactual, as may well occur in the yeast genetic test (24), and indicated that it has functional conse-

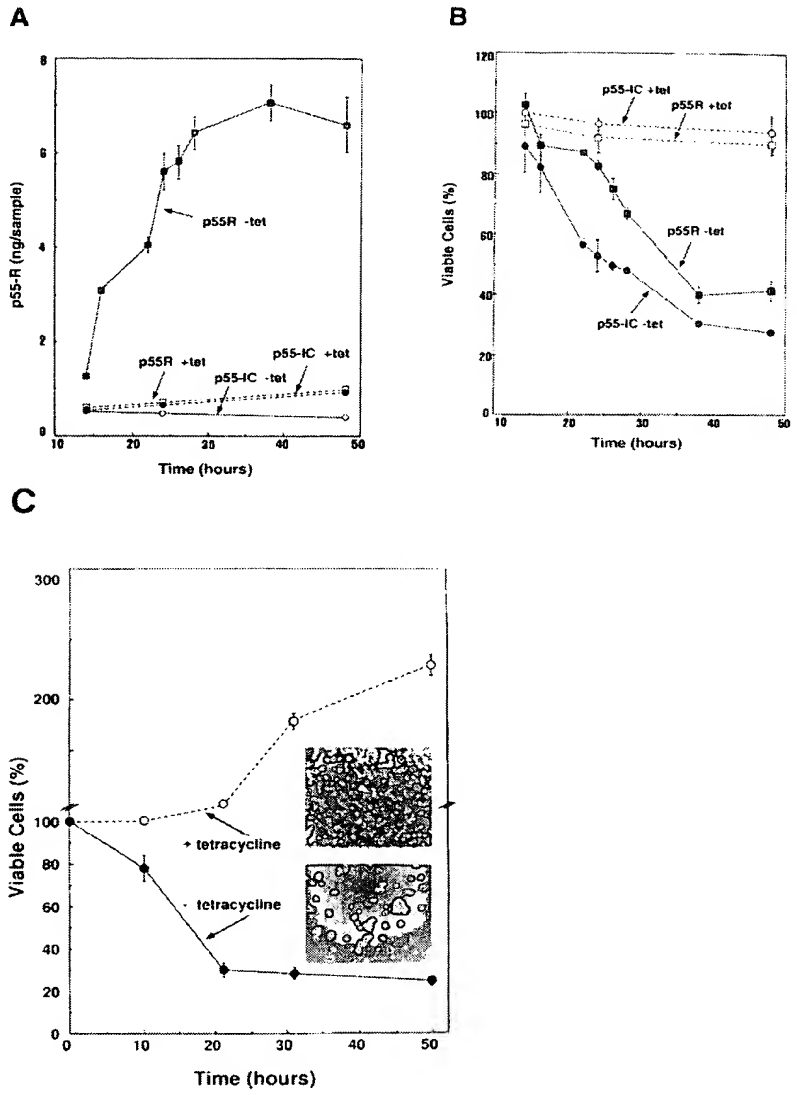

FIG. 3. **Ligand-independent triggering of a cytocidal effect in HeLa cells transfected with p55-R or its intracellular domain: kinetic study of transient expression of the receptor and its expression in a stable transfectant.** *A*, TNF receptor expression (assessed by ELISA); *B*, cell viability, in transient transfection of the full-length receptor (■, □) and of p55-IC (○, ●) in the presence or absence of tetracycline (empty and solid notes, respectively), assessed at various times after incubation with the transfected DNA; *C*, effect of p55-IC expression on the viability of cells transfected stably with this cDNA, assessed at various times after replacement of the cell growth medium with fresh medium either with or without tetracycline. Photographs were taken 36 h after tetracycline removal.

quences. The self-association could be shown to occur also *in vitro*, using GST and MBP p55-IC fusion proteins, thus ruling out involvement of yeast proteins or of the Gal4 DBD or AD in this association. Moreover, the expected functional consequence of this association could be demonstrated, namely occurrence of spontaneous signaling under conditions that permit receptor aggregation. A mere increase in p55-R expression, or even expression just of the intracellular domain of the receptor or of its death domain, was found to be sufficient to trigger signaling for cytotoxicity as well for expression of the TNF-inducible IL-8 gene within cells.

Normally, cells expressing the p55-R do not exhibit TNF effects unless exposed to this cytokine. Presumably, cells possess some mechanisms that reduce the self-association of the receptor and impose on it ligand dependence. Probably self-association of the receptors is in part restricted by mechanisms that maintain their self-surface expression at a low level. It may also be restricted by constraints imposed on the death domain in the receptor by other regions in the p55-R molecule. To some extent, self-association of the death domain seems to be inhibited by the membrane-proximal part of the intracellular domain (Table I). Crystallographic studies of the extracel-

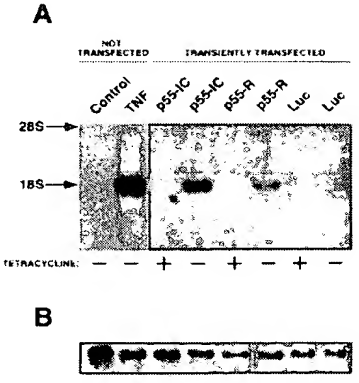

FIG. 4. **Ligand-independent induction of IL-8 gene expression in HeLa cells transfected with p55-R or its intracellular domain.** *A*, Northern analysis of RNA (7 μg/lane), extracted from HeLa (HTta-1) cells, untreated or treated with TNF (500 units/ml for 4 h; autoradiography performed for 6 h), or the HTta-1 cells 24 h after their transfection (in the presence or absence of tetracycline) with p55-IC, the p55-R or luciferase cDNA (autoradiography for 18 h). *B*, methylene blue staining of 18 S rRNA. For other details, see "Experimental Procedures."

lular domain of the receptor suggest that also this domain mediates an inhibitory effect; they indicate that, in the absence of TNF, the extracellular domains of neighboring p55-R molecules are capable of interacting in a way that obviates association of their intracellular domains.[2] Such interaction may well prevent spontaneous signaling by the receptors and allow their intracellular domains to self-associate only after TNF binding.

The intracellular domain of Fas/APO1, which bears marked structural similarity to that of the p55-R and that likewise signals for cell death, was found also to self-associate and thus trigger signaling, suggesting that this receptor, too, plays an active role in its aggregation and is subject to control mechanisms that antagonize its propensity to self-associate. This may well be the case also for a number of other receptors, for example several tyrosine-kinase receptors, including Neu/HER-2 and the epidermal growth factor receptor, that are found, just like the p55-R, to signal spontaneously when expressed at high levels as well as after deletion of their extracellular domain (see, *e.g.*, Refs. 25–27, and references therein).

Interestingly, the p75 TNF receptor, even though it has, like p55-R and Fas/APO, the ability to signal for cell death (28), does not display self-association, nor does a high level of expression of this receptor result in spontaneous signaling (29). Apparently, the mode of signaling for cell death by this receptor differs from that of the p55-R (29).

Most likely, the self-associations of p55-R and Fas/APO1 serve to fortify the aggregated state imposed on them by their ligands. Such a mechanism has certain functional advantages. It may augment signaling and also provide ways for modulation of signaling by mechanisms that act within the cell. An intriguing possibility for such modulation is indicated by the slight association between p55-IC and Fas-IC, which may allow cross-talk between the two cell death-inducing receptors (7).

The propensity of these receptors to self-associate may permit also a kind of derangement of regulation that would not be expected if their aggregation occurred in a passive manner. It can lead to spontaneous signaling, independent of the ligand, in situations in which the mechanisms restricting the self-association of the receptors fail to function properly. Such ligand-independent function is, in the case of growth factor receptors, a well known cause for the uncontrolled growth of malignant cells. In receptors that signal for cytotoxicity, it may contribute to uncalled-for death of cells, as observed, for example, in response to cytopathic viruses and various other pathogens.

[2] J. Naismith and S. Sprang, personal communication.

Acknowledgments—We are grateful to Drs. Herman Bujard and Sabina Freundlieb for providing us with the reagents for tetracycline-controlled expression and to Ada Dibeman for careful handling of the cultured cells.

REFERENCES

1. Engelmann, H., Holtmann, H., Brakebusch, C., Avni, Y. S., Sarov, I., Nophar, Y., Hadas, E., Leitner, O., and Wallach, D. (1990) *J. Biol. Chem.* **265,** 14497–14504
2. Brakebusch, C., Nophar, Y., Kemper, O., Engelmann, H., and Wallach, D. (1992) *EMBO J.* **11,** 943–950
3. Dhein, J., Daniel, P. T., Trauth, B. C., Oehm, A., Moller, P., and Krammer, P. H. (1992) *J. Immunol.* **149,** 3166–3173
4. Song, H. Y., Dunbar, J. D., and Bonner, D. B. (1994) *J. Biol. Chem.* **269,** 22492–22495
5. Tartaglia, L. A., Ayres, T. M., Wong, G. H., and Goeddel, D. V. (1993) *Cell* **74,** 845–853
6. Itoh, N., and Nagata, S. (1993) *J. Biol. Chem.* **268,** 10932–10937
7. Yonehara, S., Ishii, A., and Yonehara, M. (1989) *J. Exp. Med.* **169,** 1747–1756
8. Trauth, B. C., Klas, C., Peters, A. M., Matzku, S., Moller, P., Falk, W., Debatin, K. M., and Krammer, P. H. (1989) *Science* **245,** 301–305
9. Suda, T., Takahashi, T., Goldstein, P., and Nagata, S. (1993) *Cell* **75,** 1169–1178
10. Jones, E. Y., Stuart, D. I., and Walker, N. P. C. (1989) *Nature* **338,** 225–228
11. Eck, M. J., and Sprang, S. R. (1989) *J. Biol. Chem.* **264,** 17595–17605
12. Bartel, P. L., Chien, C. T., Sternglanz, R., and Fields, S. (1993) *BioTechniques* **14,** 920–924
13. Guarente, L. (1983) *Methods Enzymol.* **101,** 181–191
14. Fields, S., and Song, O. (1989) *Nature* **340,** 245–246
15. Frangioni, J. V., and Neel, B. G. (1993) *Anal. Biochem.* **210,** 179–187
16. Ausubel, F. M., Brent, R., Kingston, R. E., Moore, D. D., Seidman, J. G., Smith, J. A., Struhl, K., Albright, L. M., Coen, D. M., and Varki, A. (eds) (1994) *Current Protocols in Molecular Biology*, pp. 8.0.1–8.1.6, 9.1.1–9.1.2, and 16.7–16.7.8, Greene Publishing Associates/Wiley & Sons, Inc., New York
17. Gossen, M., and Bujard, H. (1992) *Proc. Natl. Acad. Sci. U. S. A.* **89,** 5547–5551
18. Wallach, D. (1984) *J. Immunol.* **132,** 2464–2469
19. Matsushima, K., Morishita, K., Yoshimura, T., Lavu, S., Kobayashi, Y., Lew, W., Appella, E., Kung, H. F., Leonard, E. J., and Oppenheim, J. J. (1988) *J. Exp. Med.* **167,** 1883–1893
20. Holtmann, H., and Wallach, D. (1987) *J. Immunol.* **139,** 1161–1167
21. Aderka, D., Engelmann, H., Hornik, V., Skornick, Y., Levo, Y., Wallach, D., and Kushtai, G. (1991) *Cancer Res.* **51,** 5602–5607
22. Stamenkovic, I., Clark, E. A., and Seed, B. (1989) *EMBO J.* **8,** 1403–1410
23. Smith, C. A., Davis, T., Anderson, D., Solam, L., Beckmann, M. P., Jerzy, R., Dower, S. K., Cosman, D., and Goodwin, R. G. (1990) *Science* **248,** 1019–1023
24. Fields, S., and Sternglanz, R. (1994) *Trends Genet.* **10,** 286–292
25. Lonardo, F., Di Marco, E., King, C. R., Pierce, J. H., Segatto, O., Aaronson, S. A., and Di Fiori, P. P. (1990) *New Biol.* **2,** 992-1003
26. Downward, J., Yarden, Y., Mayes, E., Scrace, G., Totty, N., Stockwell, P., Ullrich, A., Schlessinger, J., and Waterfield, M. D. (1984) *Nature* **307,** 521–527
27. Haley, J. D., Hsuan, J. J., and Waterfield, M. D. (1989) *Oncogene* **4,** 273–283
28. Heller, R. A., Song, K., Fan, N., and Chang, D. J. (1992) *Cell* **70,** 47–56
29. Bigda, J., Beletsky, I., Brakebusch, C., Varfolomeev, Y., Engelmann, H., Bigda, J., Holtmann, H., and Wallach, D. (1994) *J. Exp. Med.* **180,** 445–460
30. Loetscher, H., Pan, Y.-C. E., Lahm, H.-W., Gentz, R., Brockhaus, M., Tabuchi, H., and Lesslauer, W. (1990) *Cell* **61,** 351–359
31. Goodwin, R. G., Anderson, D., Jerzy, R., David, T., Brannan, C. I., Copeland, N. G., Jenkins, N. A., and Smith, C. A. (1991) *Mol. Cell. Biol.* **11,** 3020–3026
32. Watanabe-Fukanaga, R., Brannan, C. I., Itoh, N., Yonehara, S., Copeland, N. G., Jenkins, N. A., and Nagata, S. (1992) *J. Immunol.* **148,** 1274–1279
33. Wallach, D., Boldin, M., Varfolomeev, E. E., Bigda, Y., Camonis, H. J., and Mett, I. (1994) *Cytokine* **6,** 556